Establishment of CD method for studies of amyloid-oligomerization process during Alzheimer disease

Master thesis

Jana Vilímová

Charles University in Prague
Department of Physical Chemistry
University of Vienna
Department of Medicinal Chemistry

Supervisors:

o. Univ.-Prof. Dipl. Ing. Mag. Dr. Christian Roland Noe
(Department of Medicinal Chemistry, University of Vienna)

Dipl. Ing. Dr. Winfried Neuhaus
(Pharmacon GmbH, Vienna)

Doc. Ing. Alice Lázníčková, CSc.
(Department of Physical Chemistry, Charles University)

Acknowledgment

I would like to thank Prof. Christian R. Noe of the Department of Medicinal Chemistry, University of Vienna for the opportunity to work on this project and for the financial support. Special thanks are going to Dr. Winfried Neuhaus for supervising and supporting me during my work on experiment and also for editorial support. I would like to thank the whole lab-crew for the cooperation and friendly environment. I also want to thank my supervisor in the Czech Republic, doc. Alici Lázníčkové.

I would like to thank my parents, Břetislav and Hana, my brother, Tomáš and also my boyfriend Michael for supporting me.

I declare that this thesis is my original copyright work, which I have drawn up separately. All literature and other resources, from which I drew in the processing, are written in references and theses are properly cited.

Abstract

One of the main features of Alzheimer‘s disease (AD) are senile plaques in the brain. They are composed of β-amyloid (Aβ) peptides, which oligomerize and form fibrils during pathological conditions.

Inhibition of this oligomerization process is believed to be a possible therapy to prevent the progression of AD. Circular dichroism (CD) spectrometry is an optical method which enables to follow changes in the secondary structures of proteins. Within this study a CD-method was established by which the oligomerization process of synthetic Aβ 42 was monitored. During the validation of the method several parameters as the influence of several organic solvents as Ethanol, Methanol and DMSO on the spectra and the solvent solution and concentration of Aβ 42 were assessed. Then it was investigated if the addition of proposed disintegrating substances (natural compound, fluorescence dyes and antibiotics) resulted in a delayed onset of the oligomerization process of Aβ 42. Since these substances were dissolved in different solvents, the possible effects of the solvents alone as appropriate blank values were also carried out. The oligomerization experiments were carried out at 37 °C and CD-spectra were recorded at several time points (0, 7, 24, 48 hours).

In general, resulted CD-spectra showed concentration dependent effects on the Aβ 42 oligomerization caused by the inhibitors used. Thus, a CD-method was established which can be used to characterize the influence of compounds on Aβ 42 oligomerization and moreover to screen for potential substances maybe leading to drug candidates against Alzheimer‘s disease (AD).

Abstrakt

Jedním z hlavních znaků Alzheimerovy nemoci jsou senilní plaky, nacházející se v mozku. Plaky jsou tvořeny z fibril, které za patologických podmínek vznikají oligomerizací z Aβ.

Jednou z možných terapii Alzheimerovy nemoci je zastavení nebo zpomalení procesu oligomerizace. Pro experiment byla použita optická metoda, CD-spektrometrie, která umožnuje sledovat změny v sekundární struktuře proteinu. V rámci této práce byla CD- metoda použita k monitorování oligomeračního procesu syntetického Aβ. Pro validaci metody byl testován vliv různých rozpouštědel (EtOH, MeOH and DMSO) na CD- spektra a byla ustanovena koncentrace Aβ 42. Dále bylo zkoumáno, zda přidání desintegračních sloučenin (přírodních sloučenin, fluorescenčních barviv a antibiotik) má vliv na zpomalení oligomerizačního procesu Aβ 42. Pro každou testovanou látku byl také připraven kontrolní vzorek. Experiment probíhal při teplotě 37 °C a měřilo se v určitých intervalech (0, 7, 24, 48).

Závěrem, použité inhibitory vykazují koncentračně závislý inhibiční efekt na Aβ 42. Tím bylo dokázáno, že CD-metoda může být použita pro detekci vlivu sloučenin na Aβ-oligomerizaci a navíc pro objevování nových substancí, které by mohli být potenciálními léčivy AD.

Obsah

1 Introduction

Evaluation of inhibitory effect of used substances on β-amyloid oligomerization by CD method

The process of Aβ oligomerization is triggered by Aβ in pathologic conditions. In human body, Aβ behaves as a common soluble peptide occuring in brain tissue. This soluble Aβ is formed by α-secretase cleavage of APP, a transmembrane glycoprotein. Mutations of genes initiate the formation of APP-protein, presenilin 1- and 2-proteins, which are cleaved by β- and γ-secretases on Aβ.

Aβ is a protein, which is composed of 39-43 aminoacids. The most common isoforms are Aβ 40 (soluble) and Aβ 42 (insoluble). The Aβ 42 is a fibrillogenic substance. It can be polymerized to oligomers and finally to fibrils. Aβ is associated with Alzheimer disease and occurs in plaques as the main feature of disease.

There are many possible targets for the treatment. The common therapy are inhibitors of cholinesterase. The most used are galanthamin and rivastigmin. These two inhibit the cleavage of Acetylcholin (Ach) by cholinesterases (acetyl- and butyrylChE). Then the amount of Ach is normalized. Other possible therapy is using inhibitor of NMDA-receptors, memantine.

Inhibitors of aggregation reaction were targets of research as a possible therapy in this thesis. The inhibitors are derived from different sources such as natural (Curcumin) or synthetic compounds (ThT, Congo Red, Meclocycline Sulfosalicylate). They have several effects such as antibacterial, antifungal, antiviral or anti-cancer. However, they can also be binded on the secondary structure of Aβ, called β-sheet and they can delay the oligomerization of Aβ. Generally, there are not used in public.

The anti-aggregation effect of inhibitors can be evaluated by CD-method. This method is used for identification of structure and conformation of proteins. Analysis of CD-spectrum can describe quantity of conformations in secondary structure. Secondary conformations as α-helix, β-sheet, β-turns and random coil can be identified. The most important was the attendance of β-sheet. Research shows that β-sheet can trigger the oligomerization process and creation of fibrils.

In this thesis, the effect of different inhibitors on β-sheet in dependance on concentration was compared.

2 Theoretical part

2.1 Dementia

Dementia, derived from the Latin words „de“ which means „out“ and „mens“ which means „the mind“ define the loss or impairment of mental powers due to a disease.

Dementia is characterized by the loss of congnitive function, which can interfere with various parts of social life.

Above all dementia effects memory, process of learning, attention, concentration, orientation, calculation and language.

A lot of causes for the initiation of dementia can be found. The most commonly believed reasons for dementias are Alzheimer disease, multiple stroke, infections of the brain (meningitis, encephalitis), severe thyroid deficiency and brain injuries (World Health Organisation, 2001).

2.2 Alzheimer‘s disease

Alzheimer's disease (AD), is a degenerative brain syndrome, characterized by a progressive decline in the same physical and psychical activities of daily living, which were described during dementia. This disease is also a more pathological condition of cells rather than a faster way of aging.

The rate of occurrence of AD doubles every five years for those between the 65 and 85 years of age, but if the onset would be delayed by five years, the number of cases worldwide would be halved.

The first mention of AD was in 1906, when the symptoms of a dementia disease were described by Dr. Alois Azheimer, a famous German pathologist.

Nowadays, AD is the most common cause of dementia, accounting for probably 50-70 % of all dementias worldwide, as proven by research studies in developed countries and ongoing investigations in developing countries (World Health Organisation, 2001).

2.2.1 Morphopathology of Alzheimer‘s disease

The main features of AD can be observed with the naked eye or by microscopic techniques.

Macroscopic signs:

The major changes are seen on the brain tissues. There are various degrees of cortical atrophy with enlarged part on the sulci and in the ventriculi, because of the loss of nerve cells or other atrophy (Toy et al., 2008).

Microscopic signs:

Major abnormalities are neurofibrillary tangles, senile (amyloid) plaques and angiopathical changes. However, there is also the nerve loss and atrophy. The neurofibrillary tangles and amyloid plaques are placed almost in the same location of the hippocampus, amygdala and cortex. Angiopathology is more connected with changes in the blood vessels.

The most important indication of atrophy is the loss of cells, which synthetize the neurotransmitter Acetylcholin (Ach). This lack of Ach might lead to the memory impairment and the synapsis connections deteriorate (Arendt et al., 1999, Toy et al., 2008).

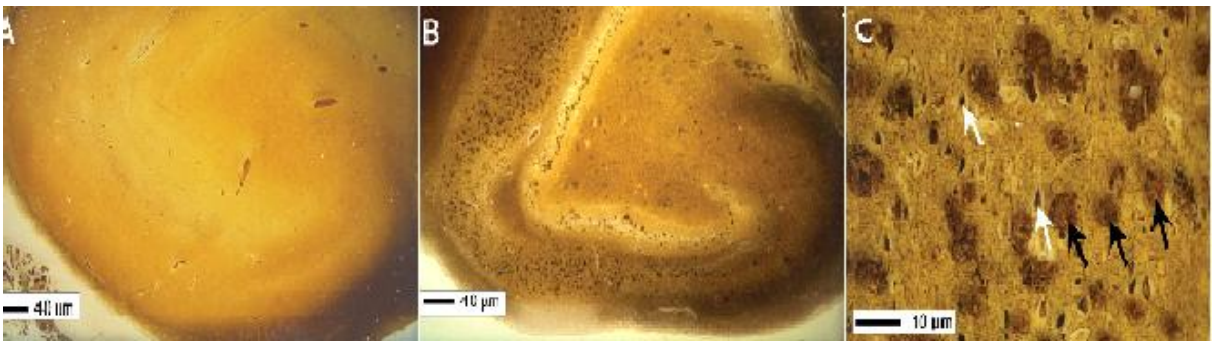

Fig 1: Normal image of hippocampus (A), pacient with AD (B), Bielschowsky stain. Dark spots are the neuritic plaques (black arrows) and tangles (white arrows) (C) (Patterson et al., 2008).

2.2.2 Physiopathology of Alzheimer disease

It is typical for AD that there is an occurance of neurofibrilar and nerve degeneration.

AD can be characterized by two types of degenerative formation, senile plaques and neurofibrillary tangles, which can lead to nerve degeneration and death (Maccioni et al., 2001).

The senile (amyloid) plaques are placed extracellularly and are generated by fibrils of Aβ. The Aβ is created by the proteolytic processing of the amyloid precursor protein (APP).

The formation of neurofibrillary tangles takes place intracellularly consisting of paired helical filaments (PHFs), which contain mainly the Tau protein. (Carter et al., 2001)

2.2.2.1 Amyloid-plaques

Amyloid plaques are mainly located in the hippocampus where the density and amount of the affected area is examined, which can be used to characterize the stages of the disease.

These plaques are the result of pathological changes in the brain tissue, which are started on the genetic level.

In studies of early-onset AD causal genetic mutations of 3 genes, namely presenilin-1 (30%-70%), APP gene(10-15%) and presenilin-2 (less than 5%), were identified. For late-onset AD no causal genetic mutation was found. (Patterson et al., 2008).

The APP gene is synthetized by neurons resulting in a transmembrane protein (Octave et al., 2005).

The difference between pathological and normal processes is in the cleavage of APP. There are two major pathways how the APP can be processed: the non-amyloidogenic and the amyloidogenic one.

During the non-amyloidogenic process APP is cleaved by α-secretase in the middle of the β-amyloid domain. The result is a soluble peptide, which normally occures in the brain tissue. The amyloidogenic way is connected with the mutation of either the APP, presenilin-1 or the presenilin-2 gene. The mutation of the genes is translated into the proteins. Then, the APP prefers the cleavage by a β-secretase and both presenilin proteins are cleaved by γ-secretase enzymes on Aβ (shown in fig. 2).

This way releases neurotoxic peptides as Aβ 40 and Aβ 42. Aβ 42 is insoluble, whereas Aβ 40 is the soluble isoform and less neurotoxic. Thus, the difference of 2 aminoacids is able to influence Aβ solubility. These proteins can form oligomers and then are transformed into the insoluble form of fibrils. These fibrils are the main component of the amyloid plaques (Patterson et al., 2008).

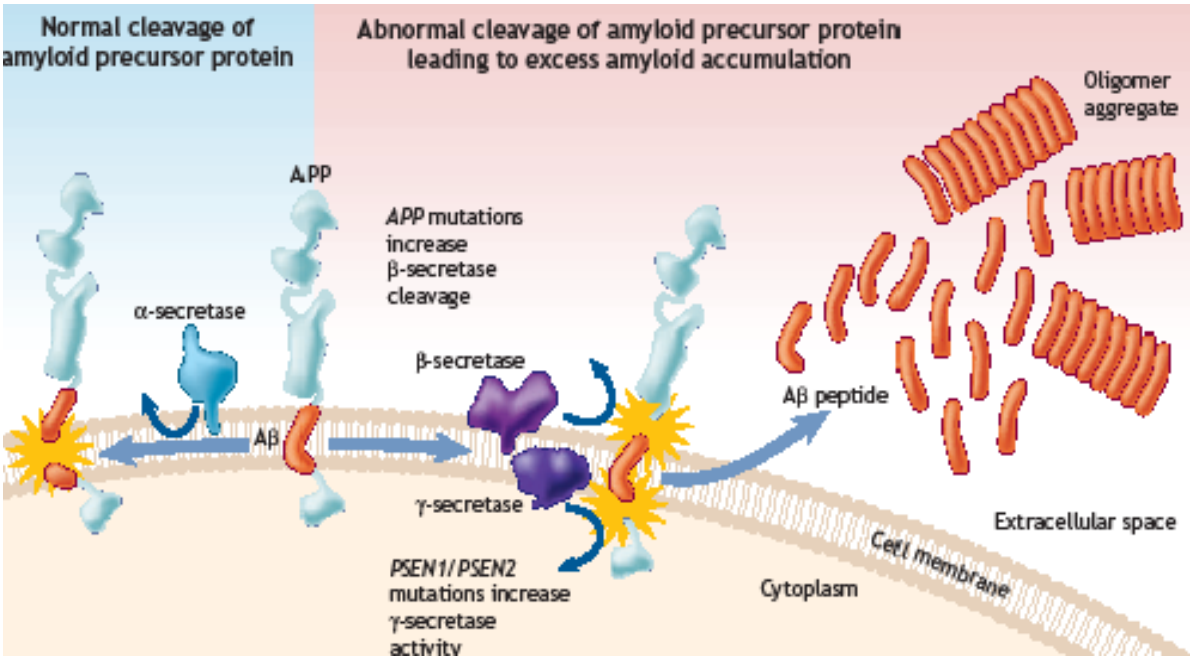

Fig 2: The proteolytic cleavage of APP by α-,β- and γ-secretase. Process leads to formation of amyloid-plaques (Patterson et al., 2008).

2.2.2.2 Neurofibrillary tangles

Neurofibrillary tangles (NFTs) are composed of paired helical filaments and are originated from microtubuli, which are associated with protein Tau. Because of its insoluble form the formation of NFTs is responsible for the dysfunction of the microtubule network, intra- and extra-cellular transport, synapsis loss and the death of nerve cell. (Octave et al., 2005)

The main factor which influences the occurence of NFTs is the modified Tau protein. This protein is also found in normal cells as a part of the cytoskeleton. The pathological progress is caused by the change of Tau protein.

In the physiological state the balance between phosphorylation (phosphatase) and dephosphorylation (kinase) regulates the function of the Tau protein. The changed Tau protein is already phosphorylated causing the formation of non-functional microtubules which then results in the death of cells.

Several researchers have shown the influence of kinases on the Tau protein-pathology. Two important kinases are known, a serine-threonin kinase (GSK 3β) and the cyclin-dependent kinase (Cdk 5), which are deregulated in pathological state. These kinases are associated with the impairment of nerves (Sperber et al., 1995).

2.2.2.3 Genetics of Azheimer‘s disease

Individual and familial genetic risks are known for the progression of AD. For the diagnosis of the familial type of AD the knowledge of the familiar medical history is very helpful. Usually, an early-onset of AD with significant genetic factors is before the age of 60.

In the familial type of AD differences with regard to the degrees of inheritance are known. For first-degree relatives (children and siblings of affected person) the incidence is about 20%, while for second-degree relatives (indirect relatives of affected person), the risk is about 10% incidence to suffer from AD (Patterson et al., 2008).

For the early-onset of the autosomal dominant familiar AD main causal mutations are on chromosome 21 (APPgene), chromosome 14 (presenilin-1) and chromosome 1 (presenilin-2). This results in an accumulation of β-amyloid fragments (Richter, 2004).

Mutations of the APP-gene leads to the exchange of only one amino acid. The APP-gene occurs in more than 20 different mutation, which can cause AD. The onset of the disease is usually from 40 to 60 years of age. Other mutations concern the presenilin genes. These genes are transmembrane proteins consisting of 448-463 amino acids with hydrophobic domains. The possibility of 160 mutations in the PS1 locus was found for the Presenilin-1 gene and the onset of AD is normally before 50 years of age.The Presenilin-2 gene exhibits a rare incidence and the onset is usually before 65^{th} year of age (Blazer et al., 2009).

The late-onset AD has no significant causal mutation. Mostly, the late-onset AD is influenced by different genetic risks. The most known is the ApoE (Apolipoprotein E) gene, ε4 allele, located on chromosome 19. The ApoE gene has 3 allels (isoforms), ε2 (8% occurence in population), ε3 (75%) and ε4 (15%). ApoE is responsible for the transport of lipids, mainly cholesterol. There is a risk of negative cardiovascular effects, such as hypertesion and diabetes, caused by the mutation. The exact mechanism is

unclear. Recently, the sortilin-related receptor gene (SORLi) was shown to play a role in the late-onset of AD and to have an influence on APP processing, which is involved in the amyloid cascade. (Patterson et al., 2008).

2.2.2.4 The „Neurodegenerative Cascade“ Hypothesis (Amyloid Cascade)

In early stages of Alzheimer disease, the amyloid plaques seem to be potentionally good therapeutic targets. These plaques are composed of amyloid deposits, microglial cells and neurites. The plaques contain mainly Aβ which is cleaved by β- and γ- secretases from APP. (Barrow et al., 2007).

During the formation of amyloid plaques glial cells are activated (astrocytes and microglial cells). These glial cells play an important role in inflammatory and neurodegenerative events and for the integrity of the blood-brain barrier.

Neurotransmitters and reactive oxygen radicals are released after activation of glial cells. Another running process is the formation of neurofibrillary tangles, which leads to the loss of neurons caused by apoptosis. Studies showed that Aβ can initiate the apoptosis process. The enzymes of apoptosis, namely caspases, are able to cleave proteins of the cytoskeleton and membranes. (Fisher et al., 1998).

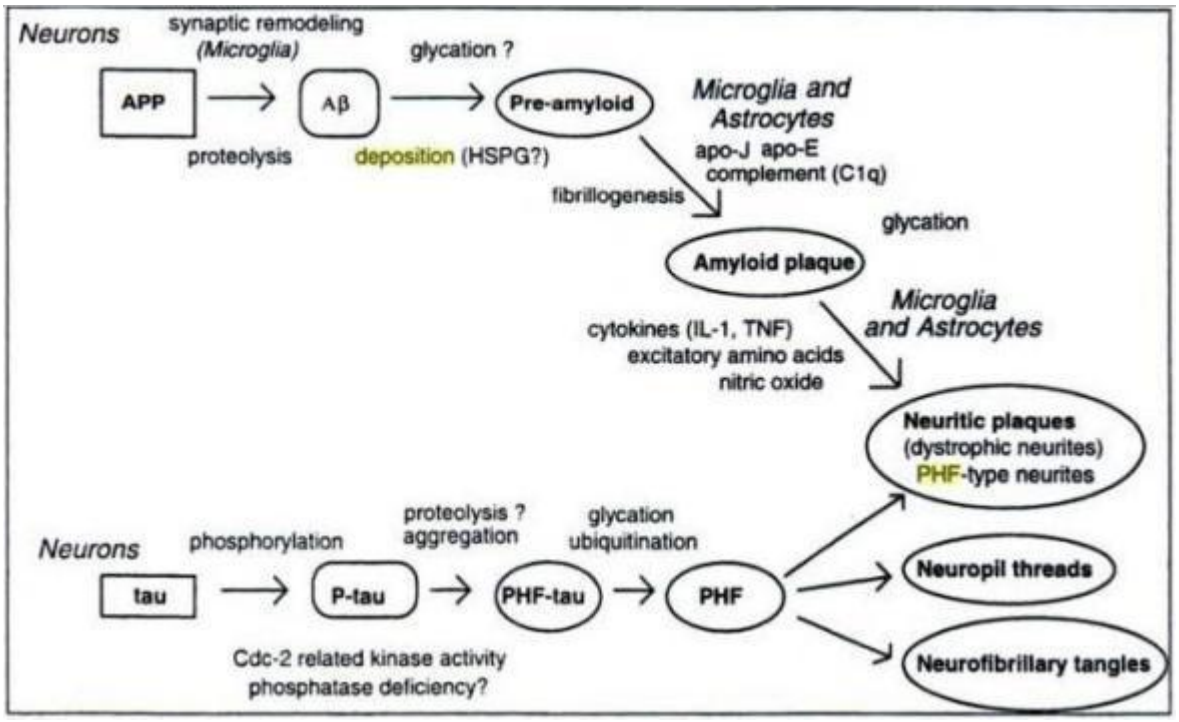

Fig 3: Amyloid deposition and PHF formation in AD (Ransohoff et al., 1996).

2.2.2.5 The „Inflammatory“ Hypothesis of AD

The inflammatory hypothesis focuses on the pathological inflammatory responses occurring during the AD. The initiative factor should be the presence of extracellular amyloid plaques. These plaques are antigens for the human body which cause an immunity reaction by increasing amount of hypertrophical astrocytes and microglial cells surrounding Aβ plaques (Hof et al., 2000).

Microglial cells are able to synthetize immuno-molecules and to secrete markers and effector molecules (MHC-1, IL-1β, TNFα). Their role is to coordinate the inflammatory process until the activation of the specific immune system (e.g. leucocytes). Leucocytes can not enter the brain tissue if the blood-brain barrier functions normally. In pathological conditions, the microglia release mediators, such as TNFα, IL-1β, nitrogenmonoxid (NO) and reactive oxygen species (ROS), which damage neurons and cause inflammation. The infiltration of leukocytes is enabled by the effects of cytokines (TNF-α, IL-1β), which can increase the permeability of the blood-brain barrier (Walz et al., 2002).

IL-1 influences the synthesis of APP and the following formation of plaques. It also leads to an increase of IL-6 and MCP1 (monocyte chemotactic protein) in blood and the induction of ICAM-I (intercellular adhesion molecule-I) on endothelial cells (Vojáček et al., 2004).

2.2.2.6 Alzheimer disease and its influence on the blood-brain barrier (BBB): The clearance of Aβ-peptides from the brain

The clearance:

After the cleavage of APP by β- or γ-secretase β-amyloid peptides are formed. They can further oligomerize, which then may build plaques. The Aβ exists both inside and outside the brain in the extracellular space, where it might be degraded by enzymes. Furthermore, Aβ is also transported across the BBB (brain to blood, blood to brain) and can be cleared by local cells (Sisodia et al., 2007).

Problems caused by increased concentration of Aβ in the brain are prevented by proteolytic cleavage or directed efflux out of the brain.

The proteolytic cleavage of Aβ is linked to two endopeptidases, the insulin degradable enzym (IDE) and the neutral endopeptidase (NEP) (Sisodia et al., 2007).

For the directed transport of soluble Aβ from brain to blood and from blood to brain, the two transporters LRP1 (low-density lipoprotein related protein receptor) and RAGE (receptor for advanced glycation end products) are used. These receptors are multifunctional scavengers which transport of huge molecules such as Aβ. LRP1 is responsible for the efflux of Aβ from the brain to the periphery and RAGE for the influx from blood to brain. The processes of transport and clearance can be influenced by chaperones that bind to molecules such as apolipoprotein E (ApoE) which are used as a ligand in a complex with Aβ. The complex is then taken up by the LRP1 receptor and is transferred by transcytosis. In the other case, Aβ binds directly to the RAGE receptor. The activity of LRP decreases according to age, on the contrary the activity of RAGE increases. Thus, the accumulation of Aβ in the brain can cause immune reactions.

The blood-brain barrier:

The blood-brain barrier influences the pathogenesis of AD. The BBB has a special clearence mechanism to prevent accumulation and aggregation of Aβ in the brain. Aβ occures around arterial vessels and celebral capillaries to influence the permeability of BBB. The change of the BBB is evidenced by the alteration of specific BBB markers. Increased levels of ICAM-I, collagen proteins and Glu-6-P and decreased level of GLUT-1, Na/K ATP, AchE, γ-Glu transferase can be detected. The result of these changes is a degenerated BBB . A disrupted BBB is typical for a late-onset AD (Sarbadhikari et al., 2006).

Clinical studies have also shown an effect of peripheral vascular changes such as hypertension, cardiovascular disease and DM on the BBB during AD (Verbeek et al., 2000).

This damage of the BBB may cause an enhanced transport of substances (also of the soluble form of Aβ to deposit in neurons) from the blood to the brain tissues. Furthermore, some of these substances act as antigenes stimulating the immune system. After activation of immunity reaction by the complement system, inflammatory processes may start. Then, the result is the damage of normal tissues and neurons (Sachdev, 2003).

Recent studies tried to determine if the alteration of the BBB has an effect on initiation of AD, but this is still unclear (Sachdev, 2003).

2.2.3 Symptoms of AD

The occurance of symptoms in AD patients differs from individual to individual. The behaviour symptoms depend on the degree of illness. There are three stages of AD.

Early stage:

The symptoms of the early-stage are thought to be related to age or manifestation of stress. There are headache, nausea and vertigo. Then, the more specific symptoms start such as impairment of the short-term memory, language or orientation.

Moderate stage:

In the moderate stage a progressive deterioration, speech difficulties, inability to recall vocabulary (paraphasias) are observed. The loss of the abilities to write and read, long-term memory and performing normal daily living activities are further symptoms of the moderate stage of AD. The person is not able to recognize close relatives. Also, neuropsychiatric manifestations, wandering, sundowing, irritability and labile symptoms may occur. In some cases urinary incontinence appears.

Advanced stage:

In this phase the language consists only of simple phrases or single words. It leads to complete loss of speech. Because of this loss patients start using emotional signals. This may turn out as aggressiveness, apathy and exhaution. Patients need assistance for simple tasks (e.g. eating). The muscles and mobility are getting worse. Death is normally caused by an other illness (flu, pneumonia and pressure disease).

2.2.4 Diagnosis of AD

The diagnosis of AD should involve 5 main steps: using the patient´s medical records, interviewing a person close to the patient, physical tests, cognitive tests and basic laboratory tests (Feldman et al., 2008).

Typical factors for dementia as vascular factors, hypertension, DM, smoking, renal failure and alcohol should be written down in the medical history of patient. Also genetic factors which occur in family history such as stroke, lipid status, dementia or head trauma should be noted.

Physical tests consist of the examination of risk faktors. Special attention is paid to signs of stroke, hyperreflexia, apraxia, palsy and the presence of small-vessels.

Cognitive tests evaluate the ability of memory, attention, orientation and construction. For earlier diagnosis these examination should be more used by general practitioners. The most often used method is the mini-mental state examination (MMSE). It recognises the difference between the moderate stage of dementia and the normal recognition abilites within 10 minutes. Examples for other tests are the clock-drawing examination to evaluate visuospatial abilities or the general practitioner assessment of cognition. Special manuals for exact diagnosis of dementia exist, as e.g. Diagnostic and Statistical Manual of Mental Disorders (Feldman et al., 2008).

Laboratory tests are composed of neuroimaging with computed tomography or magnetic resonance imaging in order to find atrophies in the hippocampus or the gyrus or to detect the presence of treatable diseases such as renal failure, brain tumour, normal pressure hydrocephalus or subdural hemorrhages. Then, basic investigations of blood, thyroid stimulating hormon, serum calcium, electrolytes and glucosis count is recommended. Other tests are optional, which are dependent on the medical history of the patient. The optional examinations include tests for serum vitamin B_{12}, folate levels, homocysteine, syphilis screening and HIV antibodies. In laboratory tests, measurements of biological markers are often included. The main markers are levels of Aβ, Tau and phospho-Tau proteins in the cerebrospinal fluid (Feldman et al., 2008). However, the only proof to diagnose AD definitely is to investigate the brain tissue post-mortem.

2.2.5 Therapy of AD

The therapy of Alzheimer‘s disease should start with non-pharmacological trials at the beginning of the illness. With the progressing disease the non-pharmacological therapy should be substituted by a pharmacological treatment with drugs.

2.2.5.1 Non-pharmacological treatment

The non-pharmacological therapy is convenient for patients during the onset of AD. In the non-pharmacological treatment it is important to involve caregivers and members of the family. For patients, cognitive training (memory, self preservation, orientation, attention and memories) and rehabilitation (physiotherapy, physical activities for improving the movements and logopedics) is recommended to improve their quality of life. Individualized exercise programs are created.

2.2.5.2 Pharmacological treatment of AD

The treatment of AD is actually only directed againts the symptoms. The patient should agree with the initiation of therapy. Furthermore, an individual treatment for each patient has to be devised.

o) Cholinesterase inhibitors:

AD is characterized by the lack of acetylcholin (Ach). The absense of this neurotransmitter is caused by degeneration of the nerve tissue, especially the part of Meynert basal cores which produce Ach. Ach effects memory and learning processes in the brain. The lack of Ach is the reason for an impairment of these functions.

Ach is degraded to acetyl-CoA and cholin by the enzymes acetylcholinesterase and butyrylcholinesterase.

Nowadays, four inhibitors of cholinesterases are approved by the FDA: Tacrine, Donepezil, Rivastigmin and Galantamin. (Schneider et al., 2003. Ibach et al., 2004). The mechanism of these inhibitors is to block cholinesterases. Due to the inhibition of the hydrolysis the amount of Ach increases and the functions return to the normal conditions. Tacrine is rarely used against AD because of its hepatotoxicity. Donepezil and Galantamin are selective inhibitors of acetylcholinesterases, whereas Rivastigmin is a general cholinesterases inhibitor (AchE and ButE).

Those are used in mild and moderate stage of AD. Their effect on slowing down the development of AD has been proven (Rattan et al., 2006).

o) NMDA- receptor antagonists:

The NMDA-receptor (N-methyl-D-aspartate) is an ion channel, which is voltage- and transmitter-dependent. The neurotransmitter glutamate can activate the NMDA-receptor. When glutamate is released and the membrane is depolarized, the channel opens. K^+ influx by e.g. an AMPA-receptor channel can activate the diffusion of Ca^{2+} ions and immediately triggers the process that is responsible for persistent modifications of synaptic strength. The depolarization of the cell membrane is important for the activation of the NMDA-receptor channel, because Mg^{2+} blocks the receptor if it is not depolarized(Rattan et al., 2006).

The continuous excitation can cause irreversible damage. The imbalance between glutamate and acetylcholin may lead to special symptoms as irritation, aggressivity and the death of cells caused by permanent excitation.

Memantine:

Memantine is a non-competetive inhibitor of the NMDA-receptor. It has a normal function in physiological enviroment, but during pathological changes it is able to inhibit excitotoxicity. Memantine is convenient for the treatment of moderate and severe AD (Rattan et al., 2006). Recent clinical studies did not show any benefit in combining Memantine with cholinesterase inhibitors (Patterson et al., 2008).

o) Other therapies:

Other therapies are targeted according to mechanism of AD: cleavage of APP, inflammation, Aβ aggregation, clearance or oxidative stress. Secretase inhibitors, NSAIDs, antioxidants, statins and metal complexes are used for the treatment.

Inhibition of amyloid formation:

The targets are β- and γ-secretase. The research is intensive, but inhibitors which were discovered until now are too toxic for their phamacological use. In recent studies, an effect of flubiprofen (NSAIDs) on the γ-secretase was evaluated. For better evaluation other tests are recommended (Rattan et al., 2006).

Inhibition of Abeta aggregation:

Metal chelators such as Cu^{2+} and Zn^{2+} can cause reversible aggregation and resistance to proteases. In a transgenic mouse model, clioquinol (chelator) was tested. During the examination decreasing levels of plaques and Aβ were proved. (Rattan et al., 2006).

Improved clearance of Abeta:

The immunisation process consists of an active and a passive part. Mechanisms are based on antibody-mediated clearance of the plaques and activation of microglial phagocytosis of the immune complex. There are three main mechanisms:

1. There is a balance of Aβ between brain and the periphery. In the periphery, Aβ is captured, which leads to decrease of Aβ in the bloodstream. The result is an increased clearence of peptides from brain to plasma due to the changed equilibrium. Due to the improved clearance it is able to remove Aβ and protect neurons against neurotoxicity.

2. Aβ antibodies have an effect of Aβ from brain.

3. Antibodies may cross the BBB, then bind to the amyloid on specific epitopes that can inhibit aggregation of Aβ itself (Rattan et al., 2006).

2.3 Inhibitors of the Aβ-aggregation process

This thesis is focused on the study of inhibitors on Aβ aggregation. There are several possible inhibitors, for which anti-aggregation effects were discovered. Curcuminoids, derivates of flavonoids, derivates of Cyclohexanehexol, stereoizomers of Cyclohexanehexol, fluorescence dyes, such as Congo Red, ThT and also antibiotics (Meclocycline Sulfosalicylate) belong to this group of compounds. These inhibitors are currently only used for research purposes.

2.3.1 Aggregation process of Aβ

In epidemiological studies it was proven that extracellular Aβ is the cause for the pathological toxicity occuring in AD. Deposition of this type of amyloid leads to insoluble aggregations and it has toxic effects on cells and tissues.

The mechanism of aggregation is not absolutly clarified. The process depends on the type of Aβ. Generally, Aβ peptides which are isolated from different sources have various properties. The oligomerization starts with non-toxic Aβ monomers which are retrieved from cleavage of the APP protein. The monomer then changes its secondary structures into β- sheet structure (dimer or β-crystallic substance). The formation of dimers triggers the fibrilar growth (toxic) and can lead to bigger aggregates (Kominos, 1995) (shown in fig. 4).

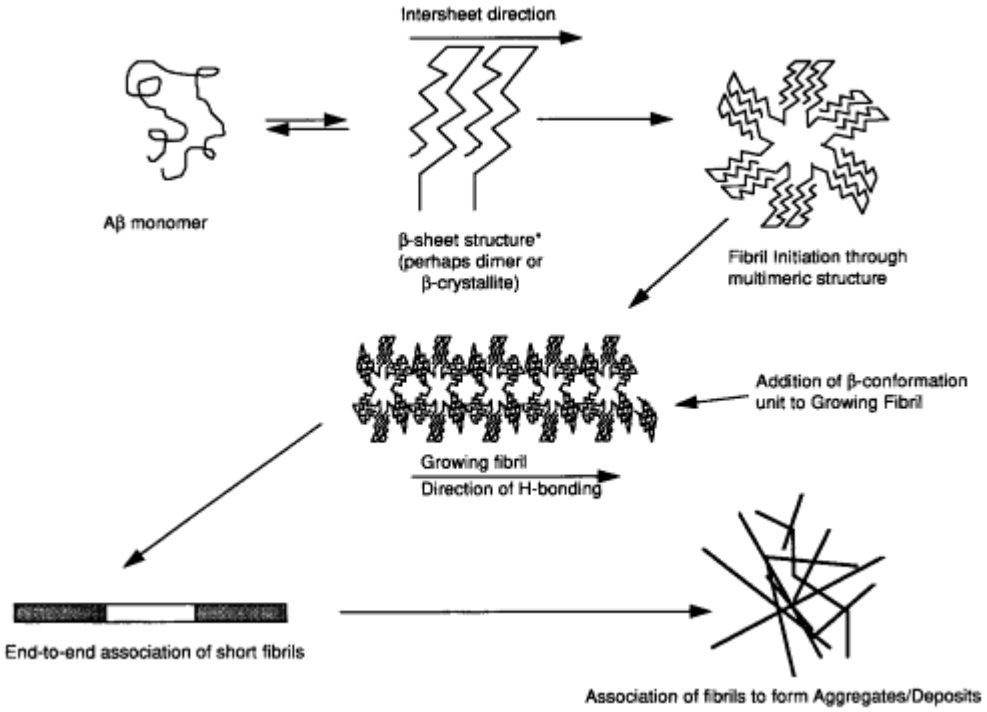

Fig 4: The aggregation of Aβ . This reaction can be activated also in in vitro enviroment. The conditions are defined by concentration and pH (Murphy et al., 1995).

The final structure of Aβ- sheets during amyloidosis are aggregates. A special form of aggregates are Lewy bodies which are often observed during dementias in Parkinson's disease and contain α-synuclein and other proteins (ubiquitin, α-β-crystalline). α-synuclein is also a component of plaques (Ahn et al., 2007).

2.3.2 Curcumin.

Curcumin is a curcuminoid and isolated from turmeric (Curcuma longa L., Zingiberaceae). Turmeric is used as traditional medicine as well as curry spice, its yellow color is caused by polyphenols. Other two important curcuminoids are desmethoxycurcumin and bis-desmethoxycurcumin. Curcumin, which is known as an antioxidant and inhibitor of the arachidonic acid cycle, suppresses oxidative damage, inflammation, cognitive deficits and amyloid accumulation. Furthermore, it acts as antiviral, antifungal and antibacterial substance and is chemoprotective against cancer (Kim et al., 2001).

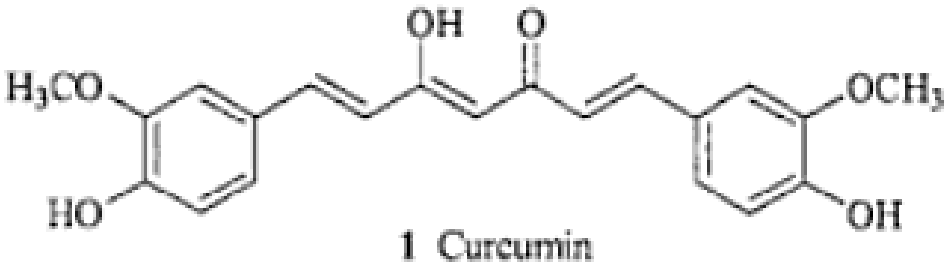

Fig 5: The structure of Curcumin. It is a polyphenol which exists in two tautomeric forms as keto- and -enol. The –enol form is the more stable one in solution as well as in solid phase (Basha et al., 2006).

Curcumin can cross the BBB and inhibits Aβ formation, binds plaques and reduces Aβ in plaques. Furthermore, Curcumin was a better inhibitor of Aβ 40 oligomerization than NSAIDs and decreased the risk of Aβ 42 oligomer formation. Curcumin is currently in the phase of clinical trials as a preventive and therapeutic drug for treatment of AD (Yang et al., 2004).

2.3.3 Thioflavin T (ThT)

ThT is structurally a benzothiazol. It is mainly used for the detection of amyloid-plaques in AD as well as other amyloid proteins by fluorimetry. A shift of the fluorescence signal induced in the presence of Aβ-fibrils resulting in a detection at around 450nm (excitation maxima) and 482nm (emission maxima). In absence of fibrils, excitation and emission maxima are 350 and 438nm (Naiki et al., 1989).

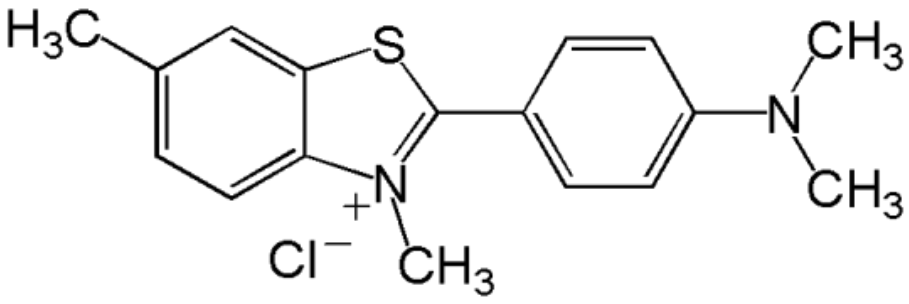

Fig. 6: The structure of Thioflavin T (Rost, 1995).

In this thesis ThT was used as an inhibitor. ThT binds normally to Aβ-fibrils, it can be used to stop the oligomerization and fibrilization of Aβ-peptides.

2.3.4 Congo Red

Congo Red (benzidinediazo-bis-1-naphthylamine-4-sulfonic acid) is soluble in water and organic solvents. It is a type of dye with toxic effect. The colour of Congo Red solutions is pH-value dependent. The solution of Congo Red is aggregating,

because of hydrophobic interactions between aromatic rings. This effect is more visible in higher concentrations.

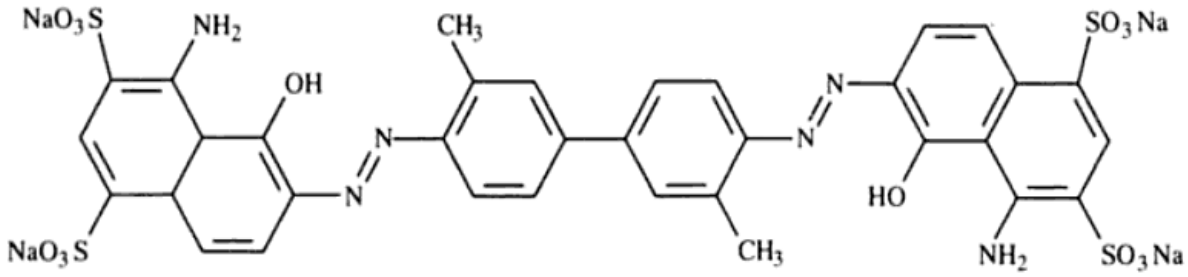

Fig. 7: The chemial structure of Congo Red (Rost, 1995).

Congo Red inhibits the fibril formation of Aβ.

Congo Red is very toxic, suppresses inflammatory activity and prevents natural formation of Aβ-oligomers (F. Yang et al. 2004).

Recent studies described pathogenic mechanism of amyloidogenic peptides, which can form ion channels in the cell's membrane. These ion channels may cause tissue destruction in AD. Congo Red was able to prevent these effects (Hirakura et al., 2000).

2.3.5 Meclocycline Sulfosalicylate

This substance is synthesized of Meclocycline and Sulfosalicylate. The Meclocycline is a tetracycline antibiotic with a wide spectrum of antibacterial and antiprotozoal activity. The Sulfosalicyte has a strong anti-inflammatory effect.

Fig. 8: The structure of Meclocycline Sulfosalicylate (www.sigmaaldrich.com).

The substance is used for the inhibition of Aβ-oligomerization and fibrilization (Necula et al., 2008).

2.3.6 Other inhibitors

Recently, inhibiting effects of Resveratrol (3, 4´, 5-trihydroxystilbene) on Aβ-oligomerization were found. Oligomers of Resveratrol are gained from Vitis amurensis (red wine). It is an antioxidative substance and has an effect against cardiovascular and neurological diseases. Resveratrol influences strongly the Aβ aggregation including α-synuclein and Aβ. Inhibition of cholinesterases were also proven (Jang et al., 2008, Ahn et al., 2007).

Other interesting compounds are flavonoids. E.g. Rhamnetin, Quercetin, Morine and Fisetin, which strongly inhibit Aβ fibril formation (efficiency decreasing in order as mentioned), were tested. Morin and Quercetin can protect nerve cells against oxidative stress, but there is no effect reducing cytotoxicity (Kim et al., 2005).

Other possible compunds are stereoisomers of Cyclohexanehexol (epi- and scyllo-Cyclohexanehexol). They can inhibit the accumulation of Aβ oligomers and their aggregation. Substances were tested on transgenic (TgCRND8) and non-transgenic mice. There,significant prophylactic, neuropathogical (plaque burden, angiopathology, glial reaction and synaptic loss) and astrogliotic responses were shown. Each response was influenced by the starting time point of the therapy for Epicyclohexanehexol (effect was more efficient at the onset of 6 weeks of age. In 5 months of age was comparable with non-transgenic mice), whereas Scyllocyclohexanehexol had a strong reducing, but application time-independent effect (McLaurin et al., 2006).

Moreover, Inositol stereoizomers stabilize oligomeric aggregates and can inhibit the fibrillogenesis (McLaurin et al., 2000).

2.4 Circular dichroism (CD)

2.4.1 Introduction of CD

CD is a valuable spectroscopic technique for studying protein structures. This method measures the difference in absorbance of right and left polarized light, which depends on the wavelength. The source of CD signals are chromophores, which are also responsible for the absorption and are determinated by the secondary structure of protein (Sigurdsson et al., 2005). There are three different types of CD spectra: the far UV, which is below 250 nm, the aromatic region in range of 250 to 300 nm and the near-UV visible region above 300 nm. The far UV region is sensitive to the secondary

structure of proteins. The near UV provides information about the tertiary structure of proteins and the region above 300nm about their conformation (Woody et al., 2000).

2.4.2 CD-method and structural model of polypeptides

The optical properties of proteins are influenced by their structure. The primary structure of protein is determined by the sequence of the amino acids. The presence of different bonds within the molecule causes different secondary structures. The tertiary structure is the whole shape of a single protein, which is composed of only α-helix, β-sheet or the combination of α-helix and β-sheet. The quaternary structure describes the structure of protein complexes and consists often of several domains.

CD-spectroscopy can differentiate between different types of secondary structures including α-helixes, β-sheets, turns and random coils.

The secondary structure is formed by a regular and repeating segment of polypeptides (backbone), which contain N-H, C_α-H and C=O bonds of each amino acid peptide. These groups can build hydrogen bonds. The secondary structureof a protein is devided in various types, which are characterized by angles. The angle of a C-N bond is called Φ(phí) torsion, in C_α -C the angle is named Ψ (psí) torsion angle (Ringe et al., 2004).

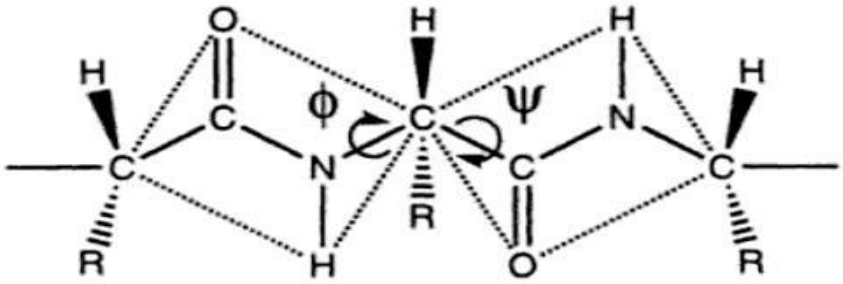

Fig. 9: Conformation of a peptide with binding angles (Φ, Ψ) (Greenberg, et al., 2000).

2.4.2.1 α-helix

The α-helix (structure shown in figure 12) is a dominant secondary structure. The conformation is stabilized by hydrogen bonds between CO- and NH- groups. It forms a structure with angles Ψ and Φ of -60° and -40°, which may cause the thickness and hydrophobic properties used in lipid bilayer. The CD spectrum of an α-helix is well

defined. The spectrum of an α-helix displays CD bands with negative ellipticity at 222 and 208 nm and positive at 192 nm. (Greenfield, 1999, Ringe et al., 2004).

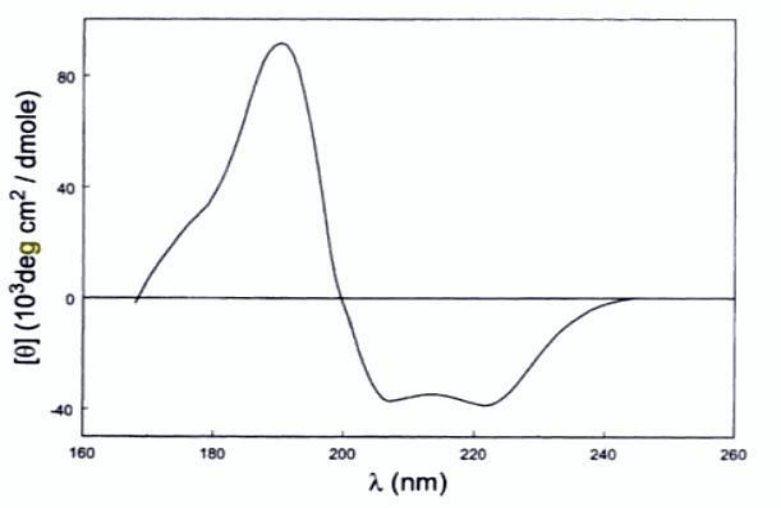

Fig. 10: CD spectrum of α-helix (Woody et al., 2000).

2.4.2.2 β-sheet (pleated sheet)

The β-sheet (structure shown in fig. 12) is another secondary structure, which consists of strands connected through hydrogen bonds forming a twisted sheet. The strands can occur in a parallel, antiparallel or mixed (both) form to each other. The connection between the first and last strand is linked through hydrogen bonds forming a closed structure of a cylinder. β-sheets are more flexible than an α-helix, but the solubility is limited. A typical CD-spectrum of a β-sheet structure is shown in fig. 11 with a positive band near 195 nm and in negative one at 216 nm (Ringe et al., 2004).

The association of β-sheets has been implicated in the formation process of protein aggregates and fibrils.

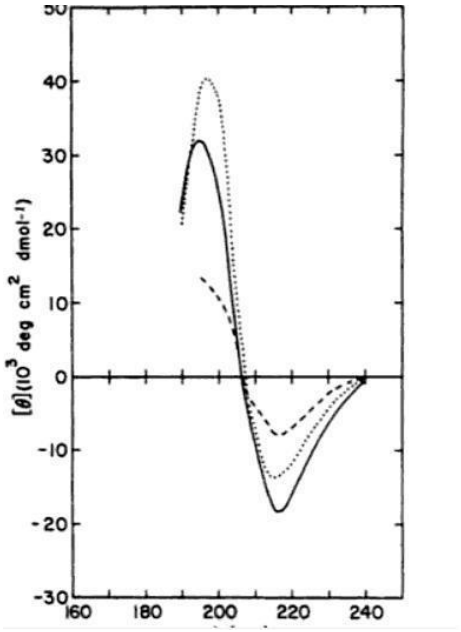

Fig. 11: CD spectrum of a typical β-sheet-like structure (Woody et al., 2000).

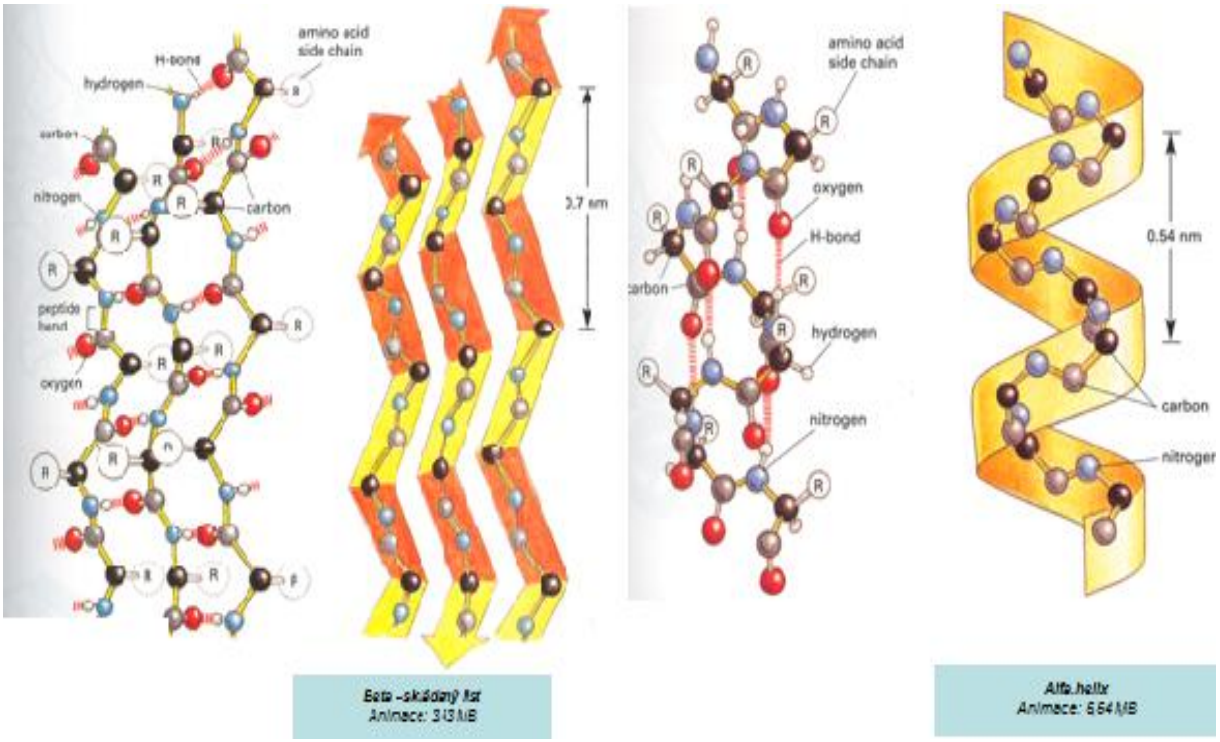

Fig. 12: Structure of a β-sheet and an α-helix structure (Ringe et al., 2004).

2.4.2.3 β-turns (reverse turn)

β-turns are the simplest secondary structure occurring in a protein. They consist of three amino acids and can reverse the direction of a polypeptide chain. The structure is very tight and can´t be enlarged. 8 different types of β-turns had been characterized according to their torsion angles (Φ, Ψ). CD spectra show also more bands because of

the various forms of β-turns. The most common one has a strong positive band at 200-205 nm, negative band between 180 and 190 nm (Woody et al., 2000).

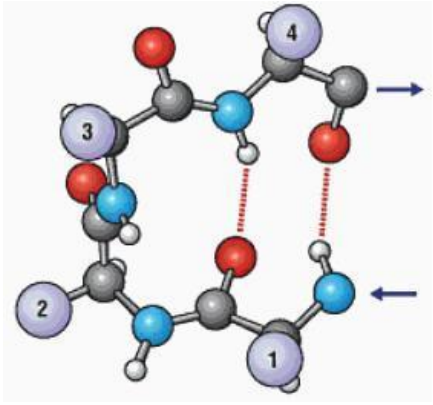

Fig. 13: The structure of β-turns. The protein is very tight. Glycine occurs more often in β-turns than in any other secondary structure. There are also hydrophobic bonds (red) and side chains (blue) (Ringe et al., 2004).

2.4.2.4 Unordered conformation (random coil)

In globular proteins unordered, unstructured and random coil conformations are preferred rather than α-helix, β-sheet or β-turn. A mostly ionized polypeptide with poly(Lys) or poly(Glu)- side chains at neutral pH represents a model for these kind of confirmation. A negative band near 200 nm and positive one near 218 nm are characteristic for a CD-spectrum (Woody et al., 2000).

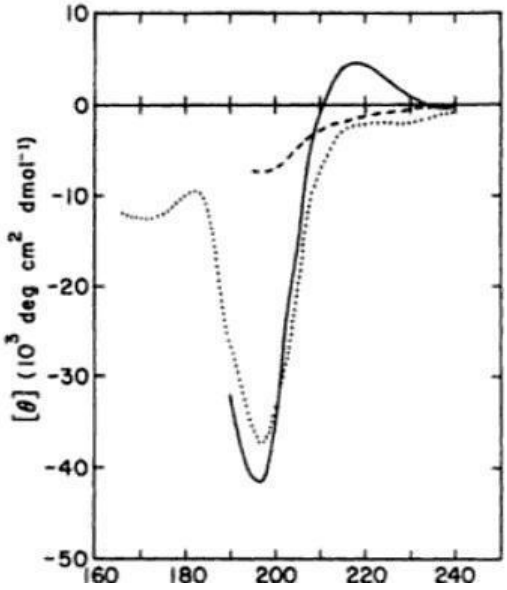

Fig. 14: CD spectrum of random coil (Woody et al., 2000).

2.4.3 The amyloidogenic peptide

Aβ 42 consists of 42 amino acids. After the onset of the oligomerization, the primary structrure of the protein is changed into the secondary structure including α-helix and β-sheets. Then, it preceeds to the fibril formation. The Aβ 42 peptide is an unstable protein influenced by pH and temperature. When Aβ 42 does not create β-sheets, the fibril formation will not take place.

Amyloidogenic peptides with charged groups can form fibrils with a net charge. In the case that the net charge is 0, β-sheets polymerize to β-sheet oligomers and then to amorphous aggregates, which remain soluble. Random coils possess the lowest net charge in all spectra and they can not form fibrils. Larger polypeptides have a higher charge balance, which complicates the creation of fibrils (Guerois et al., 2006).

2.4.4 CD Structural characterisation of proteins

The structural analysis of the secondary structure of proteins is possible because of the high sensitivity of far-UV CD for the backbone conformation.

Many methods were developed to estimate the protein‘s secondary structure from their far-UV CD spectra. The far-UV CD spectrum of a bond can be influenced by aromatic side chains, disulfide bridges and other conformations (tertially structure). It is also sensitive to its enviroment, the presence of polarity or residues as neighboured amino acids (Woody et al., 2000).

2.4.4.1 Estimation of the secondary protein structure

The protein CD spectrum can be understood as a linear combination of the components of the secondary structure spectra.

An earlier method for the estimation is to determine the helical content at a single wavelength. The simplest method is to use the CD signal at 222 nm of the fraction derived from the α-helix. Another method is the "pure component spectra". The principle of this method is the comparison of unknown far-UV CD spectrum with specrta obtained from known model compounds (Greenfield et al., 1969, Brahms et al., 1980).

A relatively novel method is based on the comparison of spectra of proteins with known X-ray structures (Johnson et al., 1981, Johnson et al., 1985, Toumadje et al., 1992).

Furthermore, computer software exist using the above described methods. The mostly used programs are SELCON 3, CDssrt, CONTIN and others.

Studies carried out by Greenfield showed that the best results were gained from a combination of SELCON and CONTIN (Woody et al., 2000).

2.4.4.2 Estimation of secondary structure in numbers

There are two methods for gaining the number of secondary structural segments.

The principle is based on a matrix descriptor analyzing the amount of β-sheet, α-helix and random coil and then estimating the number of segments in the protein. Another method is based on the estimation of the residues of α-helix and β-sheet and comparing them with the average number of residues per segment in order to determine the number of segments in the protein. This method is used by the program SELCON3 (Woody et al., 2000).

2.4.5 The use of CD-spectroscopy to follow Aβ-oligomerization

CD-spectroscopy is used to monitor the conformation of proteins (mainly β-sheet). The minimum of β-sheets of Aβ-oligomers in the CD-spectra is diesplayed at 215 and 220 nm and the maximum lies between 195 to 202 nm. The exact wavelength of the minimum or maximum depends on the sequence of the peptides and on the incubation time. Incubation of e.g. Aβ 42 with and without disintegrating substances can be used to screen for potential drugs. In general, CD-spectroscopy is a fast method for the analysis of the presence of β-sheets. (Guerais et al., 2006). During the Aβ 42-oligomerization process the amount of β-sheets will increase and this is measurable by CD-spectroscopy and comparable to appropriate blank solutions.

3 Aims of the thesis

One of the main features of AD are senile plaques in the brain. They are composed of Aβ peptides, which oligomerize and form fibrils during pathological conditions.

Inhibition of this oligomerization process is believed to be a possible therapy to prevent the progression of AD. Circular dichroism (CD) spectrometry is an optical method which enables to follow changes in the secondary structures of proteins.

The main aim of this study was to establish a CD-method which enables studies about the Aβ 42 oligomerization process. In particular, the influence of different organic solvents on the CD-spectra should be assessed. Furthermore, it should be investigated whether the addition of probably disintegrating substances as Congo Red, Meclocycline Sulfosalicylate, Thioflavin T, Curcumin and further in-house available substances can inhibit the Aβ 42 oligomerization process in a time – and concentration dependent manner.

Finally, the obtained data should be the basis for an evaluation about the applicability of the CD-method to screen for inhibitors of the Aβ 42-oligomerization process.

4 Experimental part

4.1 Chemicals and instruments:

4.1.1 Chemicals:

Amyloid beta (Aβ 42) solutions:

Aliquots of 50 µl of a 300 µM Aβ 42 solution dissolved in 0.1 % ammonia solution

Aliquots of 100 µl of a 134 µM Aβ 42 solution dissolved in 20 mM phosphate buffer, Department of Medicinal Chemistry, University of Vienna. Aβ (1-42), human (107761-42-2; P10128) Aroz Technologies LLC, Cincinnati, OH, USA

50 mM phosphate buffer prepared from:

Na_2HPO_4, Sigma-Aldrich chemie GmbH, Steinheim, Germany.

bidistilled H_2O (aqua purificata), Department of Medicinal Chemistry, University of Vienna

HCL 0,5 N, Department of Medicinal Chemistry, University of Vienna

0,1 % ammonia sol., Department of Medicinal Chemistry, University of Vienna

Thioflavin T, 88630, Fluka, Sigma-Aldrich, Steinheim, Germany

Dithiamazol (DMSO), Methanol (MeOH), Ethanol (EtOH), Acetonitril (CH_3CN), Merck KgaA, Darmstadt, Germany.

Curcumin, 28260, Fluka, Sigma-Adrich, Steinheim, Germany

Congo Red, 229620050, Acros Organics, New Jersey, USA

Meclocycline sulfosalicylate, M1388, Sigma-Aldrich, Steinheim, Germany

4.1.2 Instruments:

CD-Spectropolarimetr JASCO J 810, Biolab, Vienna, Austria

Analytical weights Sartorius, type Cp 124S/7, Göttingen, Germany

Thermomixer comfort, type Eppendorf 1,5 ml, Hamburg, Germany

pH-meter InoLab 720, WTW, Austria

Shaker Vortex-genie 2, USA

Freezer where the samples were stored at -80 °C, Laboratory and Pharmatechnic, Wien and at -20 °C.

4.2 Overview of the CD-studies

Frozen powder of synthetic Aβ 42 was dissolved as two different solutions. One Aβ 42-solution was prepared in 20 mM phosphate buffer (pH = 7,4), the second one was made in 0.1 % ammonia solution. These solutions were stored in small aliquots at -85 °C until usage.

Every time at the beginning of an experiment aliquots were thawed on ice. Ice was necessary to delay the oligomerization reaction until the start of the measurement. Then, other solutions such as phospate buffer, ammonia solution and solutions of inhibitors were prepared, also appropriate blank samples were made.

First, the effects of organic solvents on CD spectra were tested. Solutions were prepared from EtOH, MeOH and DMSO in different concentrations. The aim was to check possible influences of organic solvents on the CD-spectra without and with addition of Aβ 42. The experiments should enable to choose appropriate organic solvents for further experiments with inhibitors of the Aβ 42 oligomerization process. The lowest influence on CD spectra was in solutions with EtOH as well as with MeOH. Conversely, significant influences on CD-spectra were found with DMSO. The finally chosen concentration of Aβ 42 for further studies with inhibitors was 20 µM.

In the second part, Aβ 42-fibril disintegrating inhibitors were tested. First, the solubility of inhibitors in EtOH, MeOH and DMSO was checked. Thioflavin T was dissolved in a 20 mM NaOH-Glycin buffer, Curcumin was best soluble in DMSO, worse in EtOH and worst in MeOH. Substance H was soluble in MeOH. Congo Red and Meclocycline sulfosalicylate were dissolved in water. The used concentrations of each stock solution are mentioned later in the according experimental descriptions.

Results from previous tests were used for the experiment with Aβ 42 solutions. CD-spectra were measured of each sample after incubation for at least 0, 7, 24 and 48 h at 37 °C.

For the first experiment different concentrations of ThT were added to solutions containing Aβ 42 and phosphate buffer.

The second experiment was with Curcumin dissolved in EtOH. Different concentrations of Curcumin were prepared and added to Aβ 42 solutions to study the influence on the oligomerization process.

The third experiment was Curcumin dissolved in DMSO.

For the fourth experiment substance H was dissolved in MeOH was used. The fifth experiment was with Congo Red and Meclocycline sulfosalycilate, both substanced were dissolved in H_2O.

For the analysis CD-spectra mdeg-values were converted into molar ellipsis values by means of the special software program spectra manager was used. Molar ellipsis values are more commonly used to describe the spectra data, because these values are normalised to the corresponding concentration of the analyte (in this case Aβ 42) used. Then, time versus molar ellipsis curves were generated, the values at 0 h were set to 100 % and the slopes from 0 to 7 h, from 0 over 7 to 24 h and from 0 to 24 h at 195 nm, 220 nm and at the wavelength with the minimum value were evaluated after linear regression analysis. The comparison of the different slopes to the control samples should give an overview of the inhibiting effects of the compounds and suitability of the method.

4.3 Establishment of the CD-method

First, in order to follow the kinetics of the Aβ 42 oligomerization process with the CD spectrophotometer, samples with 2 µM Aβ 42 were tested in a 1 cm cuvette situated during the whole measurement in the CD-device at 37 °C . However, during the first 24 hours no change of the secondary protein structures was detected. Because the concentration of Aβ 42 was too low to form oligomers in this time frame, a new solution with a concentration of 20 µM Aβ 42 was measured in 1 mm cuvette. During this reaction the formation of clear β-sheet structures was detected at the minimum wavelength of around 220 nm.

Next, effects on the β-sheet formation process of the two different stock solutions of Aβ 42 dissolved in ammonia and in phosphate buffer were compared. According to the spectra shown in fig. 15. Aβ 42 dissolved in ammonia lead to a more

significant progression of the time dependent curve. The wider range of the curve was typical and the beginning of the curve started nearly in one point.

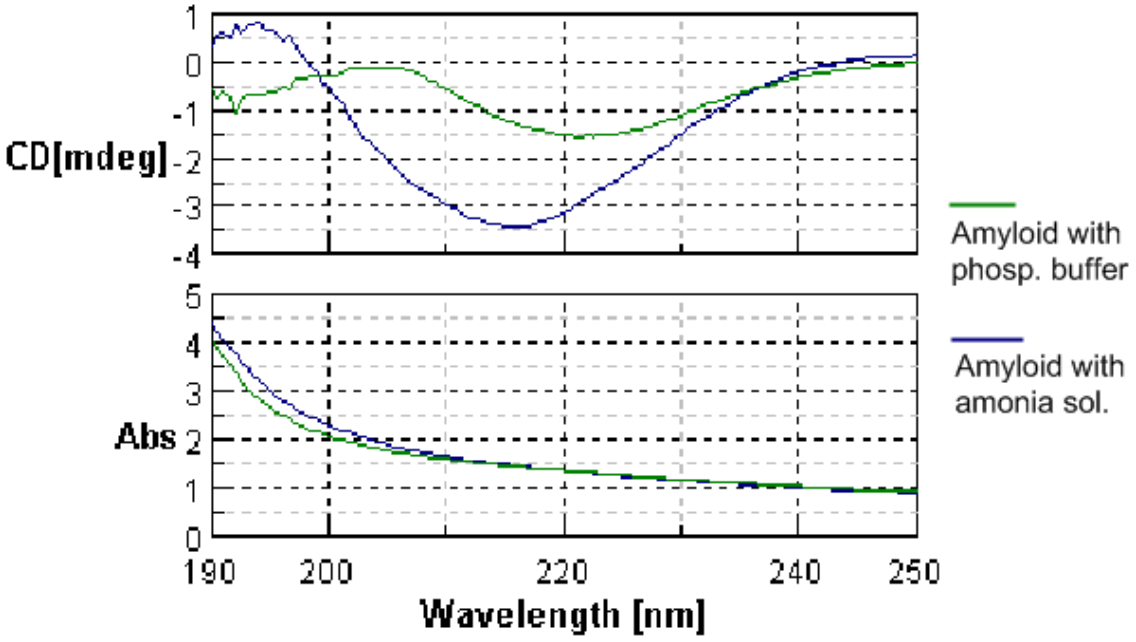

Fig. 15: CD-spectra of Aβ 42 after 8 hours incubation. Comparison of 20 µM Aβ 42 solutions obtained from stock solutions dissolved either in 20 mM phosphate buffer or in 0.1 % amonia.

The first measurement with an added possible inhibiting substance was with Thioflavin T (ThT). Firstly, no significant but expected change at 220 nm between the spectra within time were detectable. Instead in 50 mM phosphate buffer (pH = 7.4) ThT was dissolved in NaOH-Glycin buffer (pH = 8.4) in order to consider the possible role of the pH value during the oligomerization process. However, no significant change was observed.

The next suggestion was to use Aβ 42 dissolved in 20 mM phosphate buffer and to add the exact amount of 0.1 % ammonia solution in order to gain the same amount of ammonia in the sample as if Aβ 42 would have been dissolved in 0.1 % ammonia. This would unify the two advantages of a more distinct increase of the signal at 220 nm during the incubation and a lower maximum value at the beginning of the experiment.

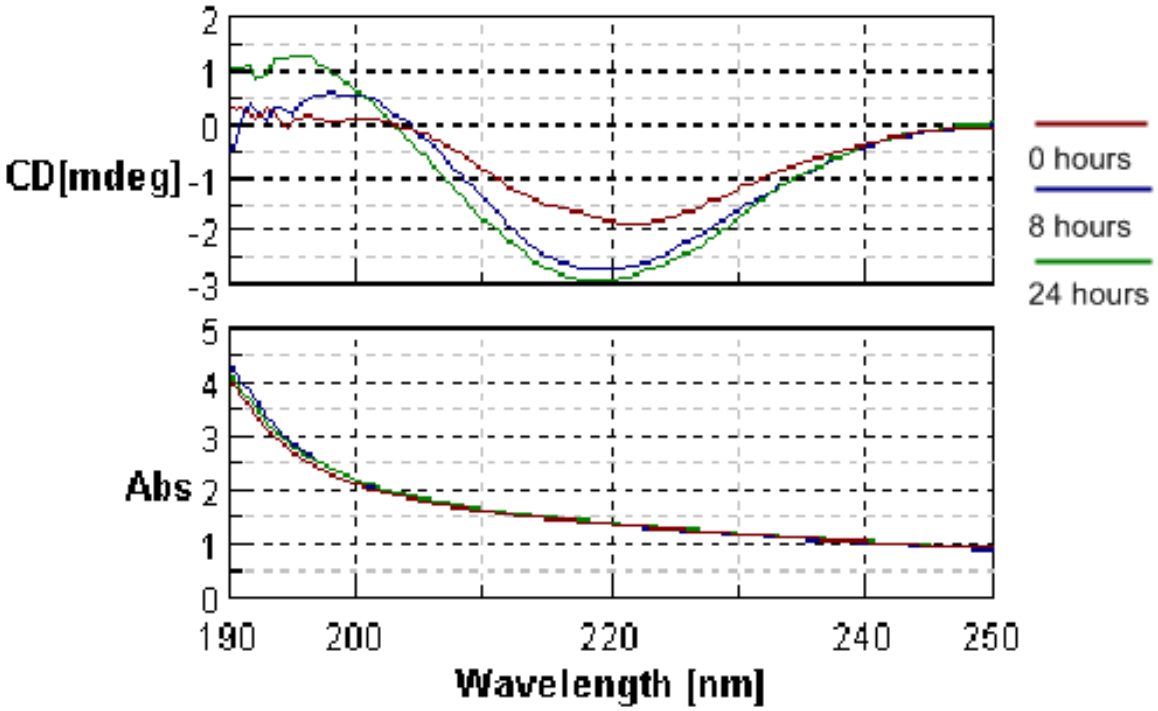

Fig. 16: Time-dependent changes of CD-spectra of 20 µM Aβ 42 dissolved in 20 mM phosphate buffer, diluted in 50 mM phosphate buffer and addition of 0.1 % NH_3.

The curves showed significant differences within time indicating that an oligomerization process of Aβ 42 took place. At 0 hour was the beginning of the reaction. Comparing to other time points as 8 and 24 hours, the progress of the reaction was examined.

4.4 Influence of several organic solvents on the CD-spectra

Another task was to find appropriate solvents for dissolving the inhibitors. The solvents should not influence the outcoming CD-spectra because of their own optical activity.

Various types of solvents (DMSO, EtOH, MeOH and CH_3CN) were analysed in various concentrations (10 %, 1 %, 0.1 %, 0.01 %, 0.001 %, 5 %, 0.5 %, 0.05 % and 0.005 %) in phosphate buffer.

According to the CD-spectra the biggest influence and thus the most optical active solvent was DMSO at a concentration of 0.1 %, 0.5 %, 1 %, and 5 %.

The other solvents did not have significant effects dependent on their concentrations on the CD-spectra. CD [mdeg] values were converted into molar ellipsis values and the resulting CD-spectra were then summarized in figures 17-22.

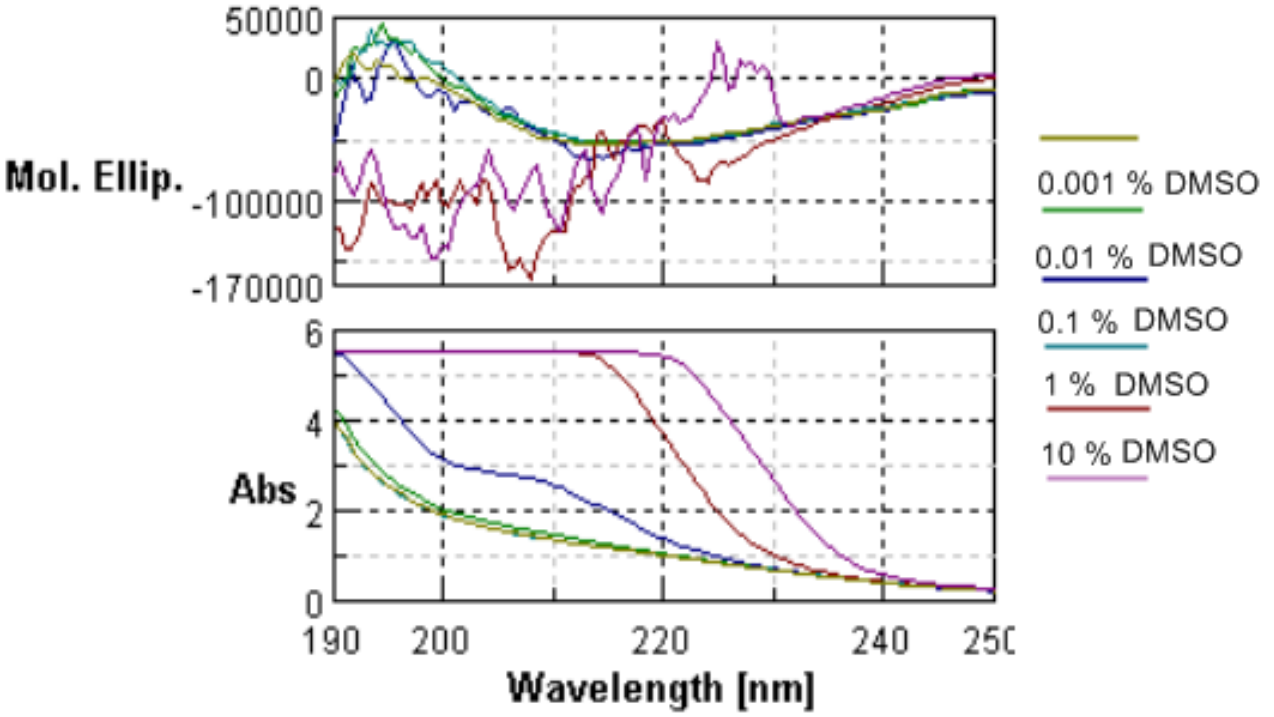

Fig. 17: Concentration dependent CD-spectra of 0.001-10 % DMSO in phosphate buffer and addition of 0.1 % NH_3 solution (dilution ratio of 1:6.7 according to solutions which contain Aβ 42).

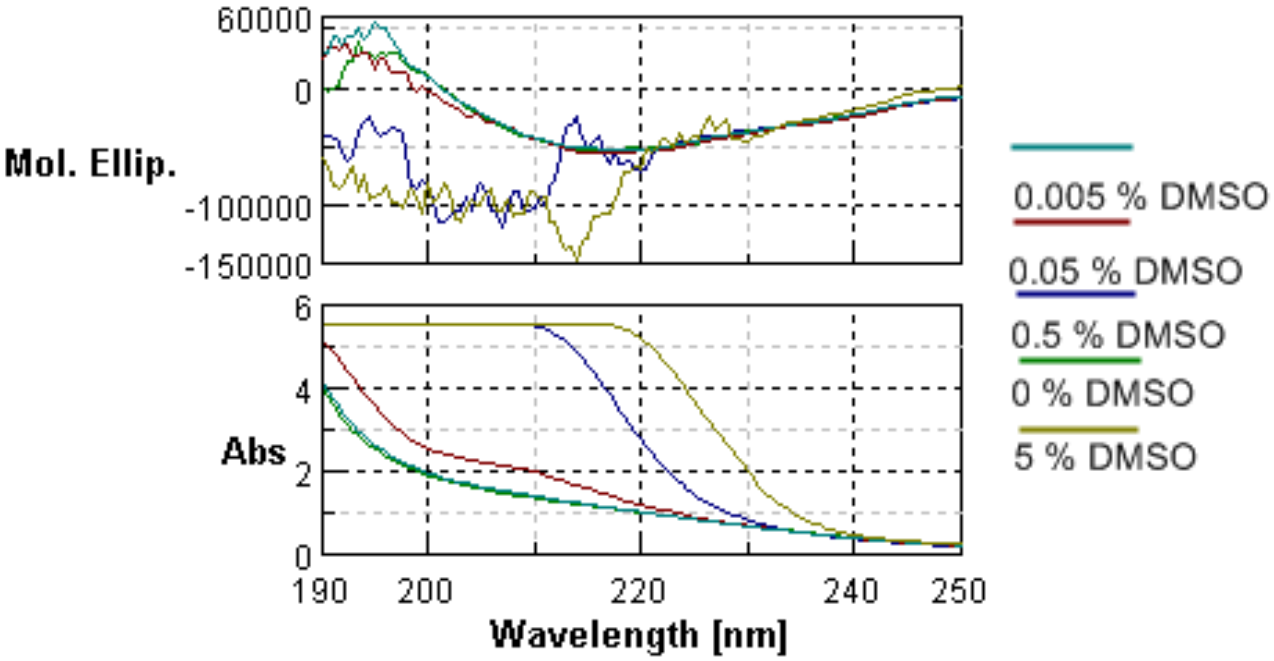

Fig. 18: Concentration dependent CD-spectra of 0.005-5 % DMSO in phosphate buffer and addition of 0.1 % NH_3 solution (dilution ratio of 1:6.7 according to solutions which contain Aβ 42).

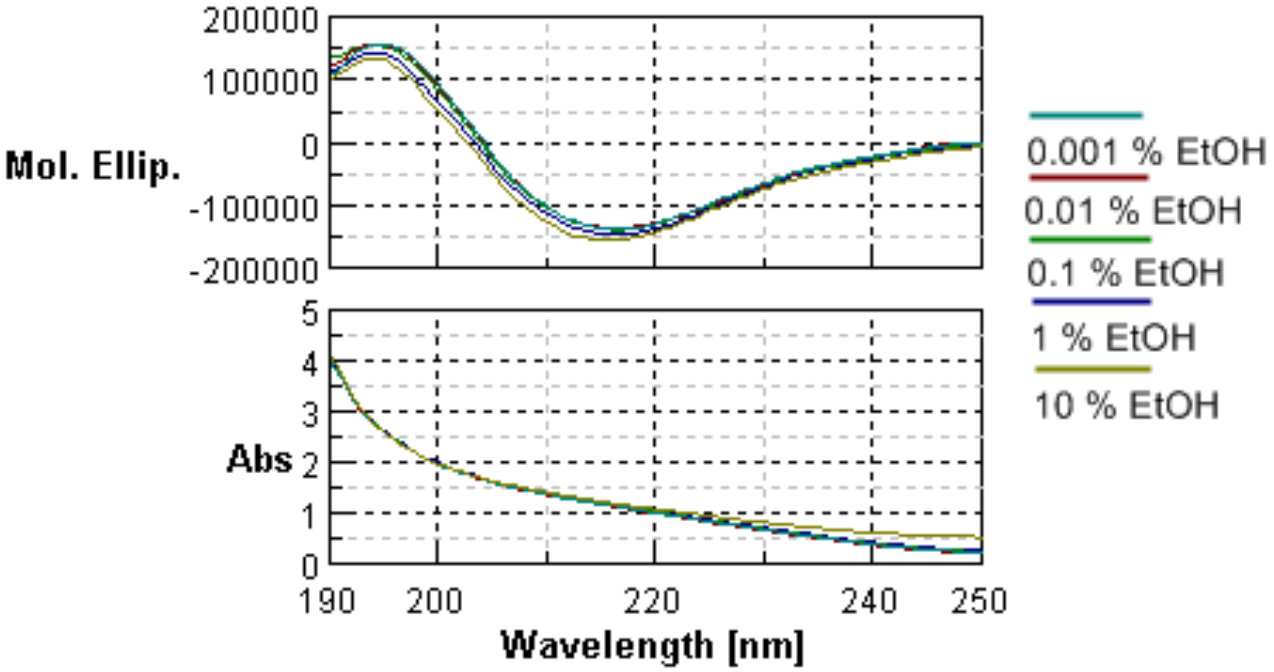

Fig. 19: Concentration dependent CD-spectra of 0.001-10 % EtOH in phosphate buffer and addition of 0.1 % NH_3 solution (dilution ratio of 1:6.7 according to solutions which contain Aβ 42).

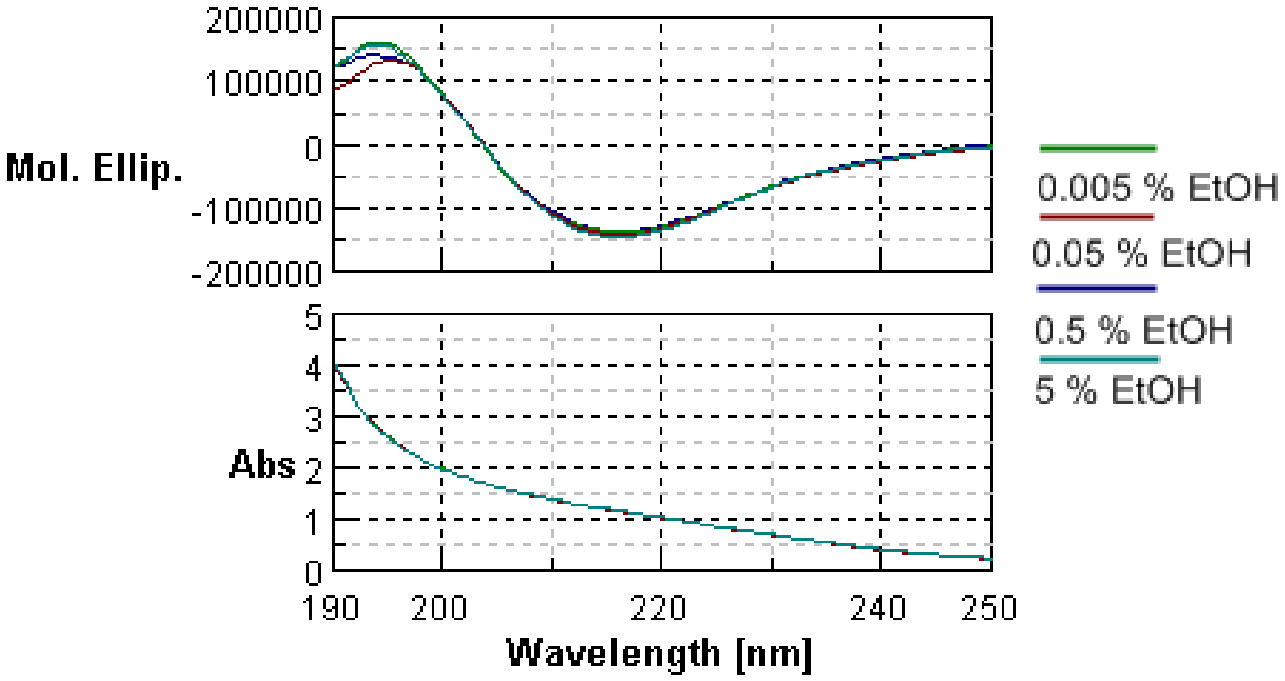

Fig. 20: Concentration dependent CD-spectra of 0.005-5 % EtOH in phosphate buffer and addition of 0.1 % NH_3 solution (dilution ratio of 1:6.7 according to solutions which contain Aβ 42).

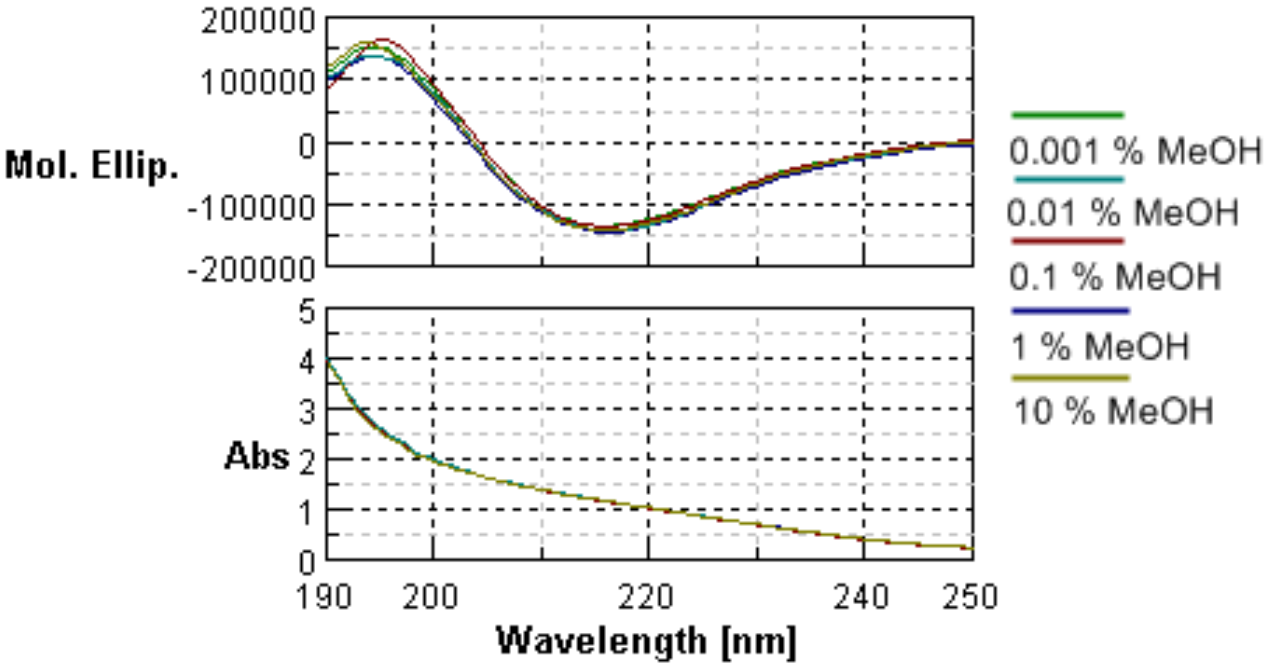

Fig. 21: Concentration dependent CD-spectra of 0.001-10 % MeOH in phosphate buffer and addition of 0.1 % NH_3 solution (dilution ratio of 1:6.7 according to solutions which contain Aβ 42).

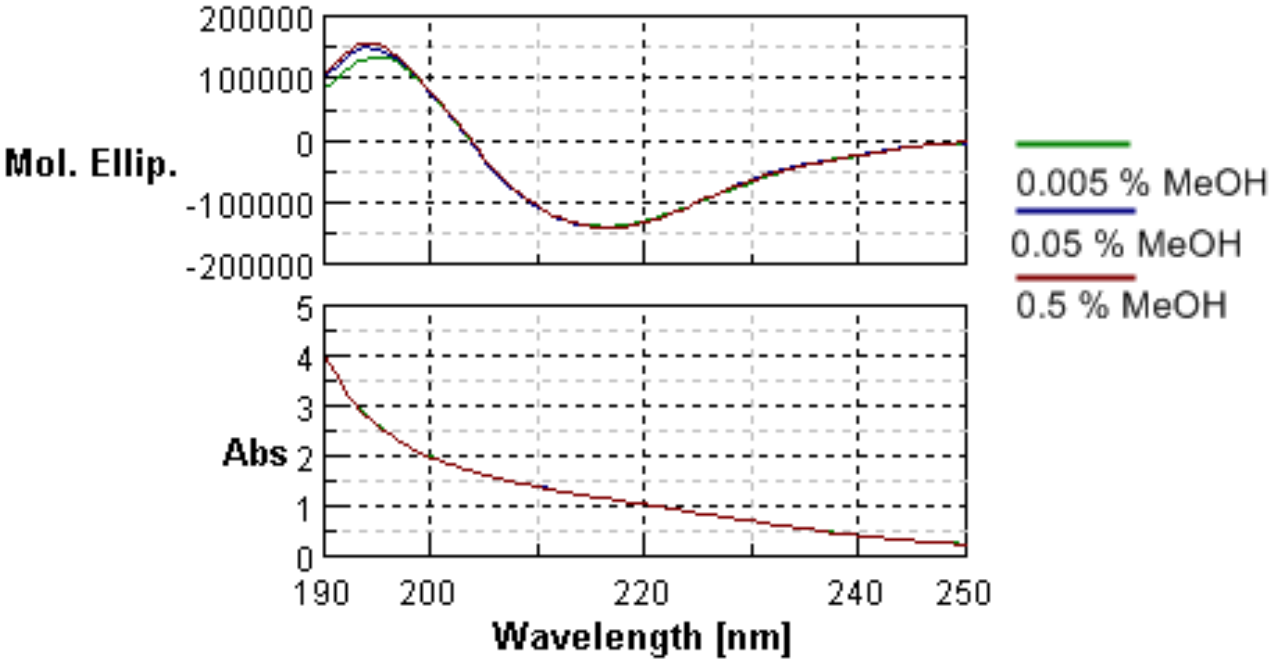

Fig. 22: Concentration dependent CD-spectra of 0.005-0.5 % MeOH in phosphate buffer and addition of 0.1 % NH_3 solution (dilution ratio of 1:6.7 according to solutions which contain Aβ 42).

For future measurements DMSO, EtOH and MeOH were used as solvents. If DMSO was used then only in lower concentrations and in order to assess the difference

using DMSO and EtOH, because the usage of DMSO could sometimes be indispensible since DMSO has to be used for some compounds with very low solubility. CH_3CN showed similar spectra as EtOH and MeOH (data not shown). So, it may be used as additional organic solvent.

4.5 Influence of inhibitors on the CD-spectra without amyloid

Next to the evaluation of the influence of organic solvents, the possible impact of the inhibitors due to their optical properties on the CD-spectra were assessed. CD-spectra of Curcumin were recorded without addition of Aβ 42. First, the solubility of Curcumin was checked.1 mg/mL of Curcumin was not soluble in 50 mM phosphate buffer. Then, the solubility of Curcumin in organic solvents DMSO, EtOH, MeOH and CH_3CN was checked. 0.0368 g Curcumin was dissolved in 10 ml of DMSO, EtOH, MeOH and CH_3CN, which corresponds to a 10 mM stock solution.

For each of these solvents different concentrations of Curcumin solutions were prepared (Table 1). Then, samples were measured at 37 °C and CD-spectra were recorded at several time points.

Different concentration of solvents:		End concentrations in sample:	
Curcumin	EtOH, MeOH, CH_3CN,DMSO	Curcumin	EtOH, MeOH, CH_3CN, DMSO
10mM	100 %	1 mM	10 %
1mM	10 %	100 µM	1 %
0.1mM	1 %	10 µM	0.1 %
0.01mM	0.1 %	1 µM	0.01 %
0.001mM	0.01 %	0,1 µM	0.001 %
5mM	50 %	500 µM	5 %
0.5mM	5 %	50 µM	0.5 %
0.05mM	0.5 %	5 µM	0.05 %
0.005mM	0.05 %	0.5 µM	0.005 %

Tab. 1: Concentrations of Curcumin solutions used tested by CD-spectrometry.

The following solutions of different concentrations were prepared from the basic solution (10 mM Curcumin in 100 %) in a ratio of 1:10.

100 µl of 10 mM Curcumin in 100 % solvent was pipetted and 900 µl of 50 mM phosphate buffer were added in order to obtain a 1 mM Curcumin solution containing only 10 % of the organic solvent.

Then, also a 5 mM Curcumin solution with 50 % of the solvent was prepared by 500 µl of 10 mM Curcumin was mixed with 500 µl of 50 mM phosphate buffer. The other solutions were prepared by 1:10 solutions in phosphate buffer. This was done in order to compare these solutions to the solutions with only the solvents.

The measured samples inside the cuvette consisted then of a total volume of 167.5 µl (139.25 µl of phosphate buffer, 11.5 µl of 0.1 % ammonia, 16.75 µl of Curcumin of different concentrations).

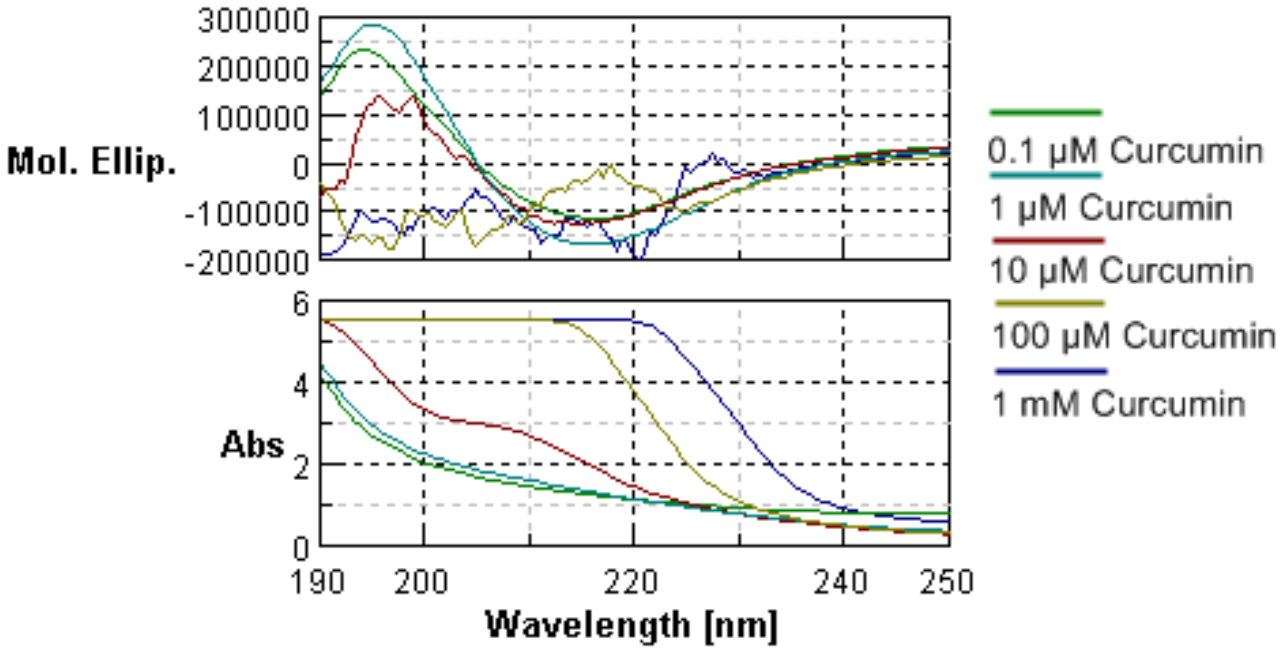

Fig. 23: Concentration dependent CD-spectra of 0.1 µM-1 mM Curcumin in DMSO in phosphate buffer and addition of 0.1 % NH_3 solution (dilution ratio of 1:6.7 according to solutions which contain Aβ 42).

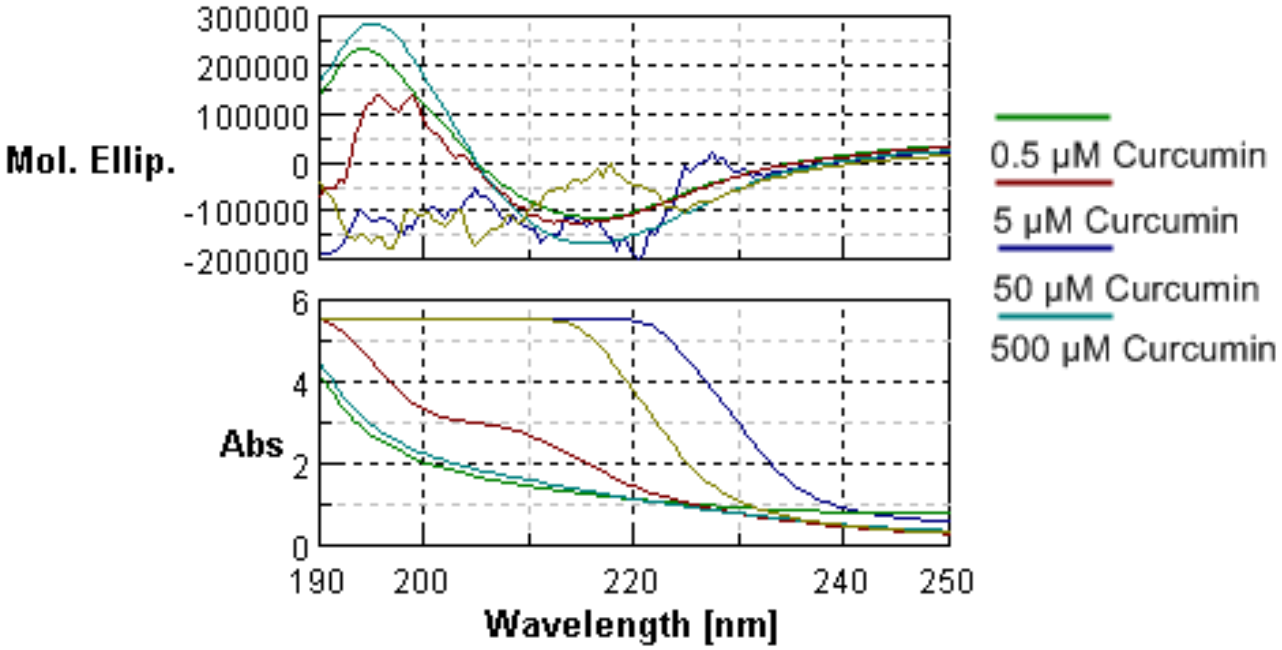

Fig. 24: Concentration dependent CD-spectra of 0.5 µM-500 µM Curcumin in DMSO in phosphate buffer and addition of 0.1 % NH_3 solution (dilution ratio of 1:6.7 according to solutions which contain Aβ 42).

The effect of Curcumin dissolved in DMSO was influenced by optical activity of DMSO. Thus, DMSO should only be used in low concentrations (max. 0.1%).

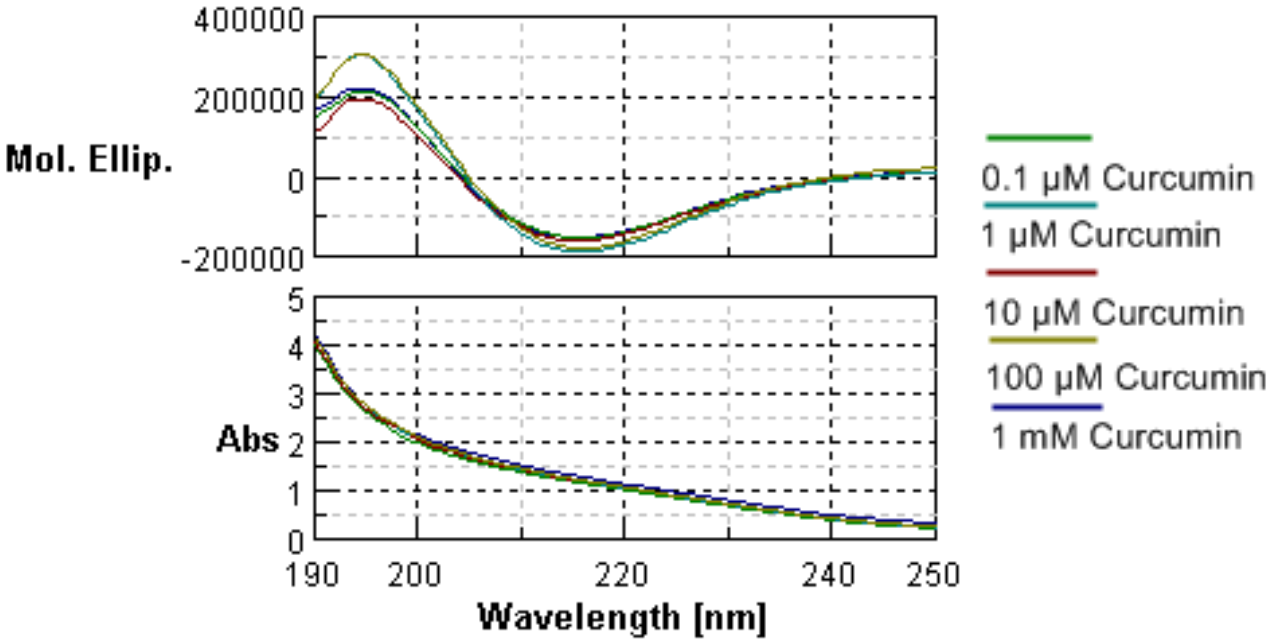

Fig. 25: Concentration dependent CD-spectra of 0.1 µM-1 mM Curcumin in EtOH in phosphate buffer and addition of 0.1 % NH_3 solution (dilution ratio of 1:6.7 according to solutions which contain Aβ 42).

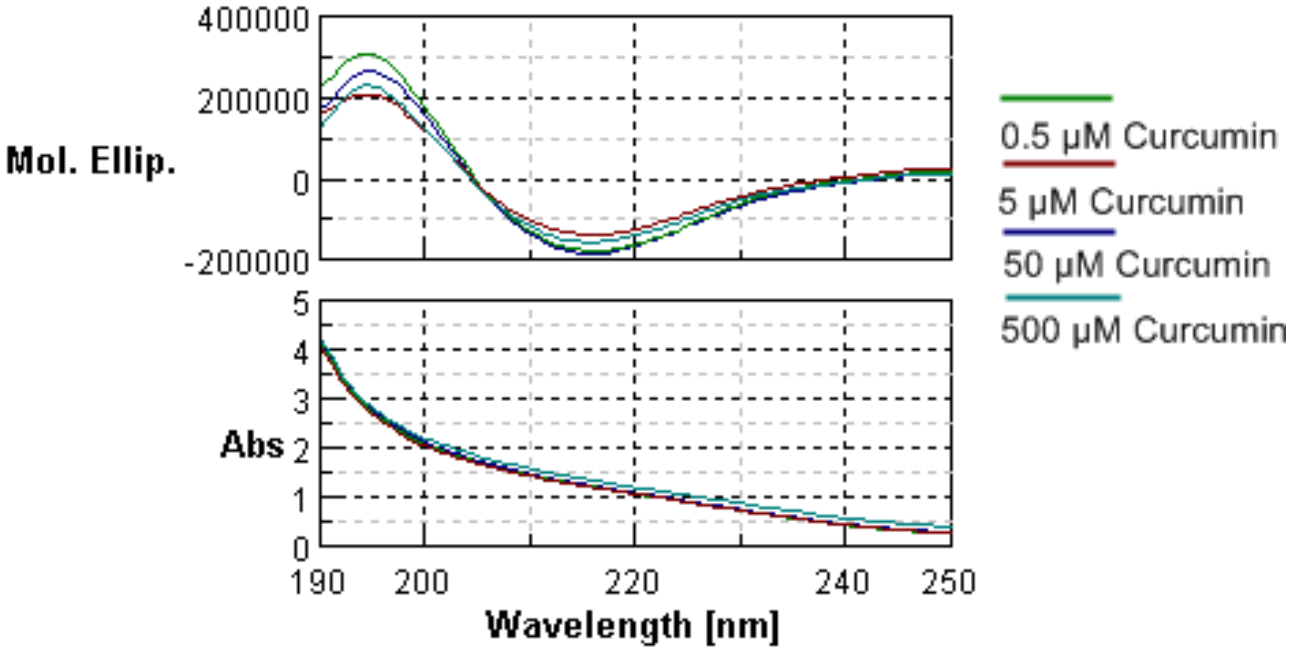

Fig. 26: Concentration dependent CD-spectra of 0.5 µM-500 µM Curcumin in EtOH in phosphate buffer and addition of 0.1 % NH_3 solution (dilution ratio of 1:6.7 according to solutions which contain Aβ 42).

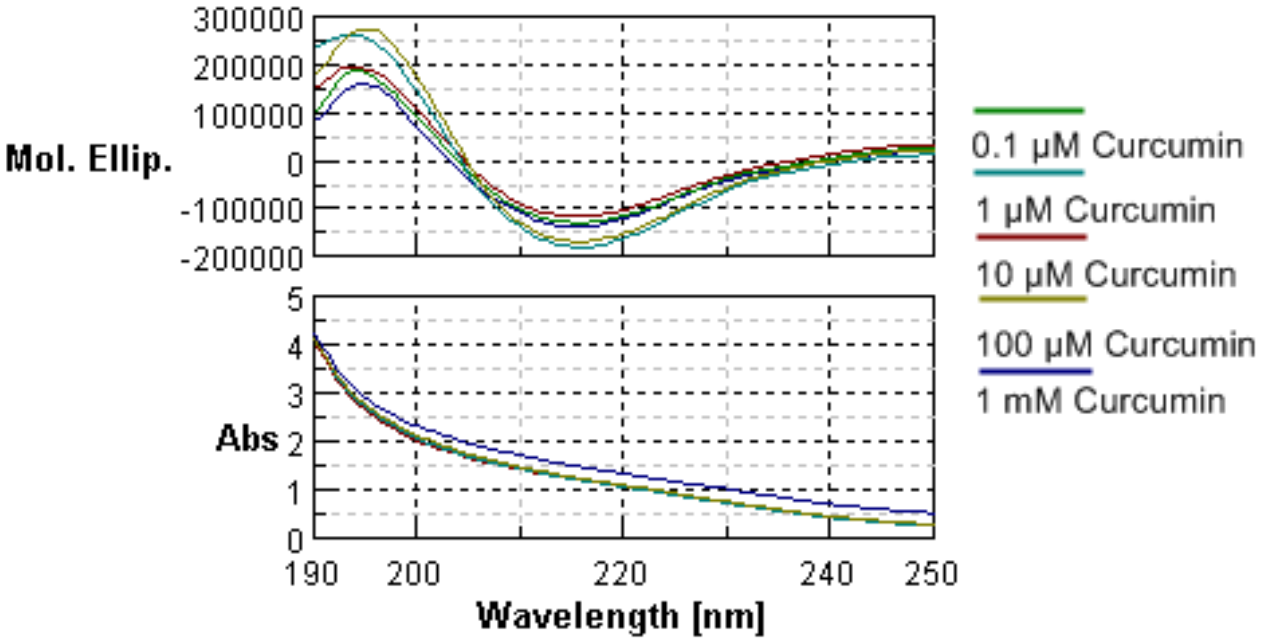

Fig. 27: Concentration dependent CD-spectra of 0.1 µM-1 mM Curcumin in MeOH in phosphate buffer and addition of 0.1 % NH_3 solution (dilution ratio of 1:6.7 according to solutions which contain Aβ 42).

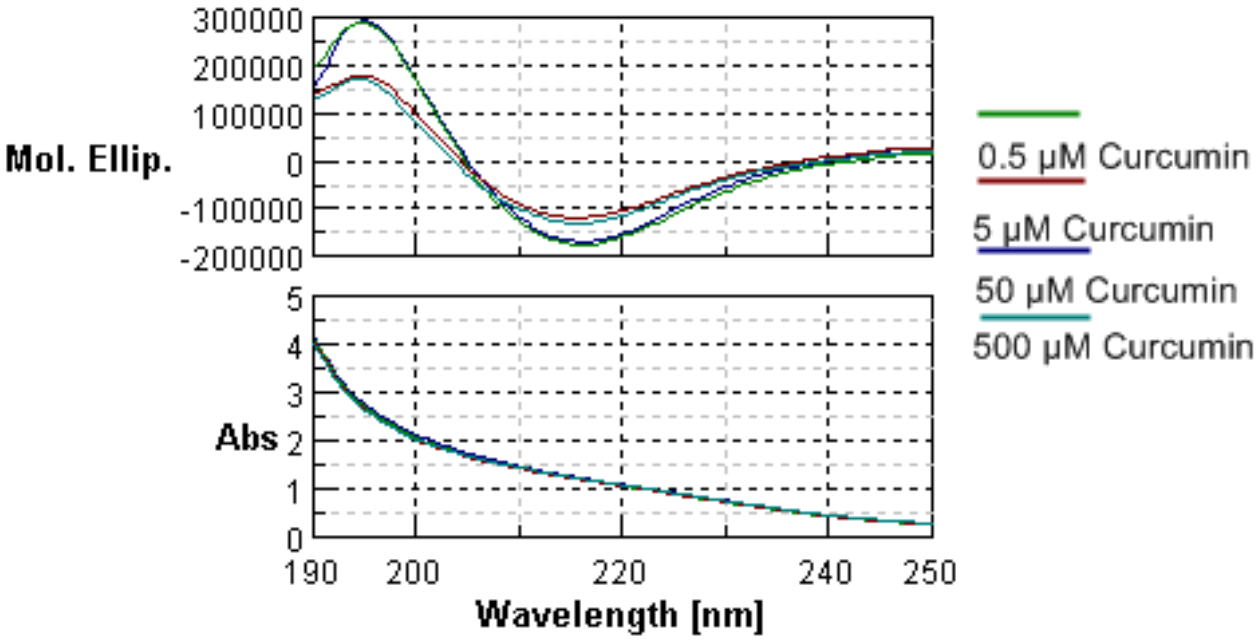

Fig. 28: Concentration dependent CD-spectra of 0.5 µM-500 µM Curcumin in MeOH in phosphate buffer and addition of 0.1 % NH_3 solution (dilution ratio of 1:6.7 according to solutions which contain Aβ 42).

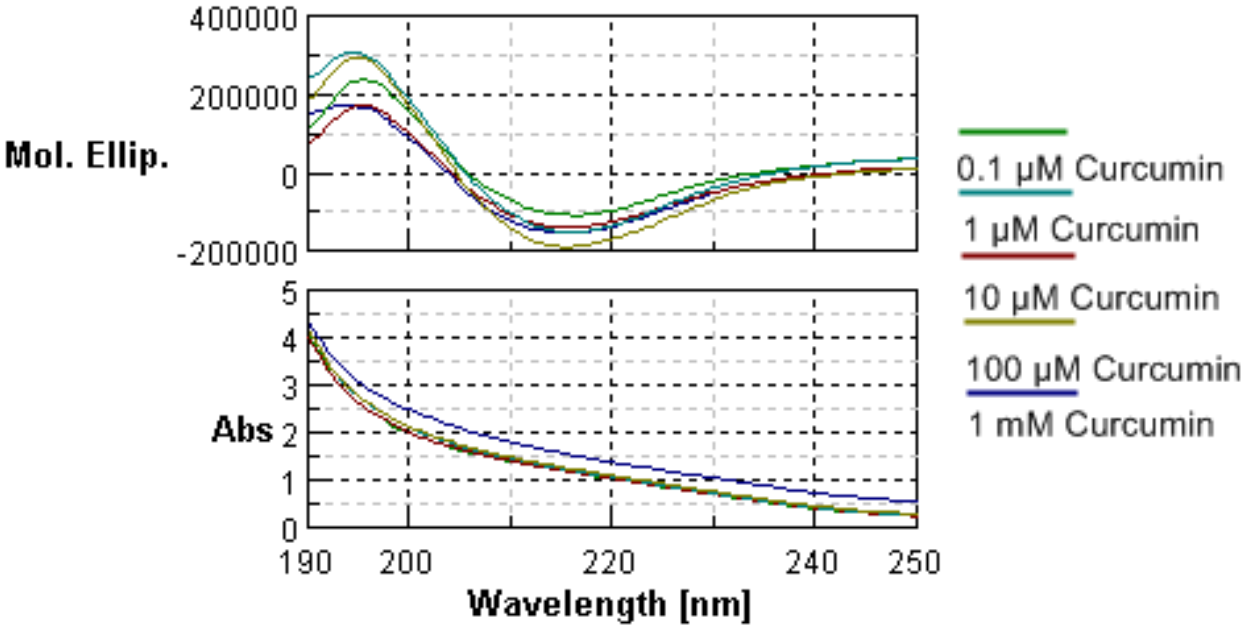

Fig. 29: Concentration dependent CD-spectra of 0.1 µM-1 mM Curcumin in Acetonitril in phosphate buffer and addition of 0.1 % NH_3 solution (dilution ratio of 1:6.7 according to solutions which contain Aβ 42).

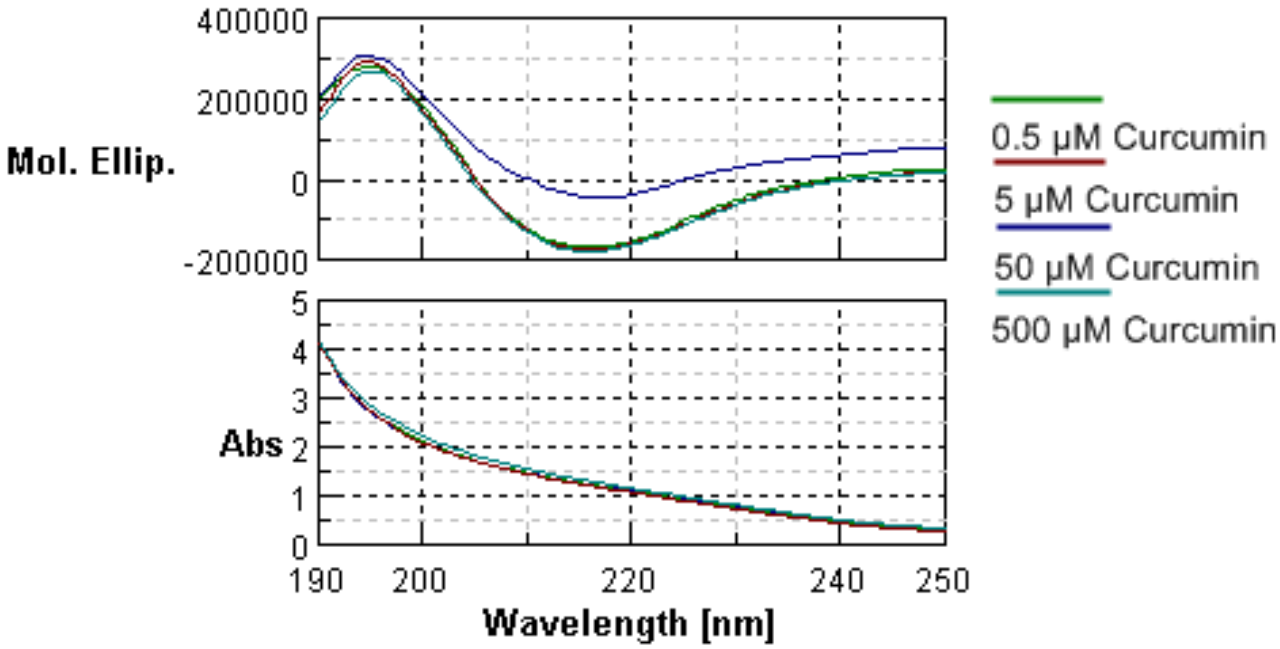

Fig. 30: Concentration dependent CD-spectra of 0.5 µM-500 µM Curcumin in Acetonitril in phosphate buffer and addition of 0.1 % NH_3 solution (dilution ratio of 1:6.7 according to solutions which contain Aβ 42).

Curcumin dissolved in EtOH and MeOH showed slightly more concentration dependent CD-spectra than these solvents alone. Thus, an additional effect caused by the presence of Curcumin can not be excluded. Curcumin dissolved in CH_3CN showed similar effects as in EtOH and MeOH.

A possible concentration dependent influence of substance H, Congo Red and Meclocycline Sulfosalicylate dissolved in the appropriate solvents on the CD-spectrum were also assessed (table 2, figures 31-36).

Different concentration of solvents:		End concentrations in sample:	
Substance H, Congo Red, Meclocycline Sulfosalycilate	MeOH, H_2O	Substance H, Congo Red, Meclocycline Sulfosalycilate	MeOH, H_2O
1mM	100%	1mM	10%
100 µM	10%	100 µM	1%
10 µM	1%	10 µM	0.1%
1 µM	0.1%	1 µM	0.01%
0.1 µM	0.01%	0.1 µM	0.001%
500 µM	50%	500 µM	5%
50 µM	5%	50 µM	0.5%
5 µM	0.5%	5 µM	0.05%
0.5 µM	0.05%	0.5 µM	0.005%

Tab. 2: Concentrations of substance H, Congo Red, Meclocycline Sulfosalicylate in solutions used tested by CD-spectrometry.

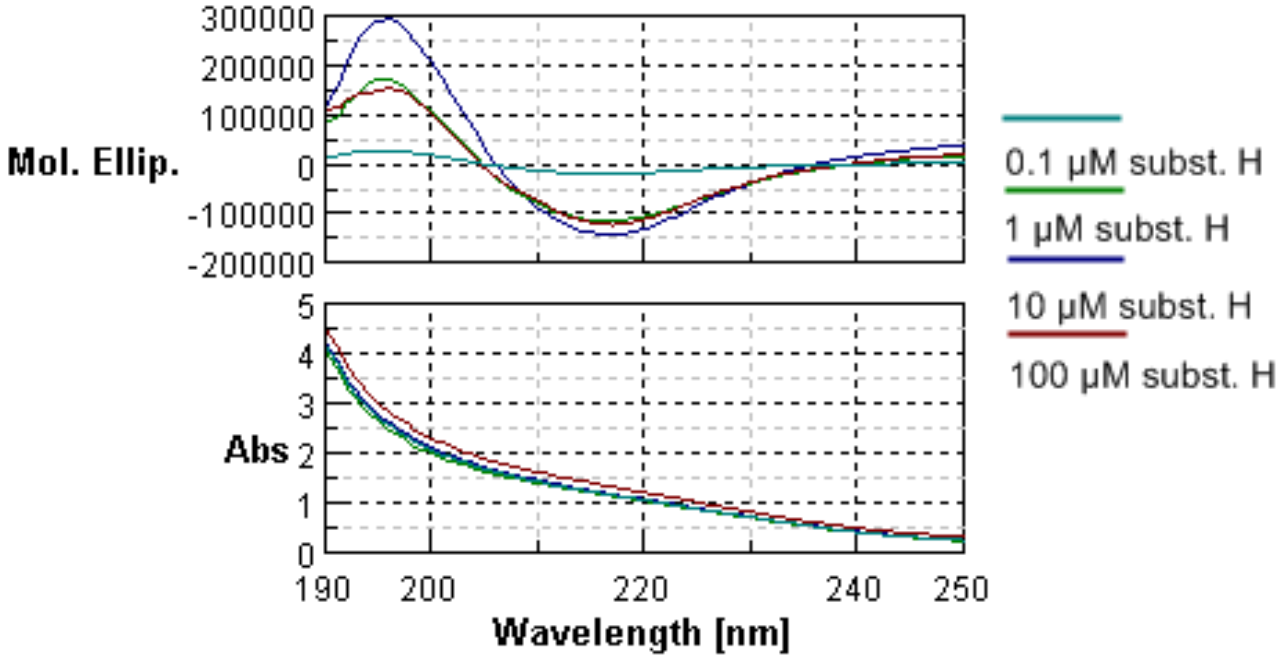

Fig. 31: Concentration dependent CD-spectra of 0.1 µM-100 µM substance H in MeOH in phosphate buffer and addition of 0.1 % NH_3 solution (dilution ratio of 1:6.7 according to solutions which contain Aβ 42).

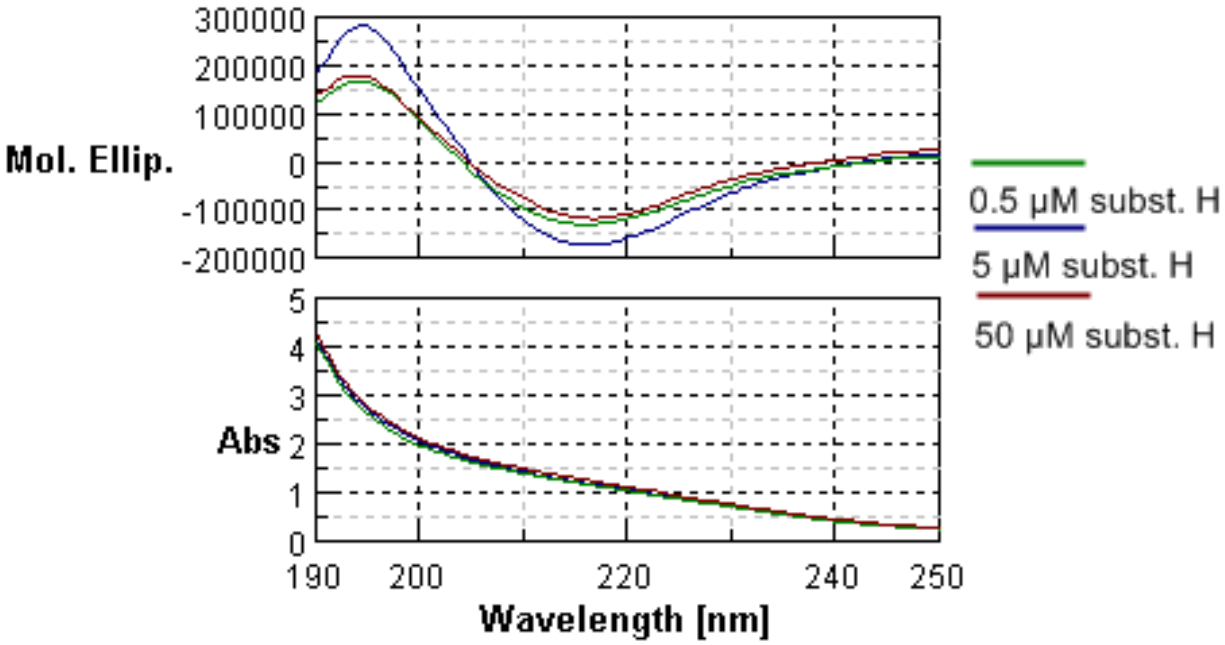

Fig. 32: Concentration dependent CD-spectra of 0.5 µM-50 µM substance H in MeOH in phosphate buffer and addition of 0.1 % NH_3 solution (dilution ratio of 1:6.7 according to solutions which contain Aβ 42).

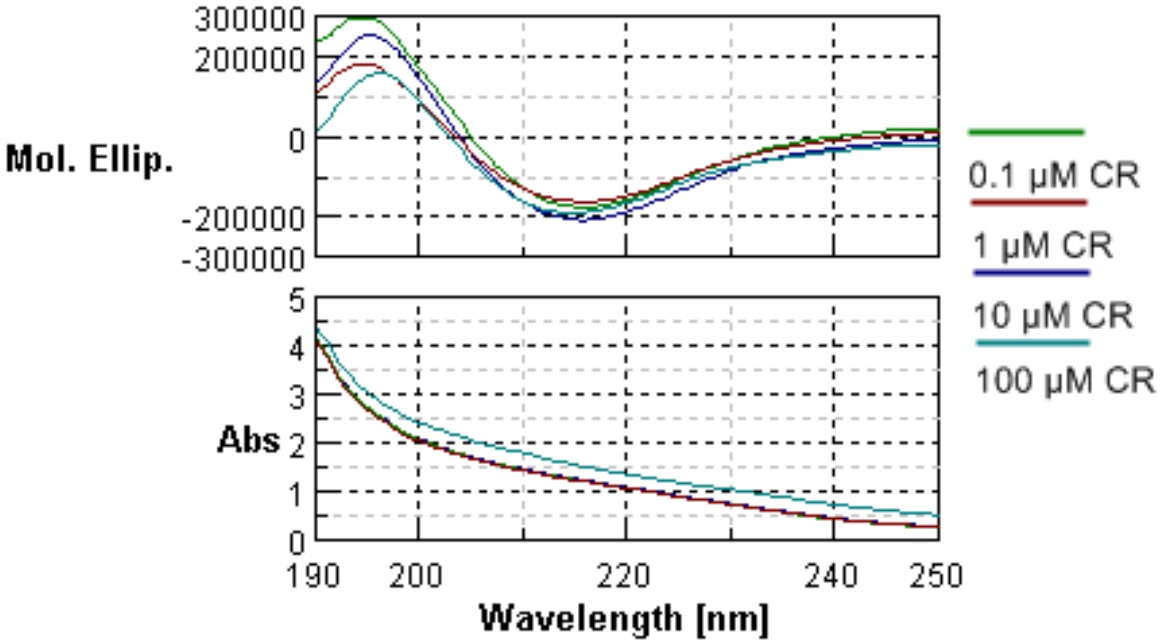

Fig. 33: Concentration dependent CD-spectra of 0.1 µM-100 µM Congo Red (CR) in water and addition of 0.1 % NH_3 solution (dilution ratio of 1:6.7 according to solutions which contain Aβ 42).

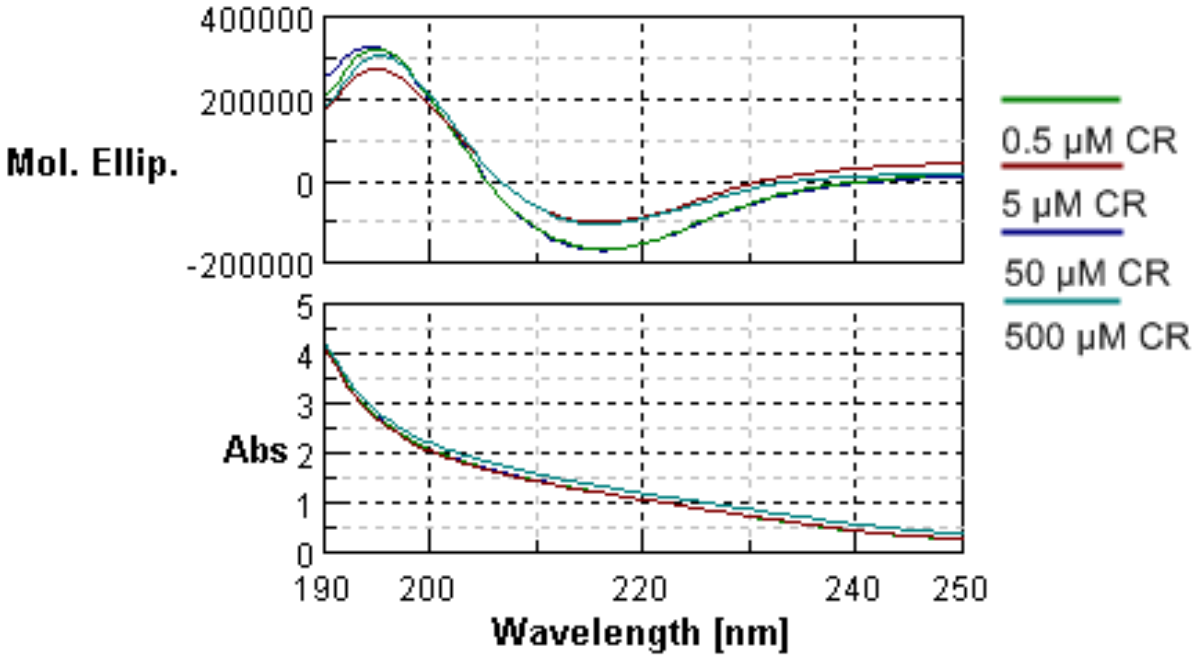

Fig. 34: Concentration dependent CD-spectra of 0.5 µM-500 µM Congo red in water and addition of 0.1 % NH_3 solution (dilution ratio of 1:6.7 according to solutions which contain Aβ 42).

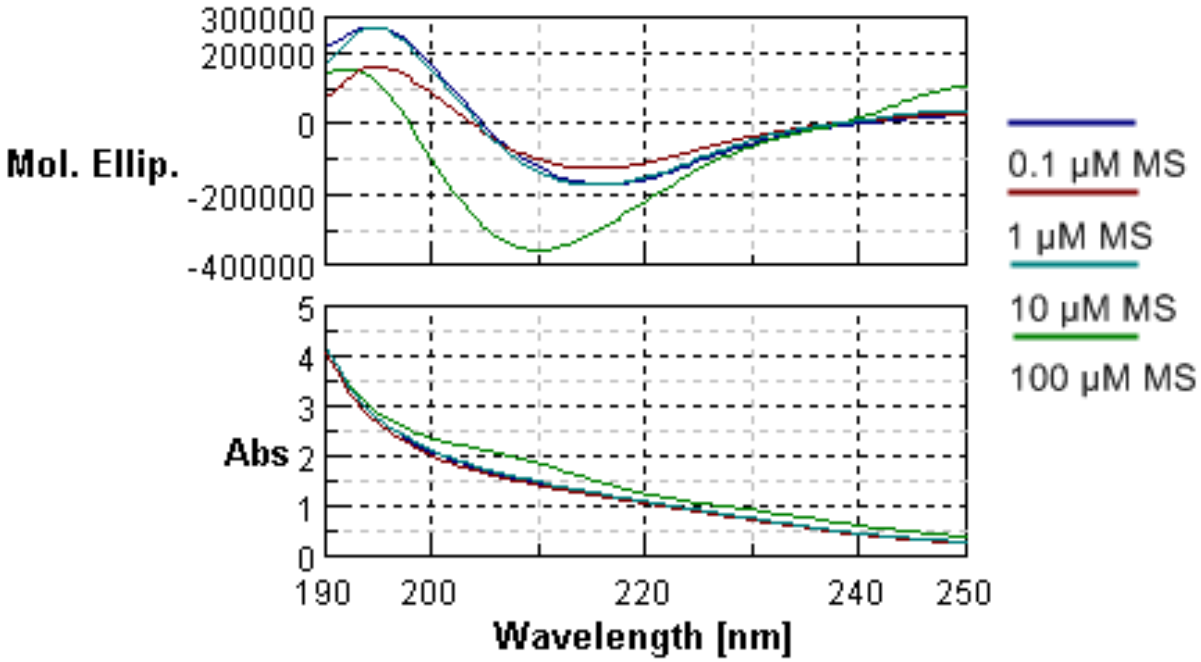

Fig. 35: Concentration dependent CD-spectra of 0.1 µM-100 µM Meclocycline Sulfosalicylate (MS) in water and addition of 0.1 % NH_3 solution (dilution ratio of 1:6.7 according to solutions which contain Aβ 42).

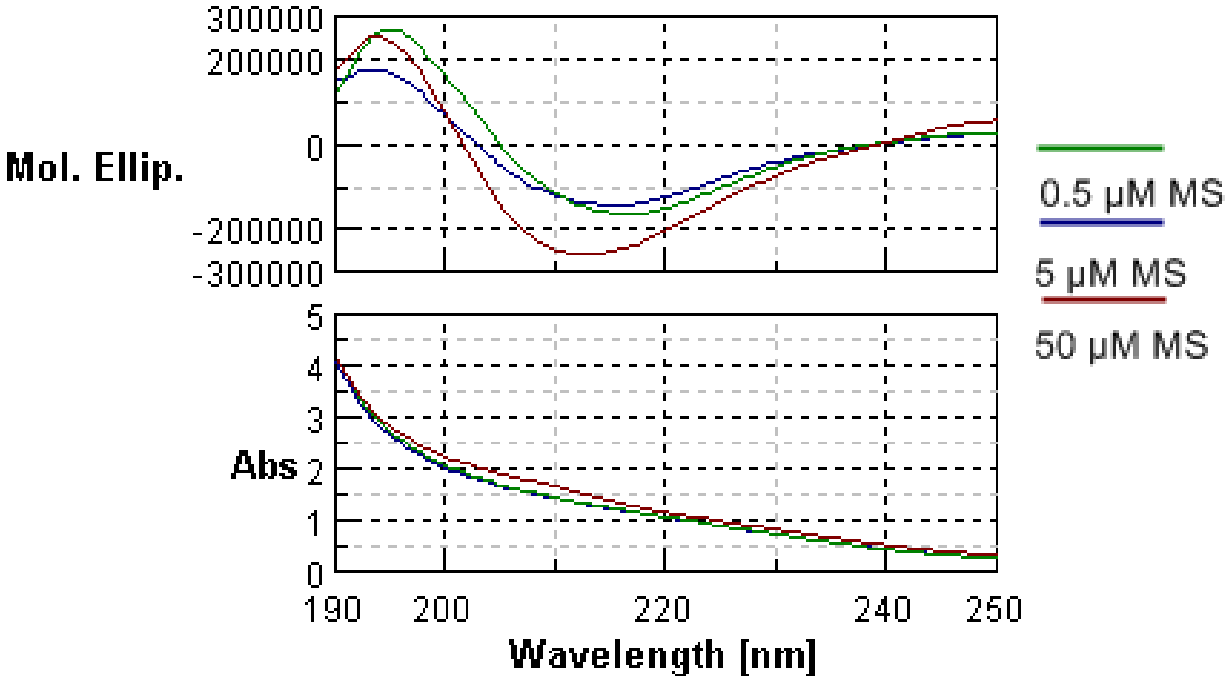

Fig. 36: Concentration dependent CD-spectra of 0.5 µM-50µM Meclocycline Sulfosalicylate in water and addition of 0.1 % NH_3 solution (dilution ratio of 1:6.7 according to solutions which contain Aβ 42).

All three substances seemed to influence the CD-spectra in concentration dependent manner. Thus, appropriate blank values of the corresponding solvent are indispensible for the following oligomerization experiments with Aβ 42.

4.6 Effects of inhibitors on the Aβ-oligomerization process

Following experiments with Curcumin, substance H, Congo Red and Meclocycline Sulfosalicylate and the according control values with the organic solvents were summarized in tab. 3.

Table of researched samples		
Sample		Concentration
Amyloid (50 µl of 300 µM) + 50 mM phosp. Buffer	Thioflavin T	0 %
		100 µM
		10 µM
		1 µM
		0.1 µM
Amyloid (100 µl of 134 µM) + 0.1 % ammonia sol. + 50 mM phosp. Buffer	Thioflavin T	0 %
		100 µM
		10 µM
		1 µM
		0.1 µM
Amyloid (100 µl of 134 µM) + 0.1 % ammonia sol. + 50 mM phosp. Buffer	DMSO	0 %
		0.1 %
		0.01 %
	Curcumin in DMSO	100 µM in 0.1 %
		10 µM in 0.01 %
		1 µM in 0.01 %
		0.1 µM in 0.01 %
	EtOH	0 %
		1 %
		0.1 %
		0.01 %
		0.001 %
	Curcumin in EtOH	100 µM in 1 %
		10 µM in 0.1 %
		1 µM in 0.01 %
		0.1 µM in 0.001 %

Table of researched samples		
Sample		Concentration
Amyloid (50 µl of 300 µM) + 50 mM phosp. Buffer	MeOH	0 %
		5 %
		0.5 %
		0.05 %
		0.005 %
	substance H in MeOH	100 µM in 5 %
		10 µM in 0.5 %
		1 µM in 0.05 %
		0.1 µM in 0.005 %
Amyloid (50 µl of 300 µM) + 50 mM phosp. Buffer	Congo Red in H_2O	100 µM
		10 µM
		1µ M
		0,1 µM
	Meclocycline Sulfosalicylate in H_2O	100 µM
		10 µM
		1 µM
		0.1 µM

Tab. 3: Summary of the inhibitor experiments with Aβ 42.

Samples with 20 µM Aβ 42 from the phosphate buffer (100 µl of 134 µM) stock solution and added 0.1 % ammonia solution or from amyloid stock solution in ammonia solution (50 µl of 300 µM) were diluted in 50 mM phosphate buffer (with or without inhibitors and organic solvants) and were measured. The measurement was carried out each time point (0, 8, 24, 72 and 96 hours) after incubation at 37 °C. The first experiment was with Thioflavin T. The control sample (without ThT) was compared to samples which contained different concentrations of ThT (100 µM, 10 µM, 1 µM, 0.1 µM.). In order to show the raw data CD-spectra [mdeg] were displayed for this experiment, whereas converted molar ellipsis spectra will be shown for all further studies. Molar ellipsis spectra are normally used to present the data normalised to the different concentrations of optical active substances. In our case, almost everytime 20 µM of Aβ 42 were used. Thus, same results should be obtained from CD values [mdeg] and molar ellipsis spectra values.

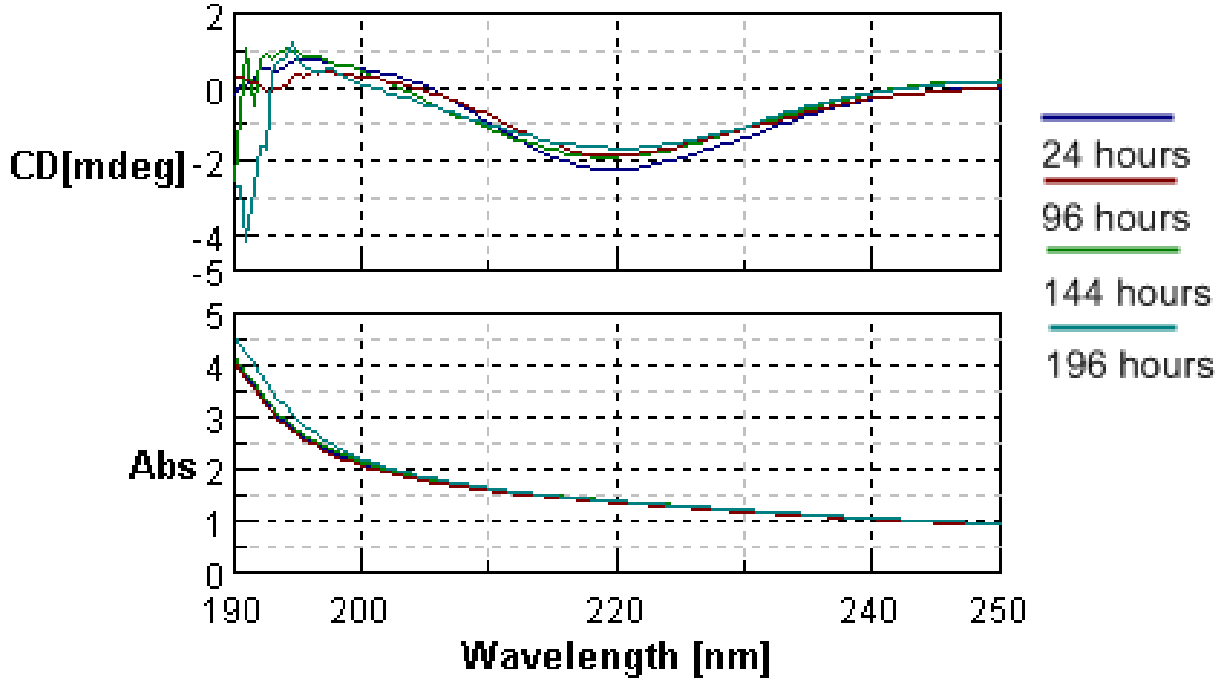

Fig. 23: Time dependent CD-spectra of 20 µM Aβ 42 from 20 mM phosphate buffer stock solution diluted with 50 mM phosphate buffer.

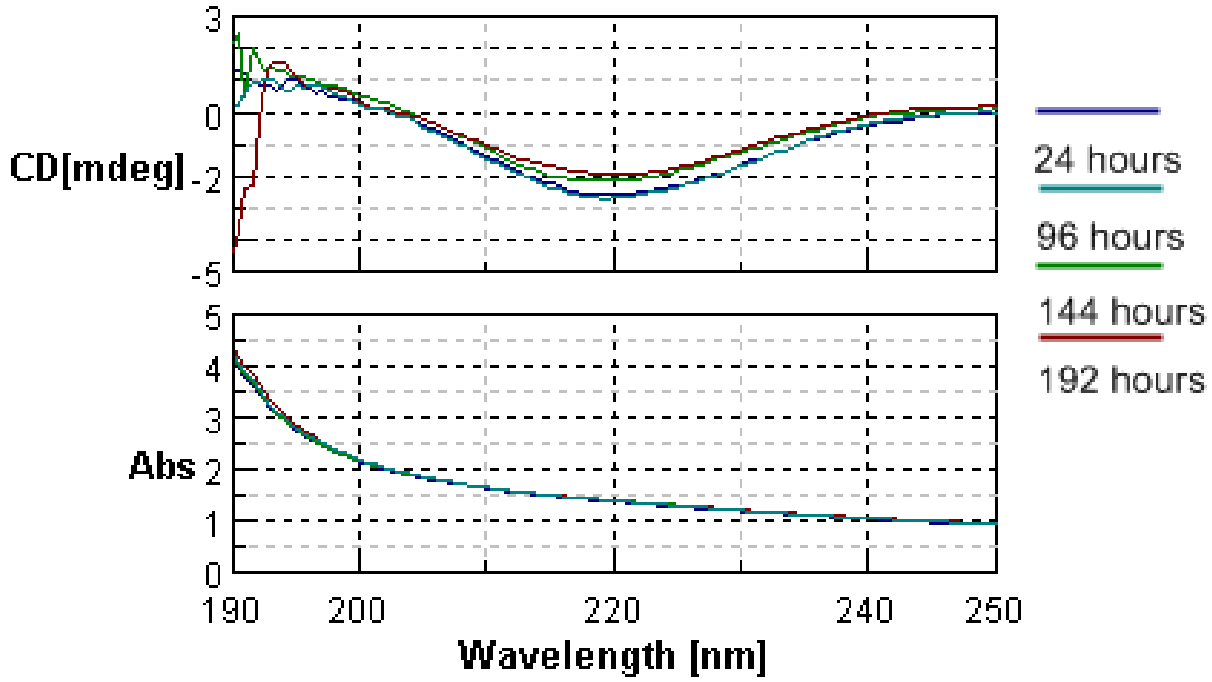

Fig. 24: Time dependent CD-spectra of 20 µM Aβ 42 from 20 mM phosphate buffer stock solution diluted with 50 mM phosphate buffer plus 1 µM ThT.

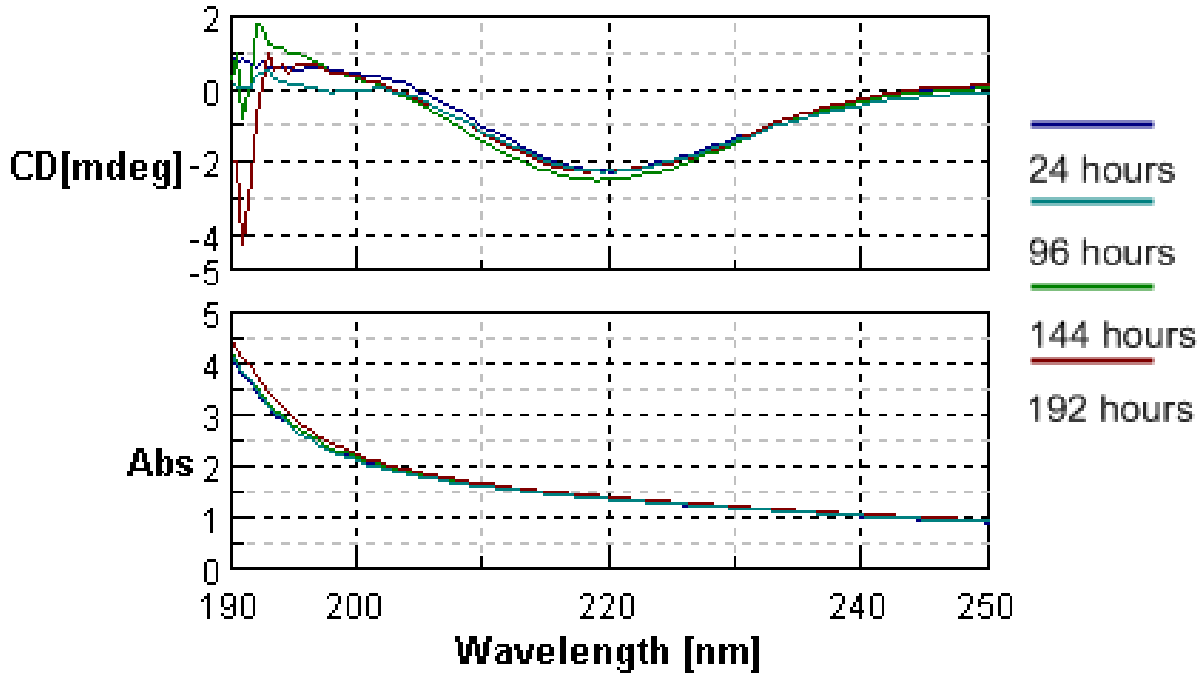

Fig. 25: Time dependent CD-spectra of 20 µM Aβ 42 from 20 mM phosphate buffer stock solution diluted with 50 mM phosphate buffer plus 10 µM ThT.

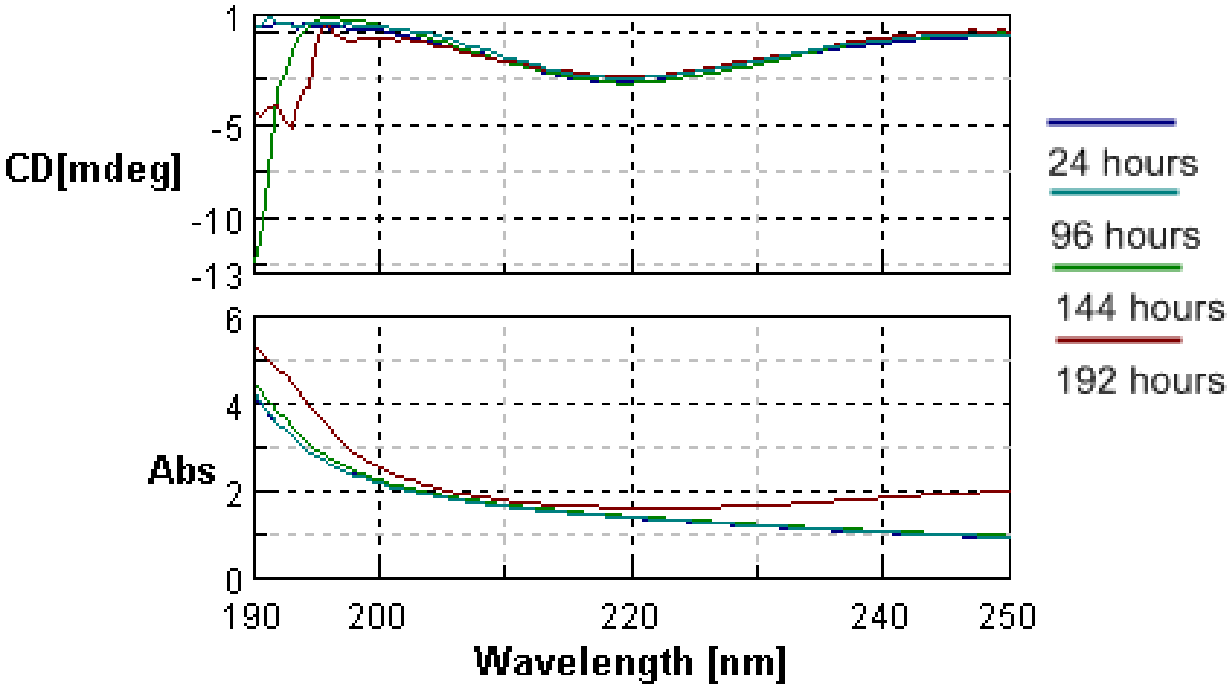

Fig. 26: Time dependent CD-spectra of 20 µM Aβ 42 from 20 mM phosphate buffer stock solution diluted with 50 mM phosphate buffer plus 100 µM ThT.

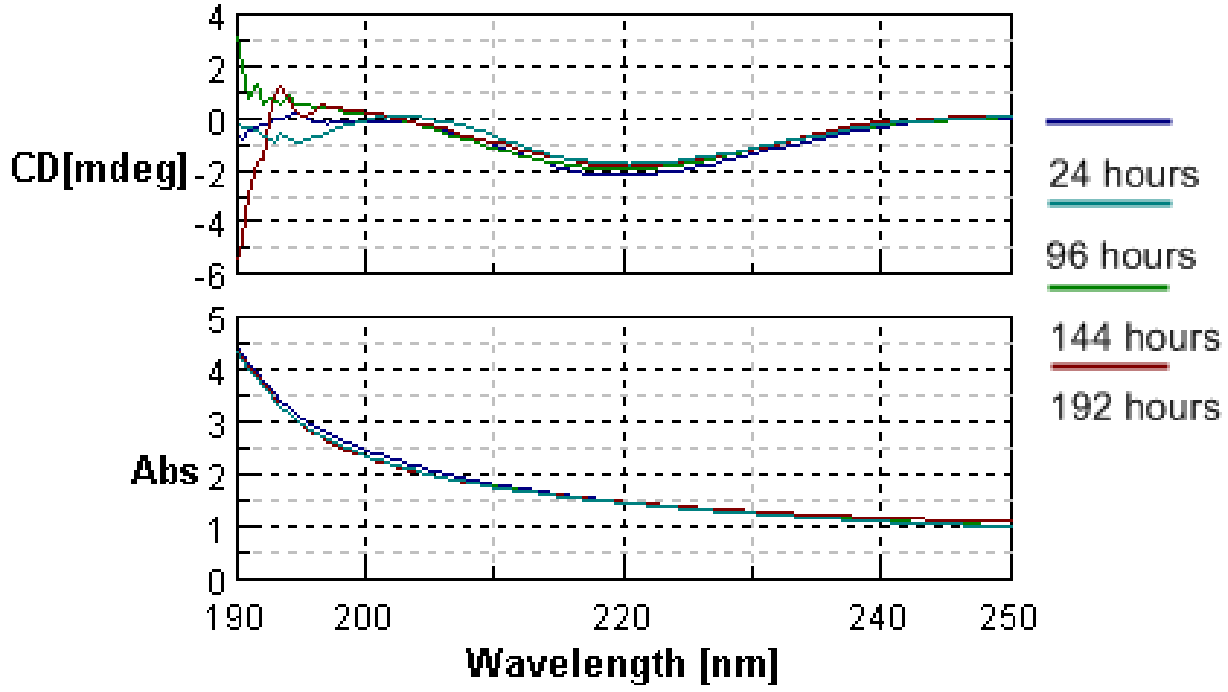

Fig. 27: Time dependent CD-spectra of 20 µM Aβ 42 from 20 mM phosphate buffer stock solution diluted with 50 mM phosphate buffer plus 1 mM ThT.

In graphs above (figures 23-27), phosphate buffer was used as dissolving and diluting agent. In the samples no 0.1 % ammonia solution was added. Graphs show very smooth curves with a lot of disturbances at the beginning. No significant differences between the curves were detected. In the next ThT experiment, two variations were considered. First Aβ 42 dissolved in 0.1 % ammonia solution could have been used or the according amount of ammonia could be added in order to reach the same ammonia concentration as if Aβ 42 dissolved in 0.1 % ammonia would have been used. Results are shown in figures 28-32.

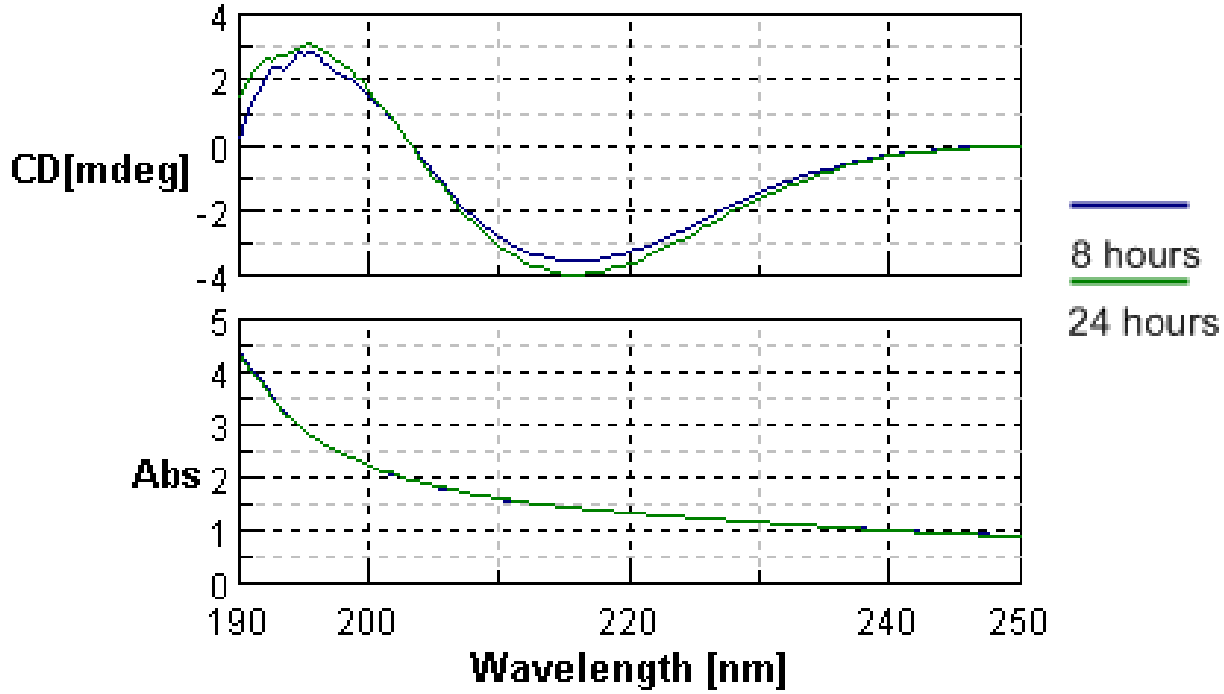

Fig. 28: Time dependent CD-spectra of 20 µM Aβ 42 from 0.1 % ammonia stock solution diluted with 50 mM phosphate buffer.

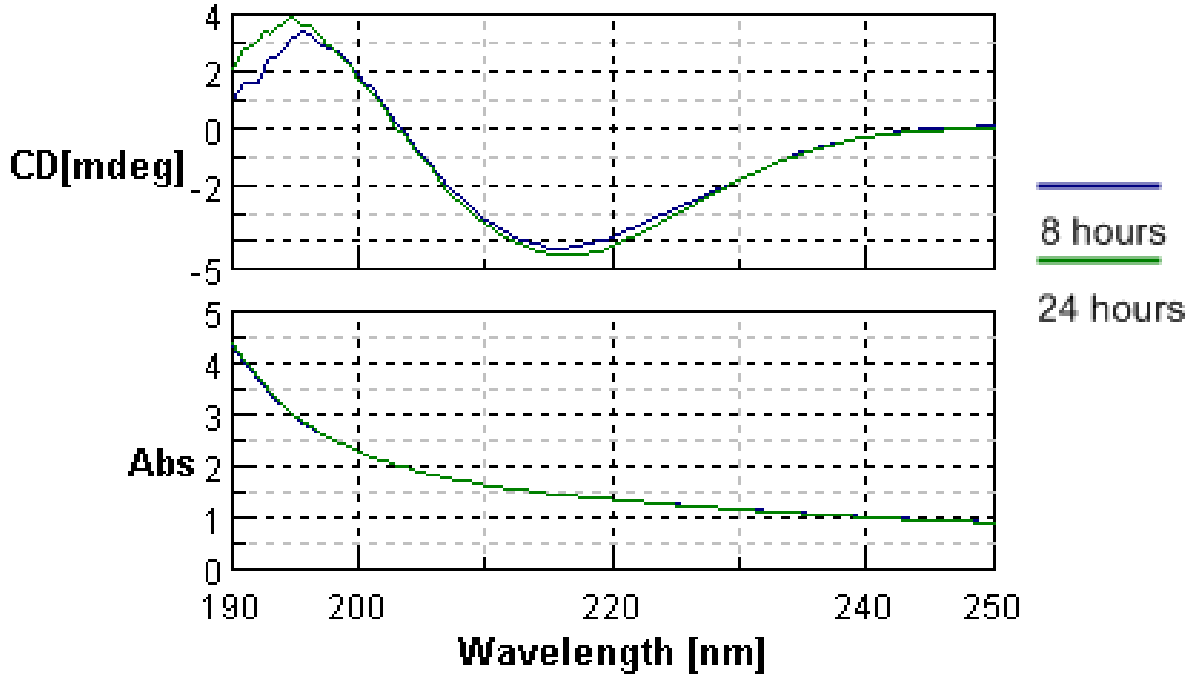

Fig. 29: Time dependent CD-spectra of 20 µM Aβ 42 from 0.1 % ammonia stock solution diluted with 50 mM phosphate buffer plus 0.1 µM ThT.

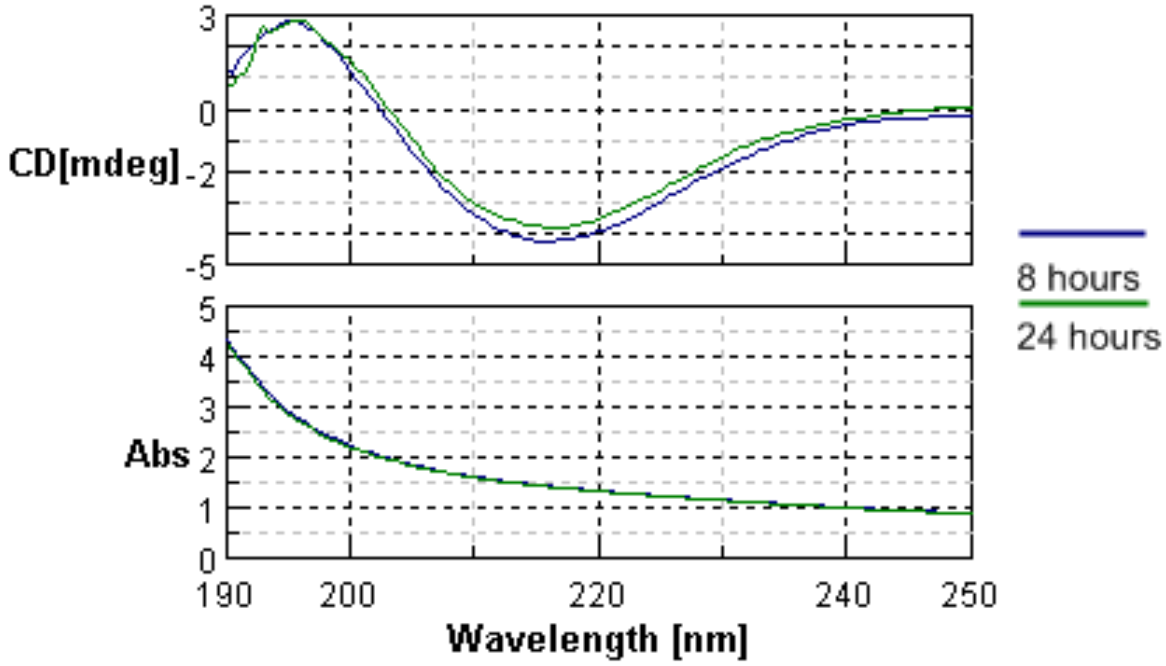

Fig. 30: Time dependent CD-spectra of 20 µM Aβ 42 from 0.1 % ammonia stock solution diluted with 50 mM phosphate buffer plus 1 µM ThT.

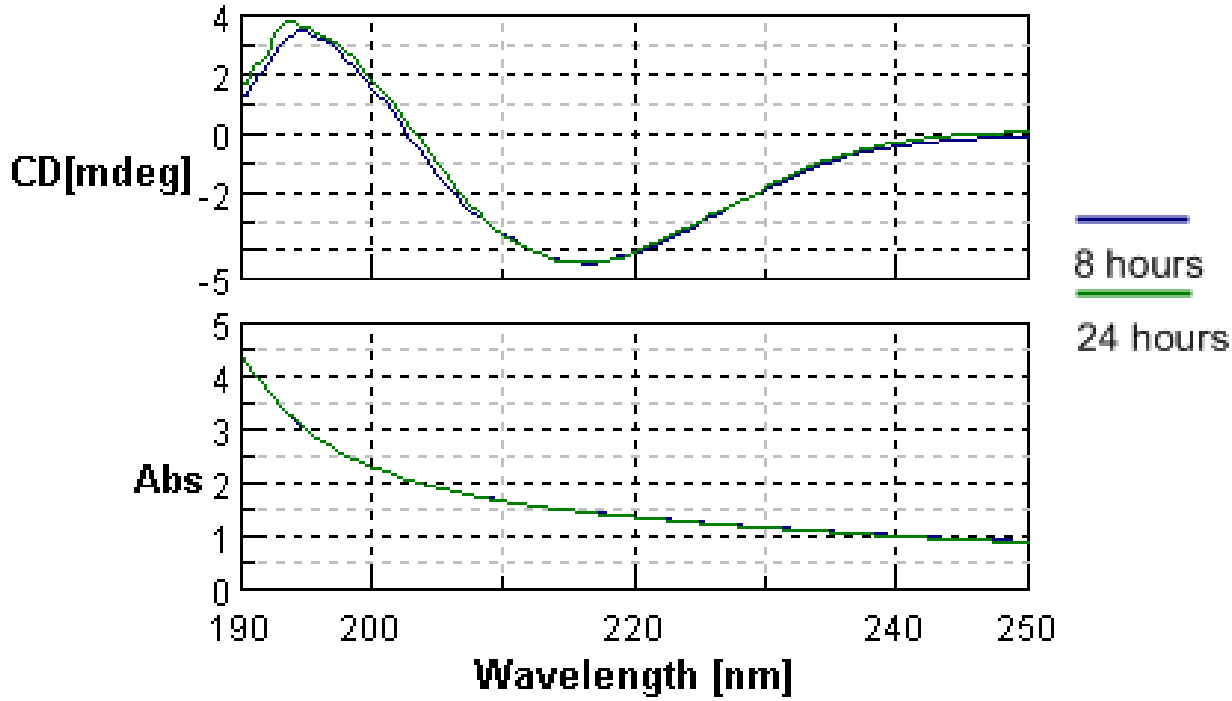

Fig. 31: Time dependent CD-spectra of 20 µM Aβ 42 from 0.1 % ammonia stock solution diluted with 50 mM phosphate buffer plus 10 µM ThT.

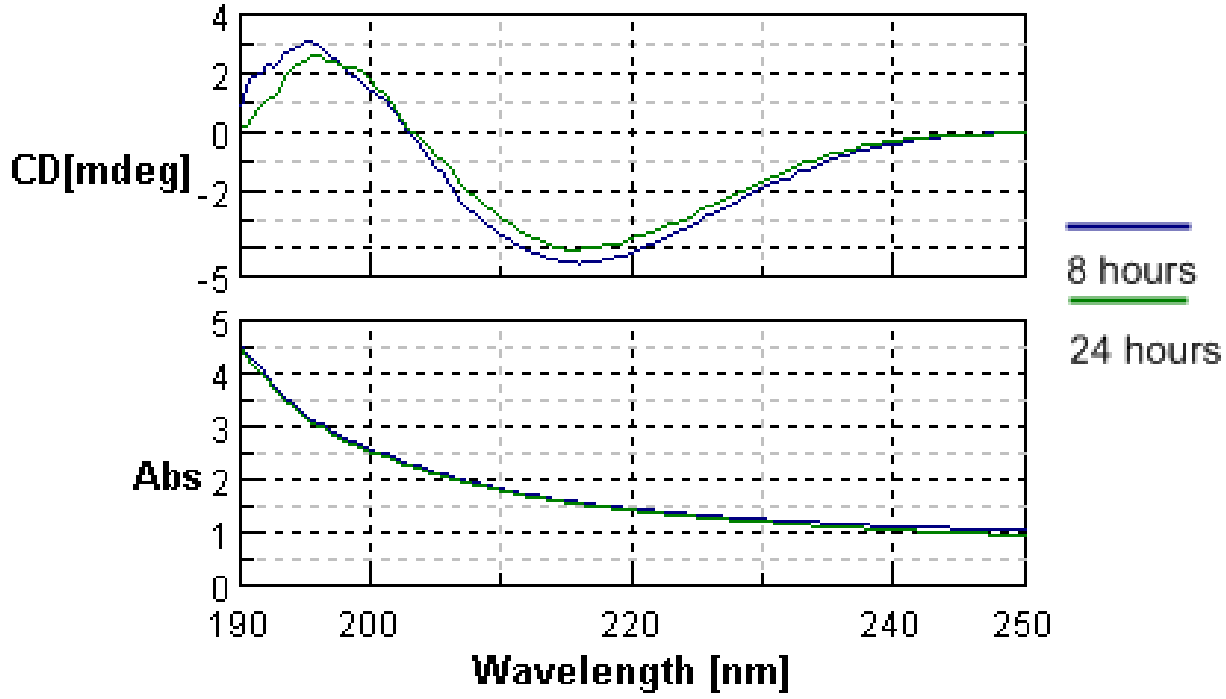

Fig. 32: Time dependent CD-spectra of 20 µM Aβ 42 from 0.1 % ammonia stock solution diluted with 50 mM phosphate buffer plus 100 µM ThT.

After use of Aβ 42 dissolved in 0.1 % ammonia, bigger differences between the curves were detected and the onset of curve was without disturbances. However, no concentration dependance of ThT was seen.

The experiment with ThT was made mainly for detecting some changes between curves after use of different Aβ solvents. Changes of curves within time were seen well. According to these changes, it was decided to use Aβ 42 dissolved in 0.1 % ammonia or addition of ammonia for the next studies.

The second experiment was with Curcumin dissolved in EtOH. 10 mM solution of Curcumin in 100 % EtOH was made and the other concentrations were prepared in 50 mM phosphate buffer in ratios of 1:10 of these solutions. 20 µl of the inhibitor solutions were then laid in before 29.9 µl of amyloid (100 µl of 134 mM), 13. 7 µl of ammonia solution and 136.4 µl of phosphate buffer were added to achieve a total volume of 200 µl. Then, different concentrations of ethanol and the control sample were prepared and were incubated for 0, 7, 24 and at least 48 hours at 37 °C..

During the measurement with the CD spectrophotometer, different curves for each concentration of Curcumin and also for concentrations of ethanol were recorded. These differences are shown in figures 33-41.

As the first one the control sample spectra were depicted at different time points. Then, graphs of various concentrations of Curcumin and EtOH were presented.

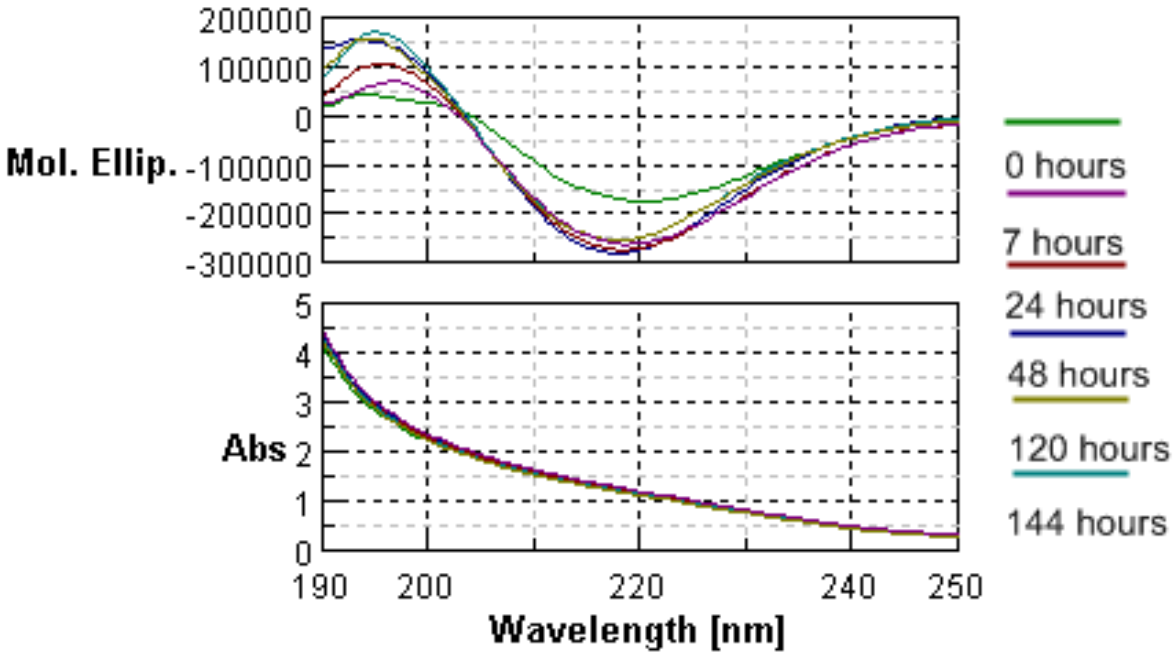

Fig. 33: Time dependent CD-spectra of 20 µM Aβ 42 from 20 mM phosphate buffer stock solution diluted with 50 mM phosphate buffer plus ammonia (=control sample, 0 % EtOH).

Control samples are important for the comparison to the graphs of solutions with inhibitors and solvents. Every curve is expected to be lower than the control curve. In that way, the effect of the inhibitor and the influence of the solvents can be seen and analysed.

In the graphs below, the difference between the curves at different time points is important, mainly at the minimum peak (around 220 nm) which reflects the formation of a β-sheet structure. The lowest values should be obtained in graphs with Curcumin because of its proposed inhibitory effects.

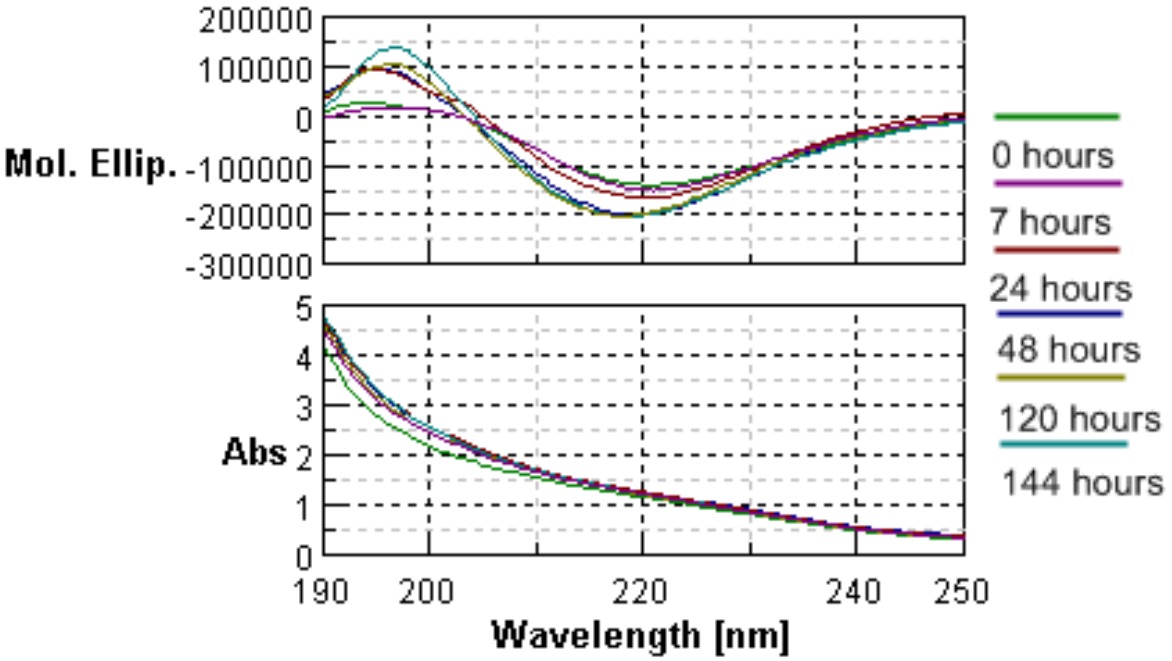

Fig. 34: Time dependent CD-spectra of 20 µM Aβ 42 from 20 mM phosphate buffer stock solution diluted with 50 mM phosphate buffer plus ammonia and 1 mM Curcumin in 10 % EtOH.

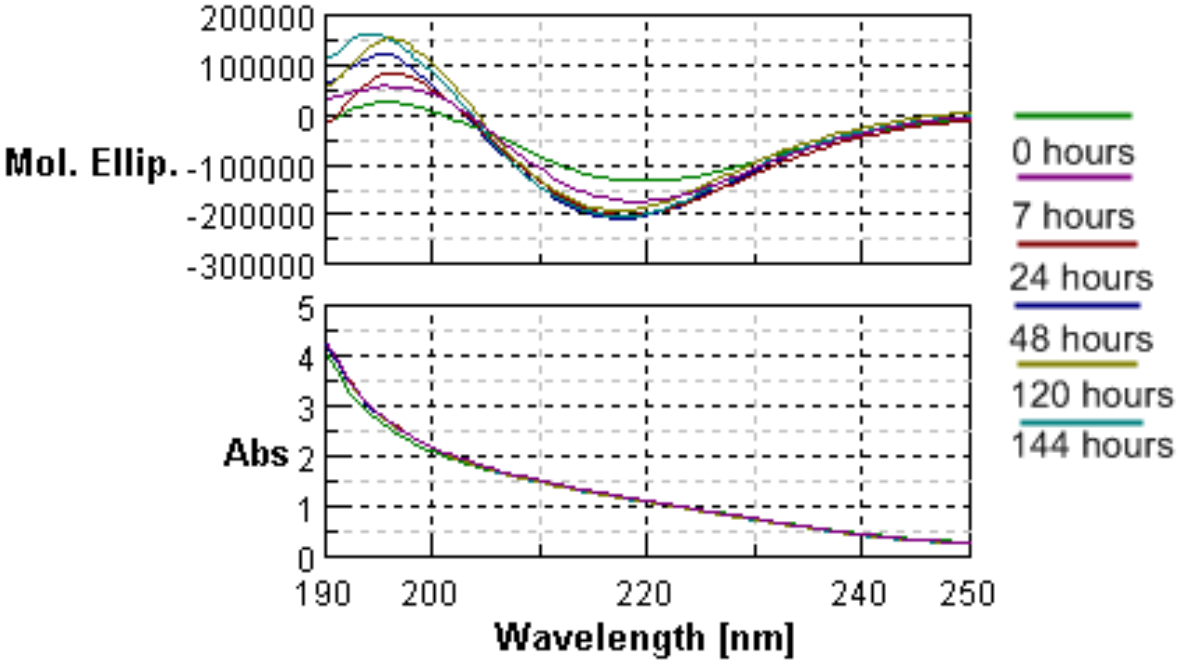

Fig. 35: Time dependent CD-spectra of 20 µM Aβ 42 from 20 mM phosphate buffer stock solution diluted with 50 mM phosphate buffer plus ammonia and 10 % EtOH.

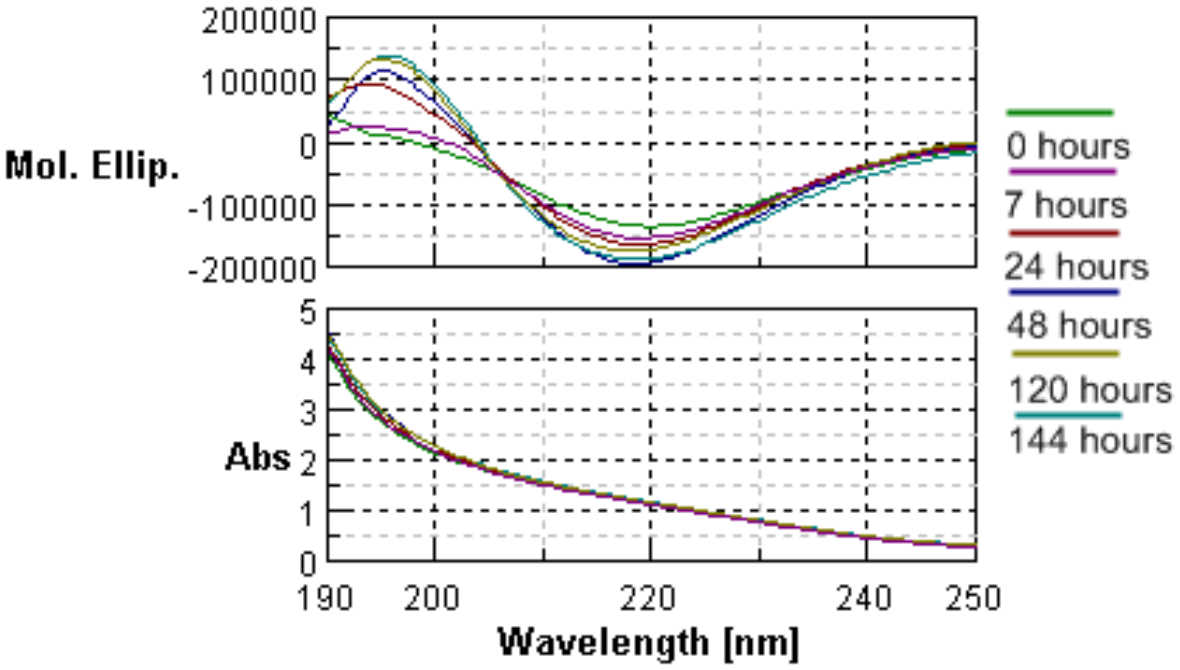

Fig. 36: Time dependent CD-spectra of 20 µM Aβ 42 from 20 mM phosphate buffer stock solution diluted with 50 mM phosphate buffer plus ammonia and 100 µM Curcumin in 1 % EtOH.

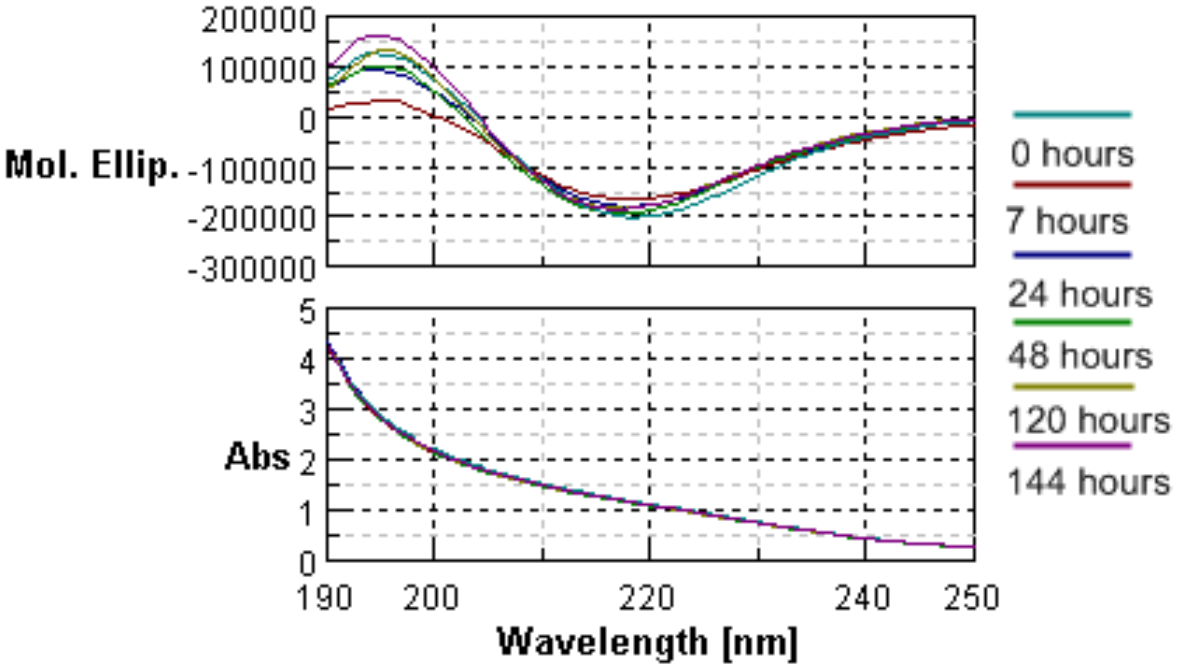

Fig. 37: Time dependent CD-spectra of 20 µM Aβ 42 from 20 mM phosphate buffer stock solution diluted with 50 mM phosphate buffer plus ammonia and 1 % EtOH.

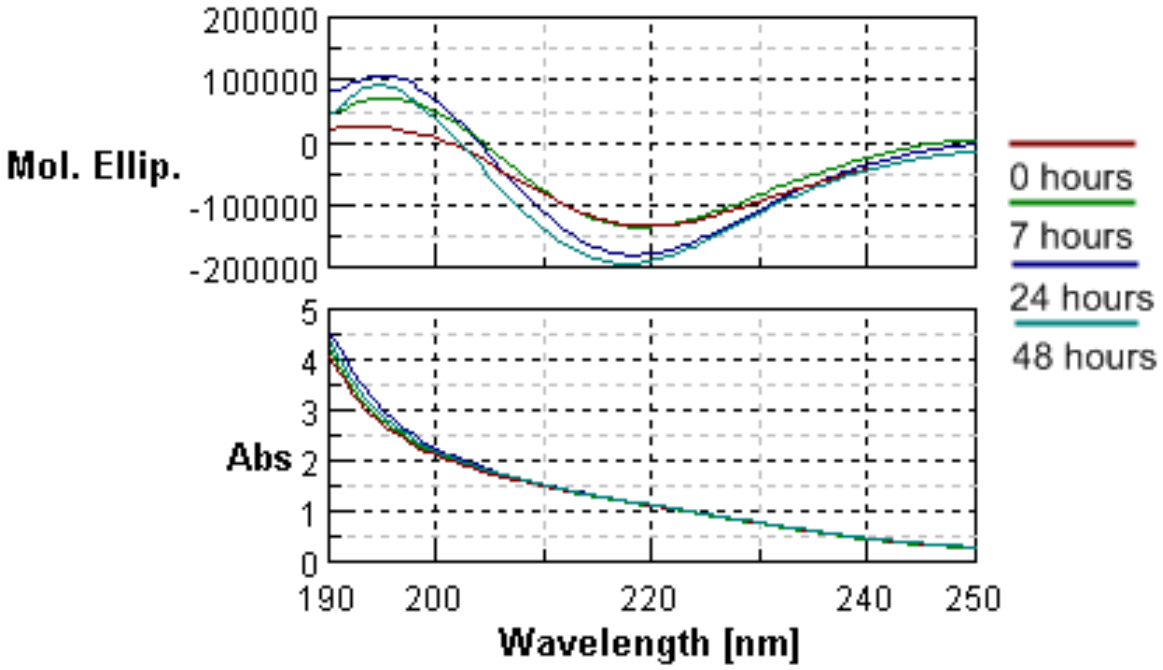

Fig. 38: Time dependent CD-spectra of 20 µM Aβ 42 from 20 mM phosphate buffer stock solution diluted with 50 mM phosphate buffer plus ammonia and 10 µM Curcumin in 0.1 % EtOH.

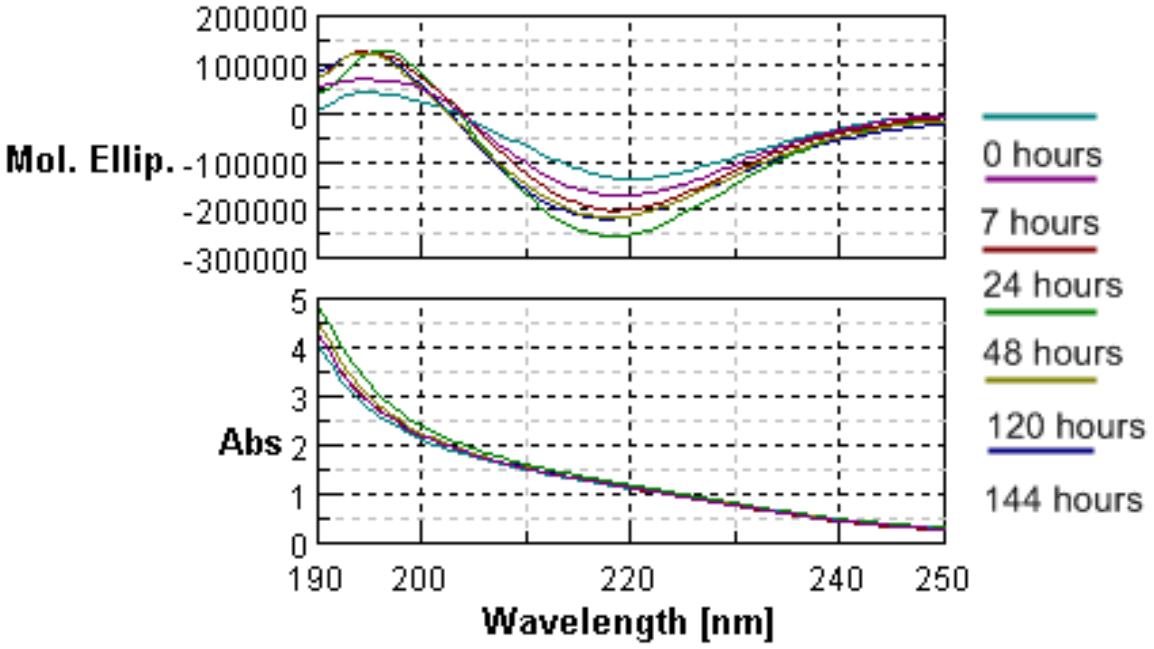

Fig. 39: Time dependent CD-spectra of 20 µM Aβ 42 from 20 mM phosphate buffer stock solution diluted with 50 mM phosphate buffer plus ammonia and 0.1 % EtOH.

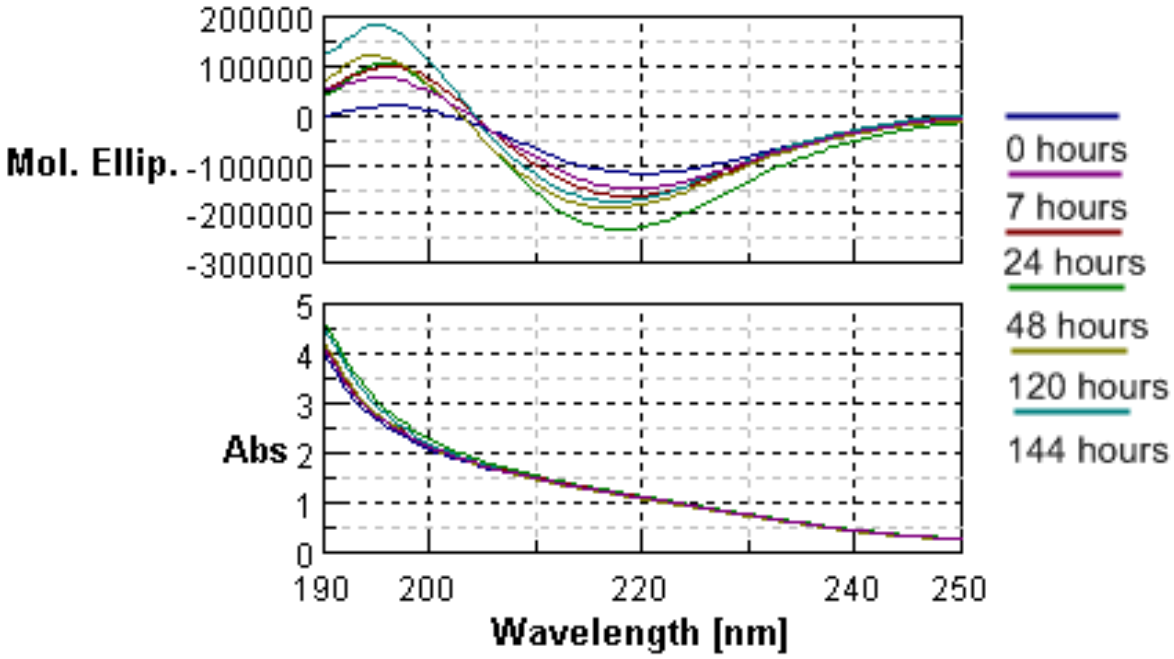

Fig. 40: Time dependent CD-spectra of 20 µM Aβ 42 from 20 mM phosphate buffer stock solution diluted with 50 mM phosphate buffer plus ammonia and 1 µM Curcumin in 0.01 % EtOH.

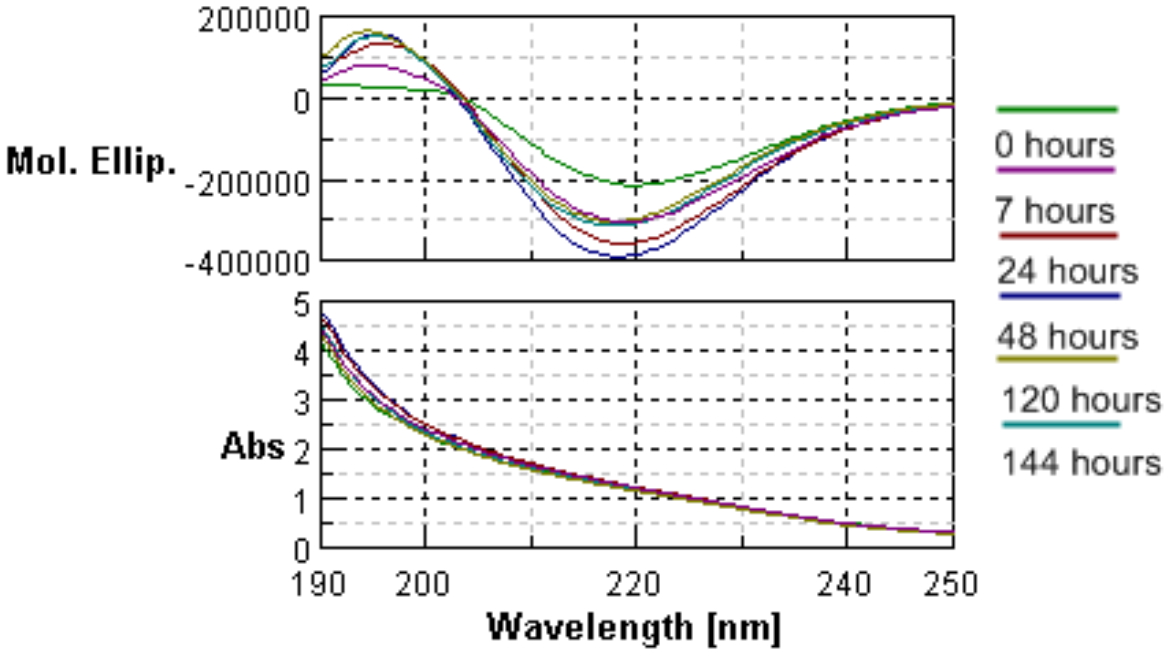

Fig. 41: Time dependent CD-spectra of 20 µM Aβ 42 from 20 mM phosphate buffer stock solution diluted with 50 mM phosphate buffer plus ammonia and 0.01 % EtOH.

According to the article in neuroscience letters (Akaishi et al., 2008), it was found that the lowest minima were obtained within the first 48 hours of the oligomerization process. In previous graphs, this progress can be clearly seen. CD-

spectra of later time points showed partly a reversed reaction indicated by increasing values at the minima at 220 nm. These later points did not provide additional information about the inhibitory effects and thus were excluded from further analysis steps. It was measured also in other time points but without any other important information.

Differences between curves, values from 0, 7, 24 h in different wavelengths (minimum, 220 nm, 195 nm) were compared. In order to normalise for possible different starting values, molar ellipsis values at 0 h were set to 100 % and graphs were drawn from 0 over 7 to 24 hours for the values at the minimum wavelengths (app. 216-219 nm), 220 nm and 195 nm. Time progressions of normalised molar ellipsis in [%] were shown in figures 42-44.

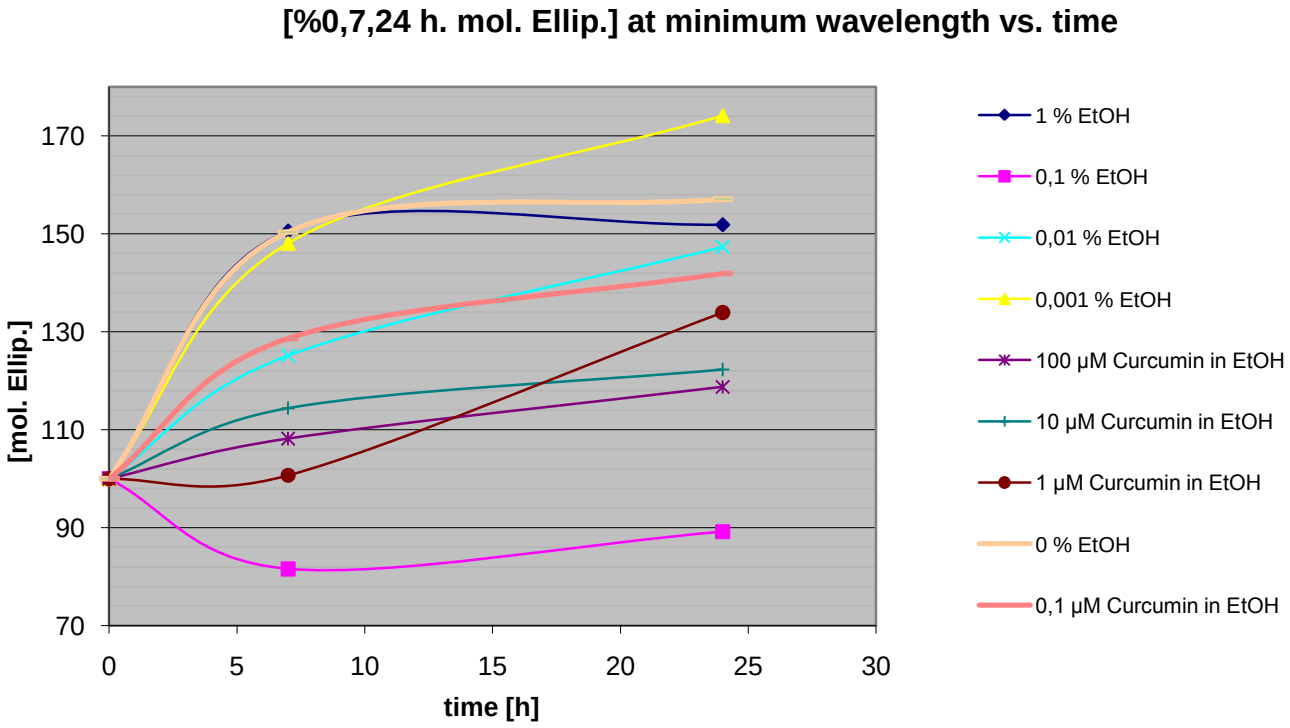

Fig. 42: Time dependent progressions of molar ellipsis values [%] at the minimum wavelength obtained from 20 µM Aβ 42 (plus ammonia) solutions with 0.1-100 µM Curcumin and/or 0.001-1 % EtOH.

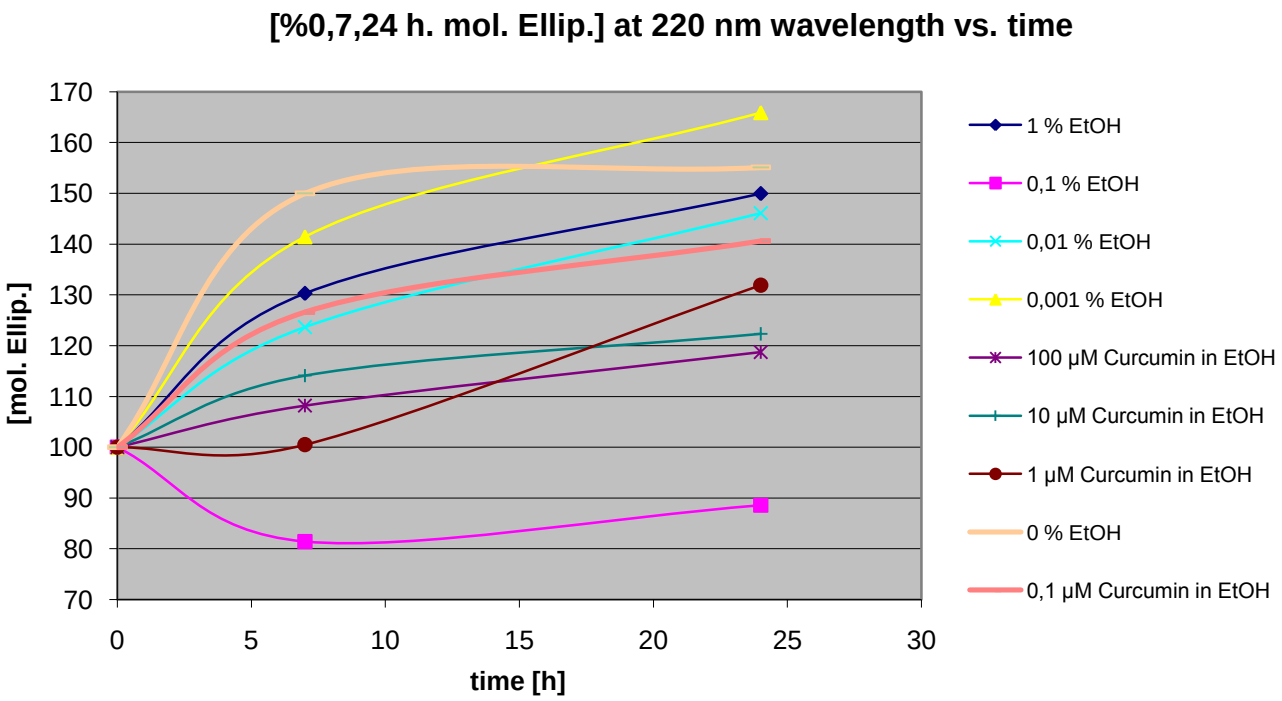

Fig. 43: Time dependent progressions of molar ellipsis values [%] at the 220nm wavelength obtained from 20 µM Aβ 42 (plus ammonia) solutions with 0.1-100 µM Curcumin and/or 0.001-1 % EtOH.

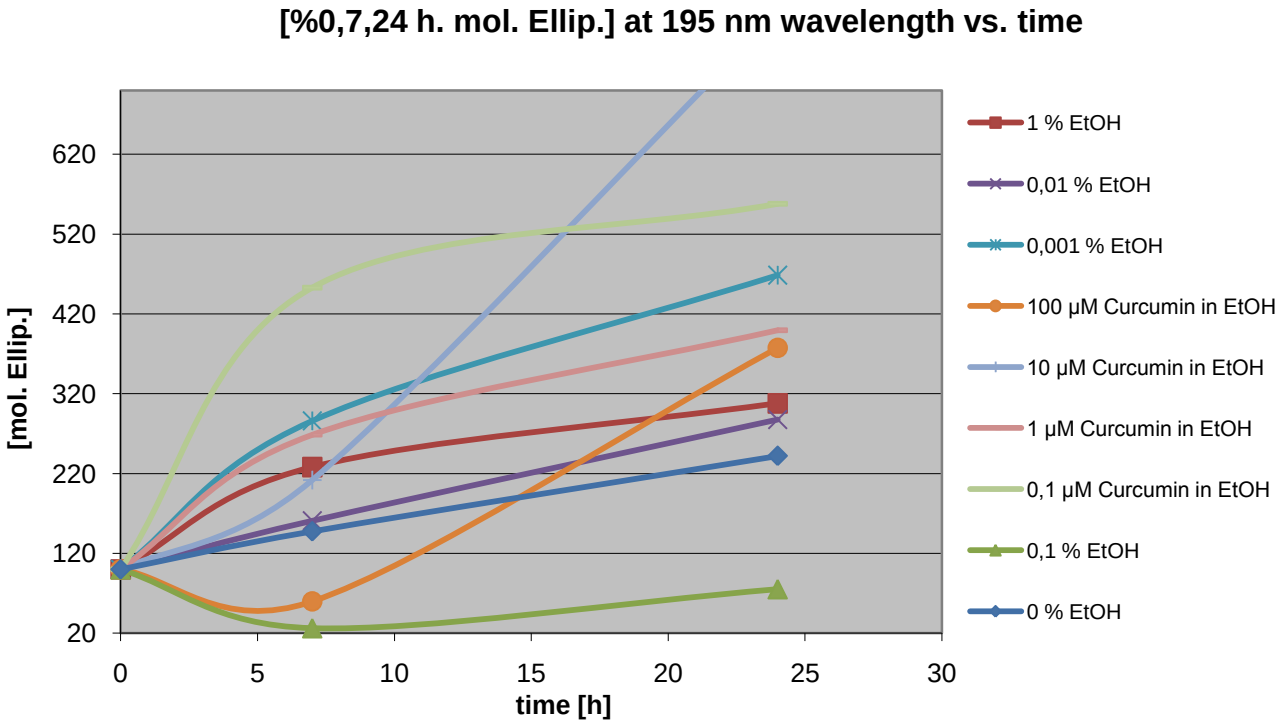

Fig. 44: Time dependent progressions of molar ellipsis values [%] at the 195 nm wavelength obtained from 20 µM Aβ 42 (plus ammonia) solutions with 0.1-100 µM Curcumin and/or 0.001-1 % EtOH.

Based on normalised molar ellipsis-graphs the slopes of these curves were calculated after linear regression analysis using points between 0 and 7 h, 0, 7 and 24 h or 0 and 24 hours. Results are summarized in tab. 4.

Curcumin in Ethanol									
	Minimum			220 nm			195 nm		
	0, 7 h	0, 7, 24 h	0, 24 h	0, 7 h	0, 7, 24 h	0, 24 h	0, 7 h	0, 7, 24 h	0, 24 h
0 %EtOH	7.1974	2.0084	2.3776	7.1398	1.9254	2.2964	6.7984	5.8505	5.9179
1 %EtOH	7.2296	1.7738	2.1619	4.325	1.908	2.0799	18.3	7.9253	8.6633
0.1 %EtOH	-2.6299	-0.2835	-0.4504	-2.6532	-0.3094	-0.4761	-10.558	-0.3059	-1.0352
0.01 %EtOH	3.5915	1.8478	1.9718	3.3788	1.8091	1.9208	8.69	7.7538	7.8204
0.001 %EtOH	6.8652	2.799	3.0883	5.9184	2.5019	2.7449	26.556	14.491	15.35
100 µM Curcumin	1.17	0.7512	0.781	1.17	0.7512	0.781	-5.7561	12.888	11.561
10 µM Curcumin	2.0603	1.1834	1.2457	2.015	0.8478	0.9309	15.983	30.017	29.019
1 µM Curcumin	0.1	1.369	1.2788	0.0715	1.4251	1.3288	24.078	11.594	12.482
0.1 µM Curcumin	4.0936	1.5216	1.7046	3.7982	1.5296	1.691	50.428	16.686	19.087

Tab. 4: Summary of slopes of normalised, time-dependent molar ellipsis curves of the experiments with 0.1-100 µM Curcumin dissolved in EtOH and 0.001-1 % EtOH as additional control samples.

In the table above, the results of slopes are shown. Different time points at different wavelengths were analysed. Slope values of using 0-24 h time frames at 220 nm (as recommended by Akaishi et al., 2008) resulted in distinct concentration dependent inhibition in comparison to the control sample (= 0 % EtOH). EtOH as solvent showed almost no significant effect except at 0.1 % EtOH. This significant decrease was reproducible after repeat of this experiments. Thus, the influence of EtOH on the Aβ 42 oligomerization process should be further investigated in another following study. The slopes at the maximum wavelength of 195 nm were higer than the control as expected, but no concentration dependent effect was clearly observable. Thus, main attention should be laid on the values obtained at 220 nm.

For the third experiment DMSO was used as an organic solvent for Curcumin. Because of its proven influence on CD-spectra it has to be used in lower concentrations than the other solvents.

The solution was 100 mM curcumin, which was dissolved in 100 % DMSO. From this solution 1 mM curcumin in 1 % DMSO, 100 µM, 10 µM, 1 µM curcumin in 0.1 % DMSO was prepared. Then, other substances in the same way as the previous experiment were arranged. Results were compared with 0.01 % DMSO, 0.1 % DMSO and control(blank) sample. Disturbances in the end concentration of 0,1 mM in 0.1 %

DMSO were examined and the inhibiting effect of curcumin on amyloid was seen. Results are shown in figures 45-51.

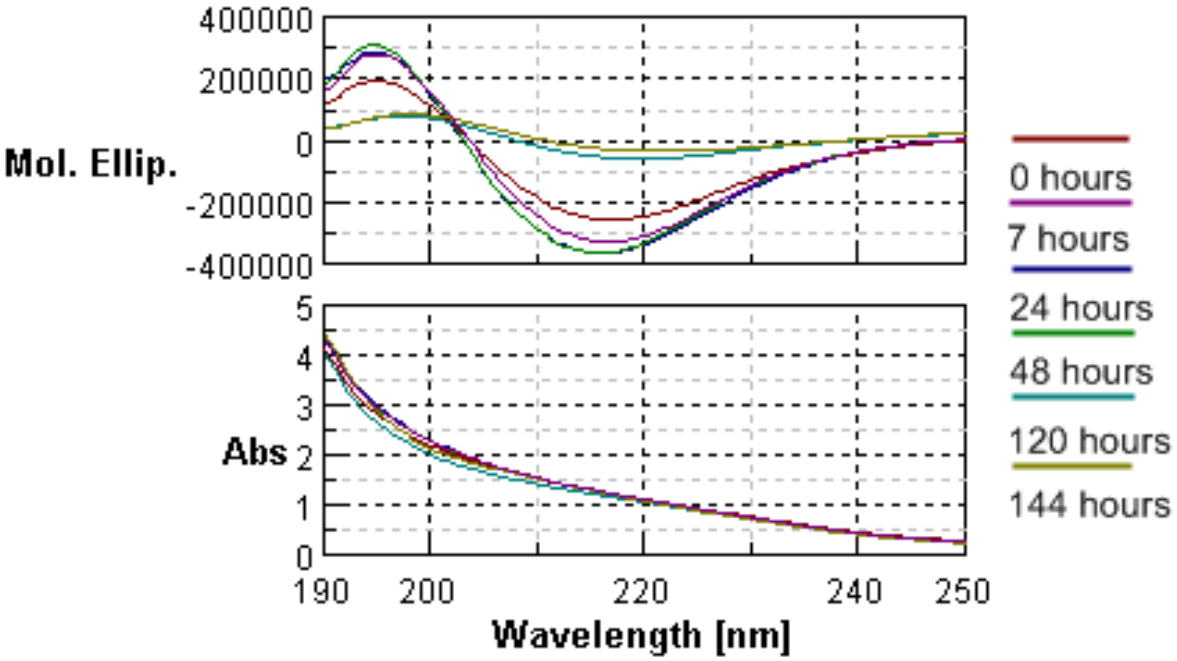

Fig. 45: Time-dependent changes of CD-spectra of 20 µM Aβ 42 dissolved in 20 mM phosphate buffer, diluted in 50 mM phosphate buffer and plus ammonia and 0% DMSO.

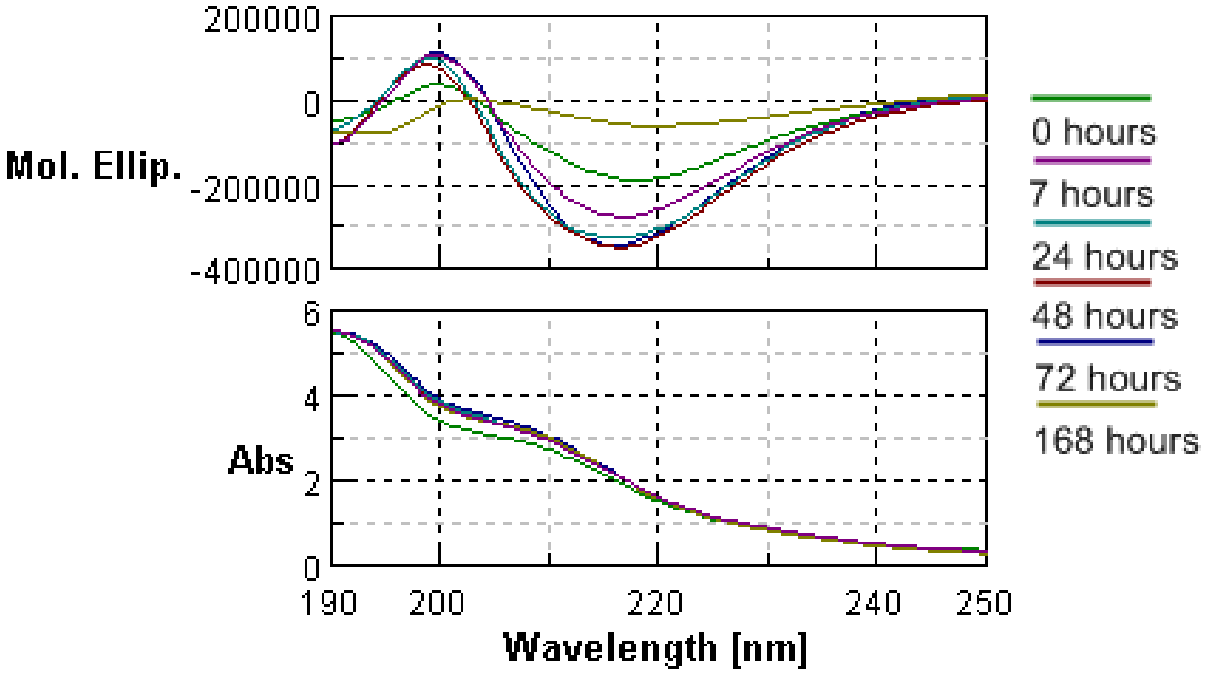

Fig. 46: Time-dependent changes of CD-spectra of 20 µM Aβ 42 dissolved in 20 mM phosphate buffer, diluted in 50 mM phosphate buffer plus ammonia and 100µM Curcumin in 0.1% DMSO.

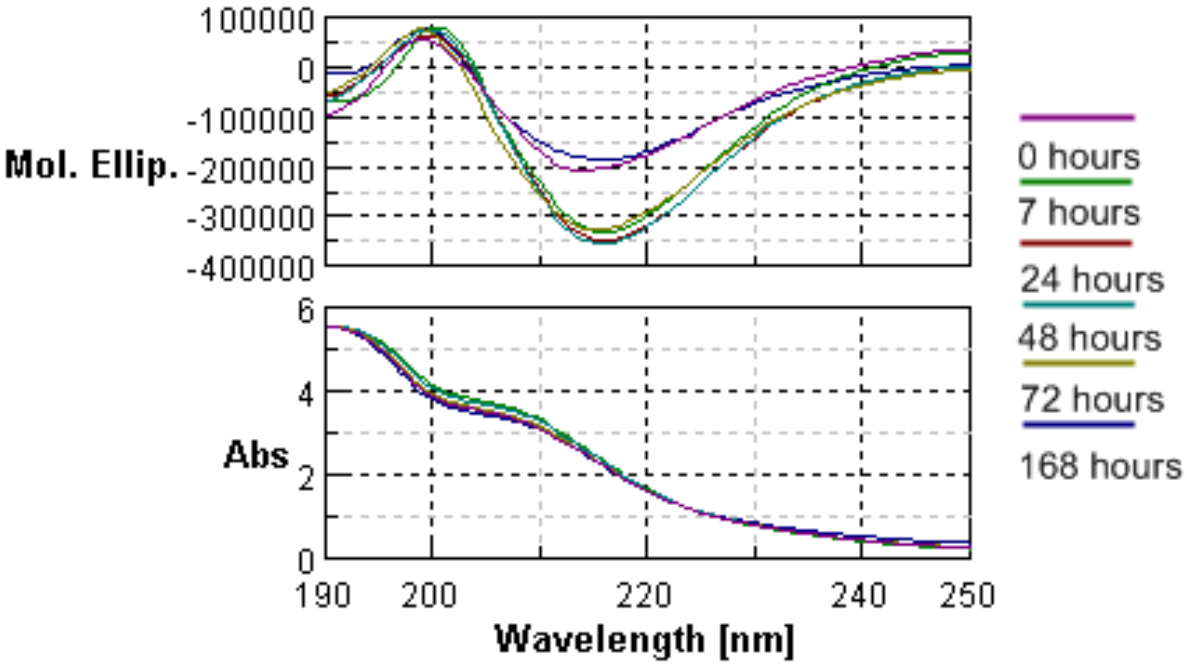

Fig. 47: Time-dependent changes of CD-spectra of 20 µM Aβ 42 dissolved in 20 mM phosphate buffer, diluted in 50 mM phosphate buffer plus ammonia and 0.1 % DMSO.

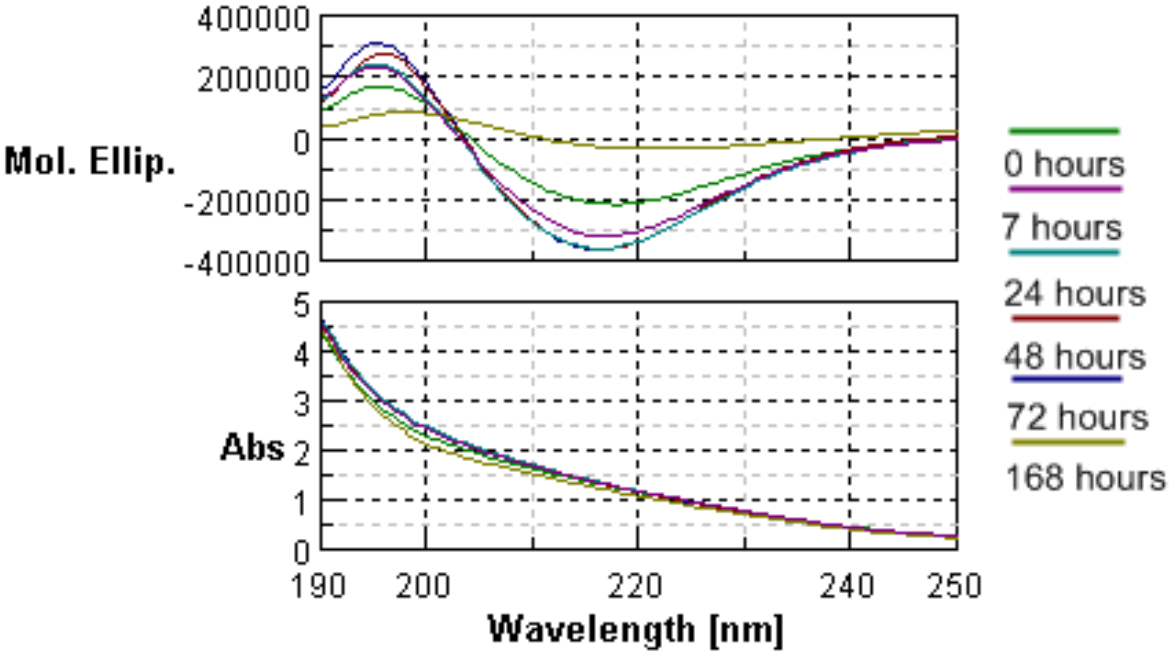

Fig. 48: Time-dependent changes of CD-spectra of 20 µM Aβ 42 dissolved in 20 mM phosphate buffer, diluted in 50 mM phosphate buffer plus ammonia and 10 µM Curcumin in 0.01 % DMSO.

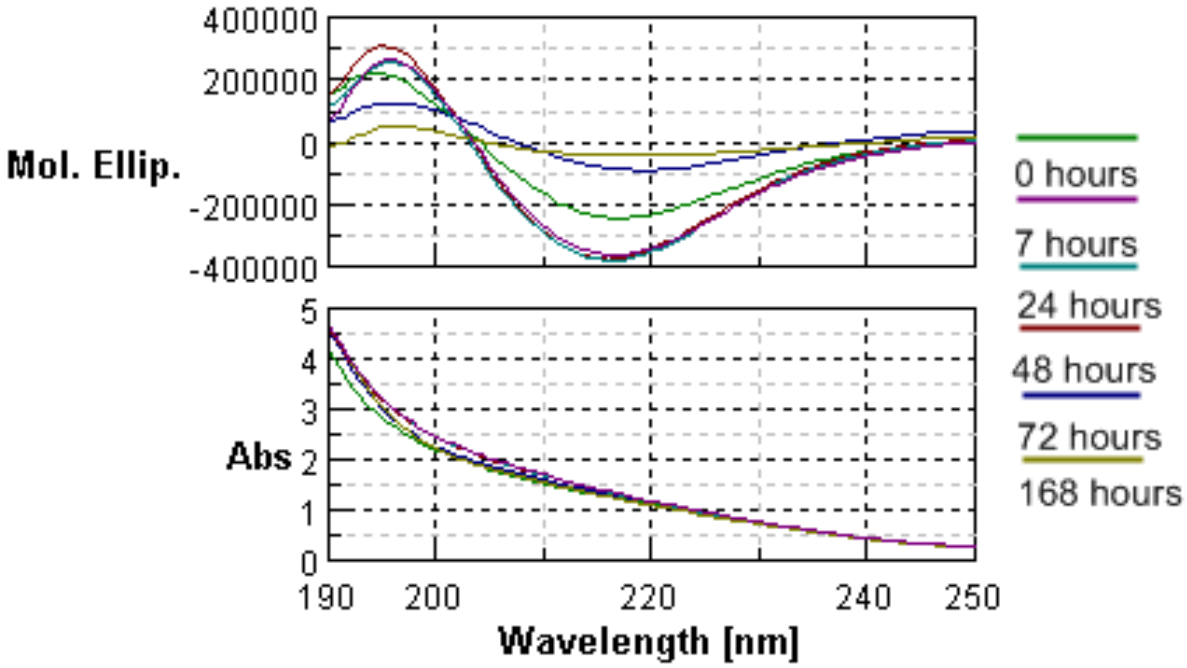

Fig. 49: Time-dependent changes of CD-spectra of 20 µM Aβ 42 dissolved in 20 mM phosphate buffer, diluted in 50 mM phosphate buffer plus ammonia and 0.01 % DMSO.

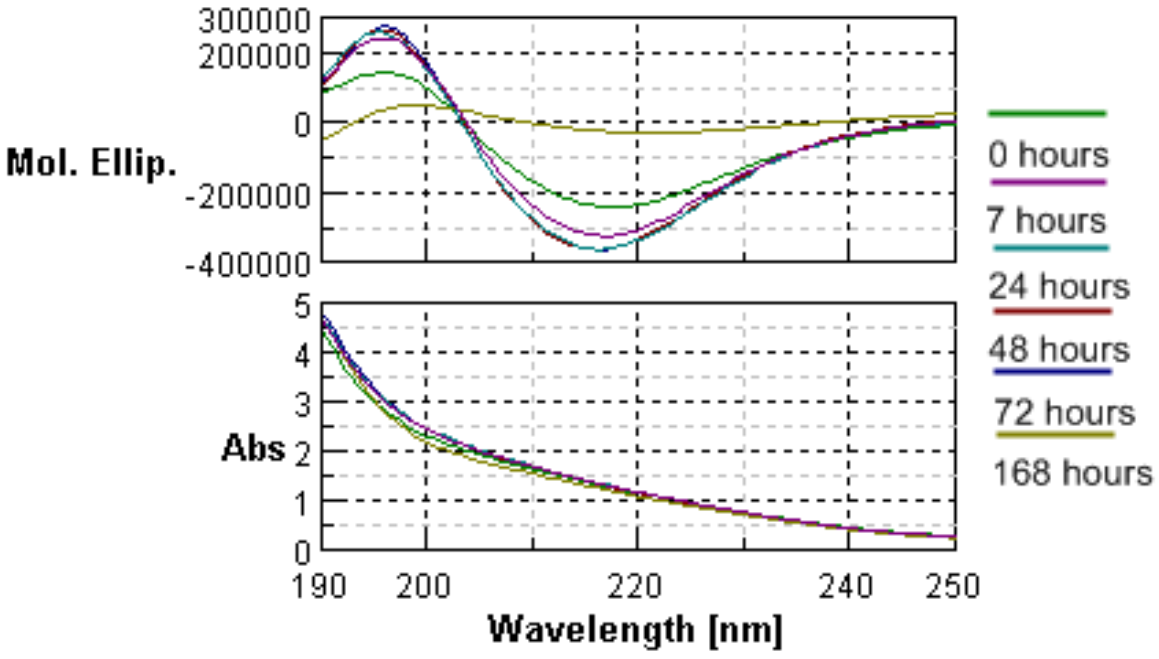

Fig. 50: Time-dependent changes of CD-spectra of 20 µM Aβ 42 dissolved in 20 mM phosphate buffer, diluted in 50 mM phosphate buffer plus ammonia and 1 µM Curcumin in 0.01 % DMSO.

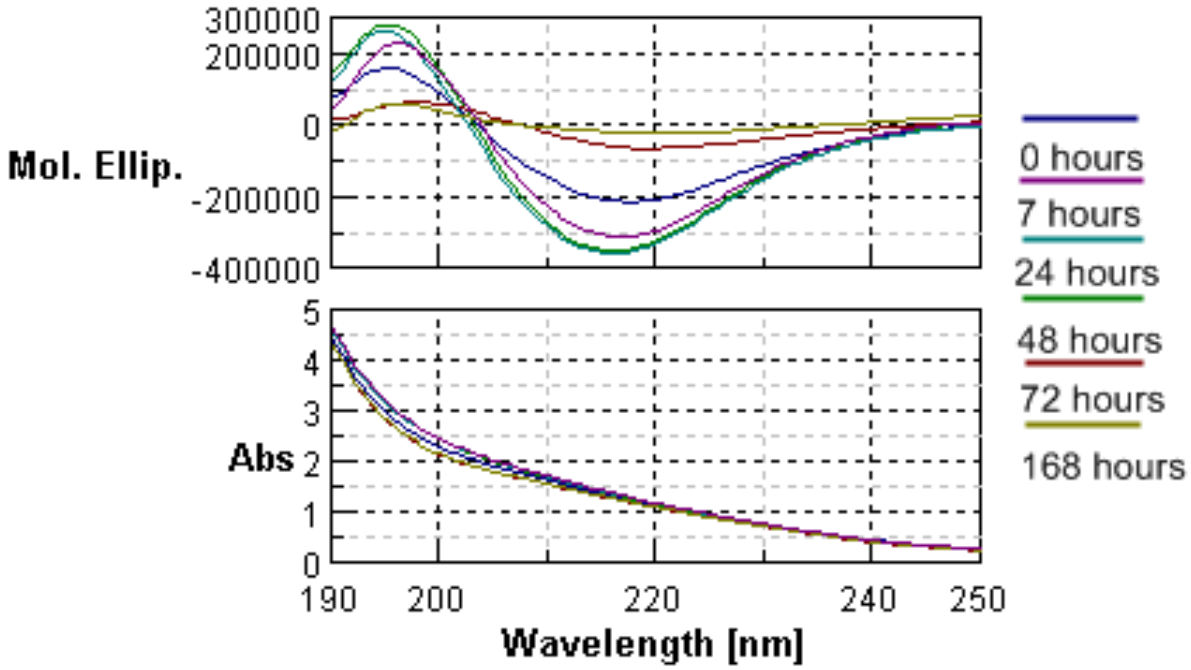

Fig. 51: Time-dependent changes of CD-spectra of 20 µM Aβ 42 dissolved in 20 mM phosphate buffer, diluted in 50 mM phosphate buffer plus ammonia and 0.1 µM Curcumin in 0.01 % DMSO.

The graph of 0.1 %DMSO, which can be used to compare graphs above is one page before.

Different concentrations of curcumin dissolved in DMSO were measured on CD spectrofotometer. Values were gained from various wavelength at minimum, 220 nm and 195 nm in time. The dependance on mol. ellips. and time of 0, 7 and 24 hours is shown in figures 52 to 54.

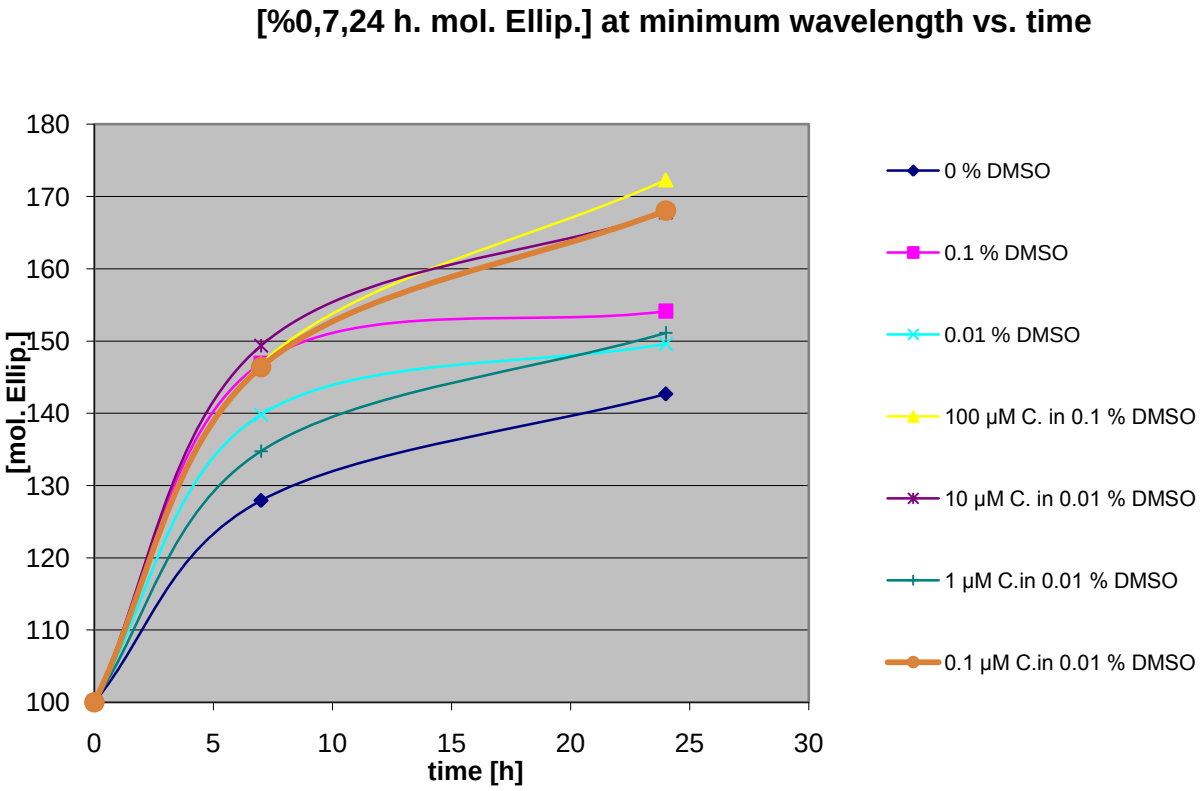

Fig. 52: Time dependent progressions of molar ellipsis values [%] at the minimum wavelength obtained from 20 µM Aβ 42 (plus ammonia) solutions with 0.1-100 µM Curcumin and/or 0.01-0.1 % DMSO.

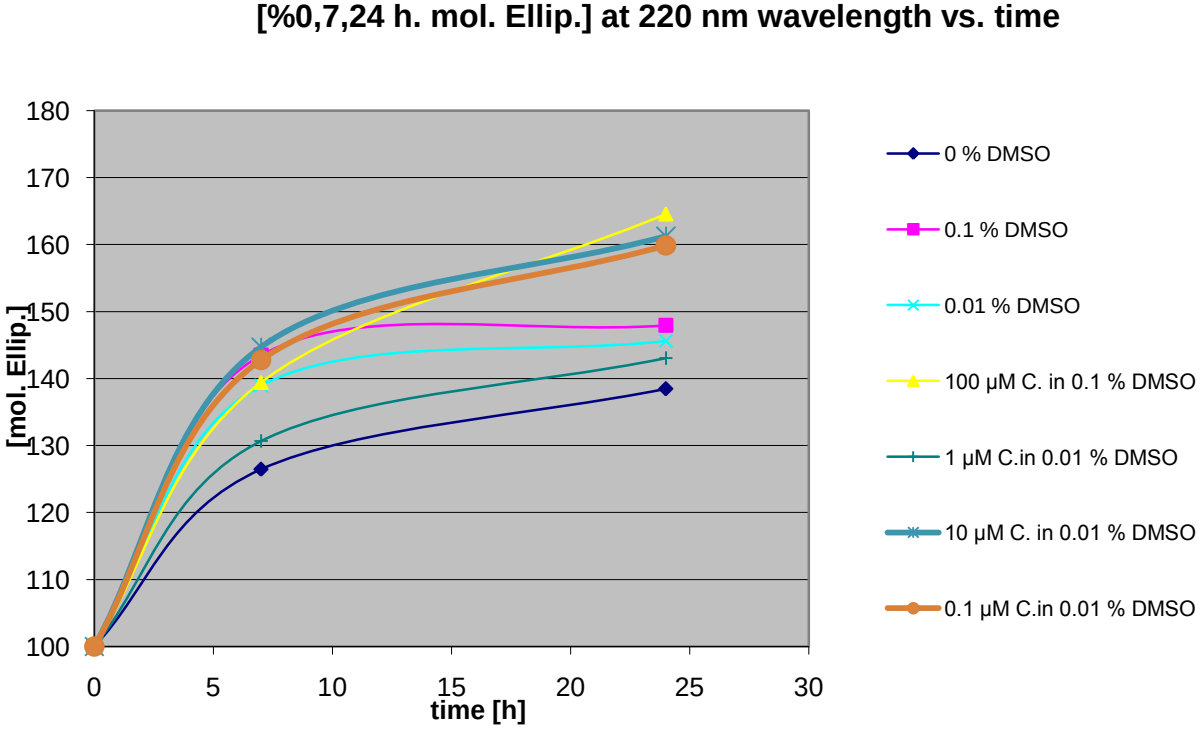

Fig. 53: Time dependent progressions of molar ellipsis values [%] at the 220nm wavelength obtained from 20 µM Aβ 42 (plus ammonia) solutions with 0.1-100 µM Curcumin and/or 0.01-0.1 % DMSO.

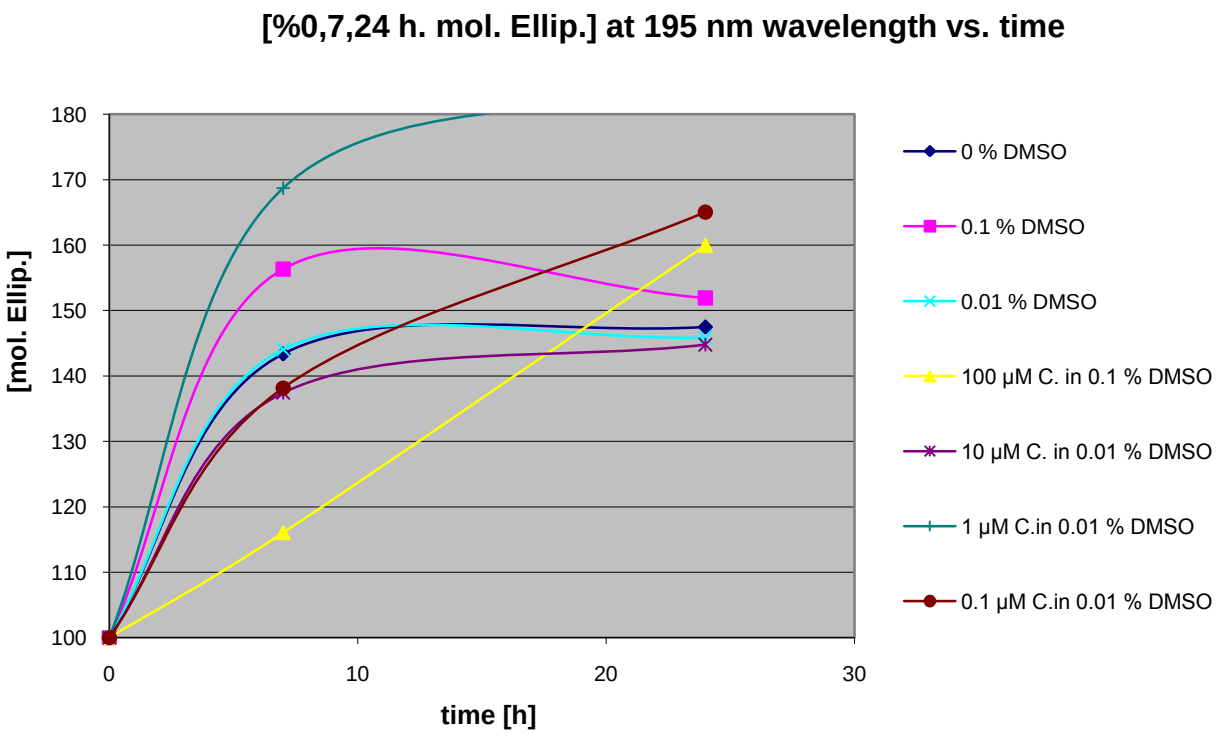

Fig. 54: Time dependent progressions of molar ellipsis values [%] at the 195 nm wavelength obtained from 20 µM Aβ 42 (plus ammonia) solutions with 0.1-100 µM Curcumin and/or 0.01-0.1 % DMSO.

Based on normalised molar ellipsis graphs the slopes of these curves were calculated after linear regression analysis using points between 0 and 7 h, 0, 7 and 24 h or 0 and 24 hours. Results are summarized in tab. 5.

Curcumin in DMSO									
	Minimum			220 nm			195 nm		
	0, 7 h	0, 7, 24 h	0, 24 h	0, 7 h	0, 7, 24 h	0, 24 h	0, 7 h	0, 7, 24 h	0, 24 h
0 % DMSO	3.9912	1.6089	1.7783	3.77823	1.4369	1.6037	6.1945	1.6554	1.9783
0.1 % DMSO	8.6109	0.7748	1.3323	6.2129	1.6749	1.9978	8.0469	1.7127	2.1633
0.01 % DMSO	6.7053	1.9146	2.2554	5.5635	1.6198	1.5658	6.291	1.5756	1.9111
100 µM C.in 0.1 %	6.6982	2.7302	3.0125	5.6341	2.4651	2.6905	2.2925	3.3956	2.4977
10 µM C.in 0.01 %	7.0513	2.5	2.8238	6.3845	2.2584	2.5519	5.345	1.5993	1.8658
1 µM C.in 0.01 %	4.9653	1.9128	2.1299	4.3801	1.5955	1.7936	9.816	3.0439	3.5256
0.1 µM C.in 0.01 %	6.6285	2.545	2.8354	6.1104	2.2175	2.4945	5.4507	2.4997	2.7098

Tab. 5: Summary of slopes of normalised, time-dependent molar ellipsis curves of the experiments with 0.1-100 µM Curcumin dissolved in DMSO and 0.01-0.1 % DMSO as additional control samples.

The fourth experiment was with an in-house provided inhibitor so-called substance H which was dissolved in MeOH. Substance H was already prepared as 2.7 mM solution in MeOH. For experiment, solution of 1 mM in 50 % MeOH was needed. The solution from 370.37 µl of 2.7 mM sol, 129.63 µl of MeOH and 500 µl of

phosphate buffer was prepared. Then, the ratio 1:10 for getting concentrations of 100 µM, 10 µM, 1 µM and 0.1 µM of substance H was used. For measurement, the solution containing the inhibitor in amount of 23 µl, 15.3 µl of amyloid (50 µl of 300 mM) and 191.7 µl of phosphate buffer were used. CD- spectra of each sample are shown in figures 55-63.

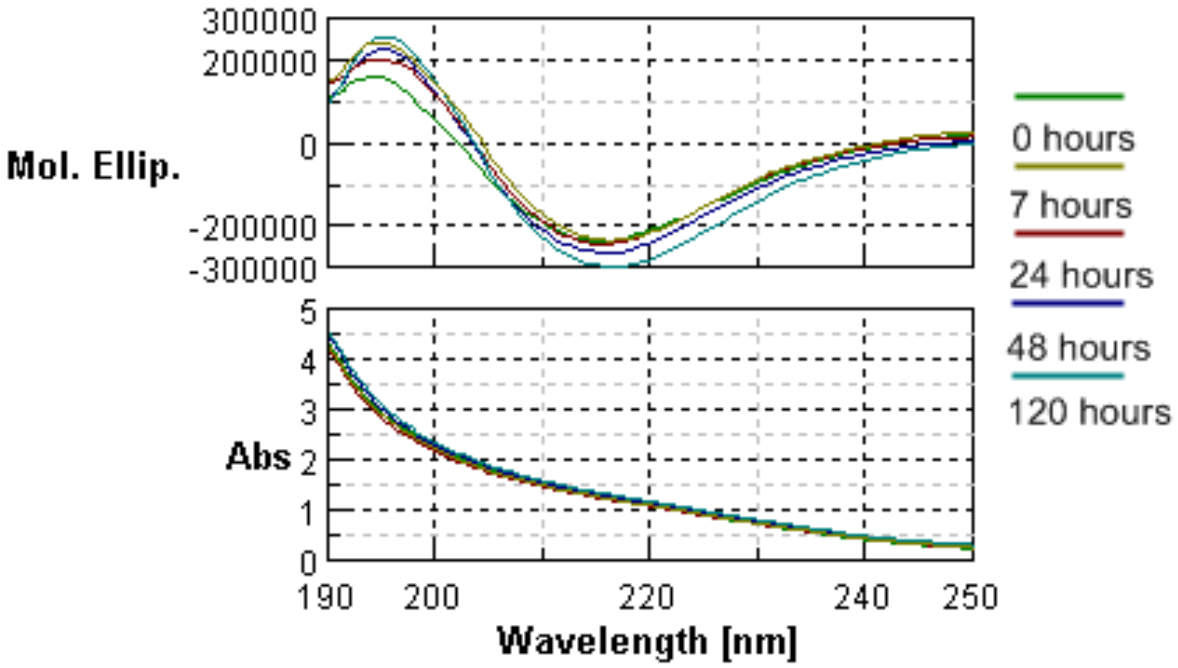

Fig. 55: Time dependent CD-spectra of 20 µM Aβ 42 from 0.1 % ammonia stock solution diluted with 50 mM phosphate buffer plus 0 % MeOH.

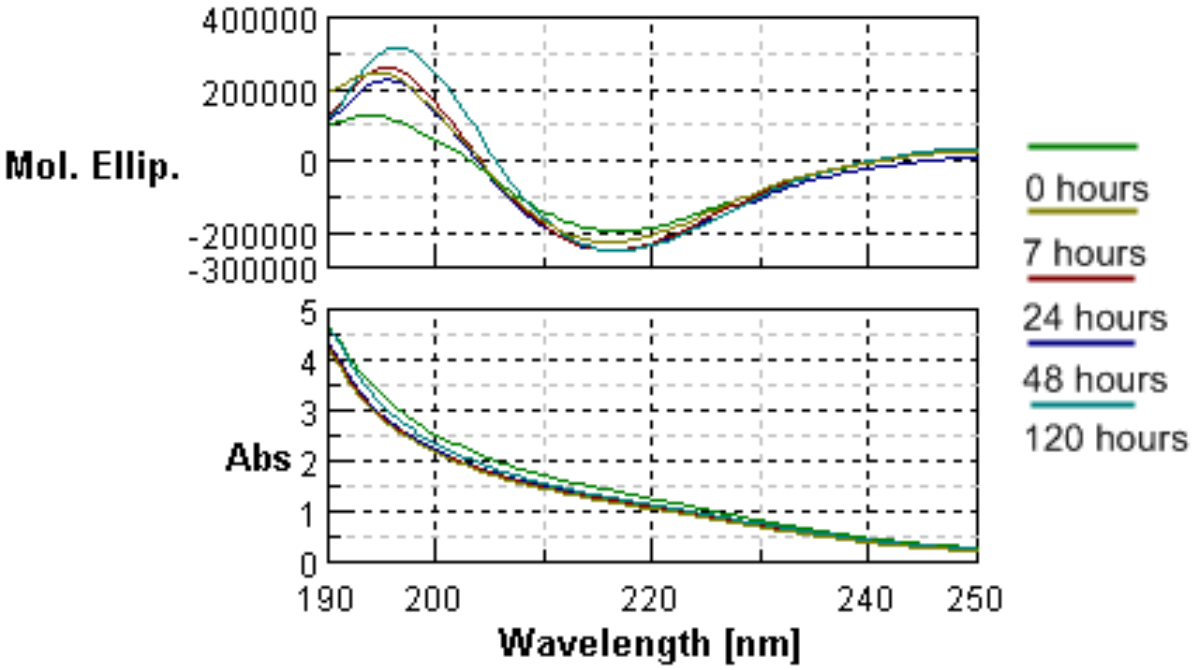

Fig. 56: Time dependent CD-spectra of 20 µM Aβ 42 from 0.1 % ammonia stock solution diluted with 50 mM phosphate buffer plus 1 mM substance H in MeOH.

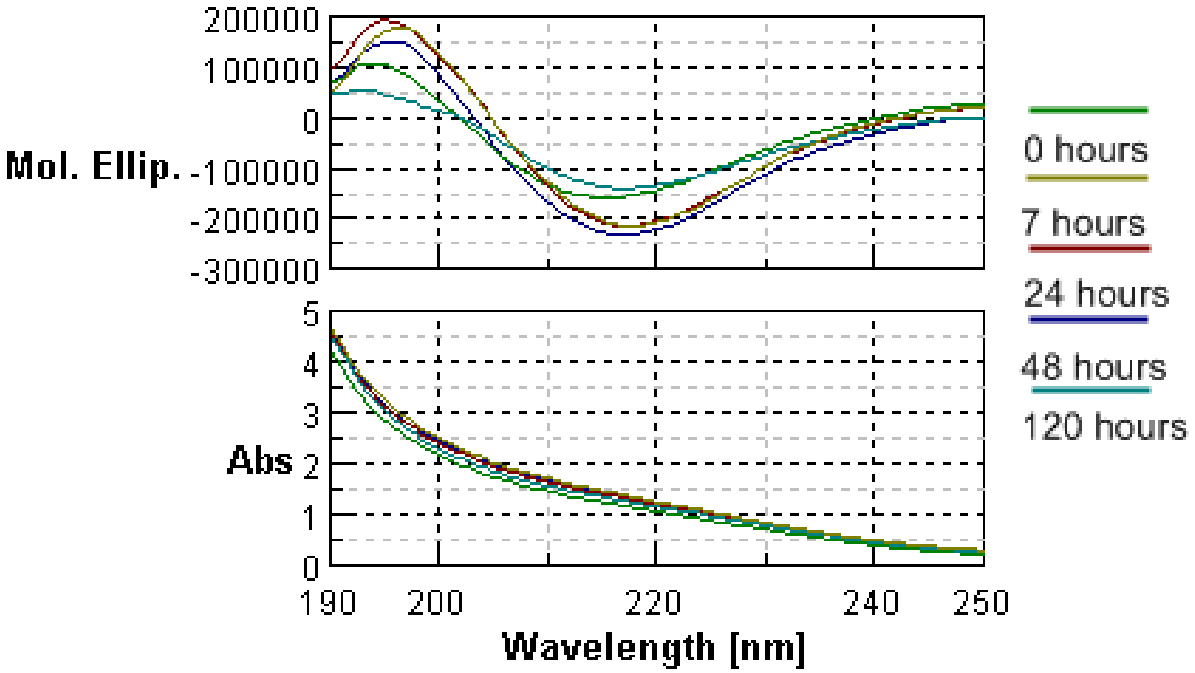

Fig. 57: Time dependent CD-spectra of 20 µM Aβ 42 from 0.1 % ammonia stock solution diluted with 50 mM phosphate buffer plus 50 % MeOH.

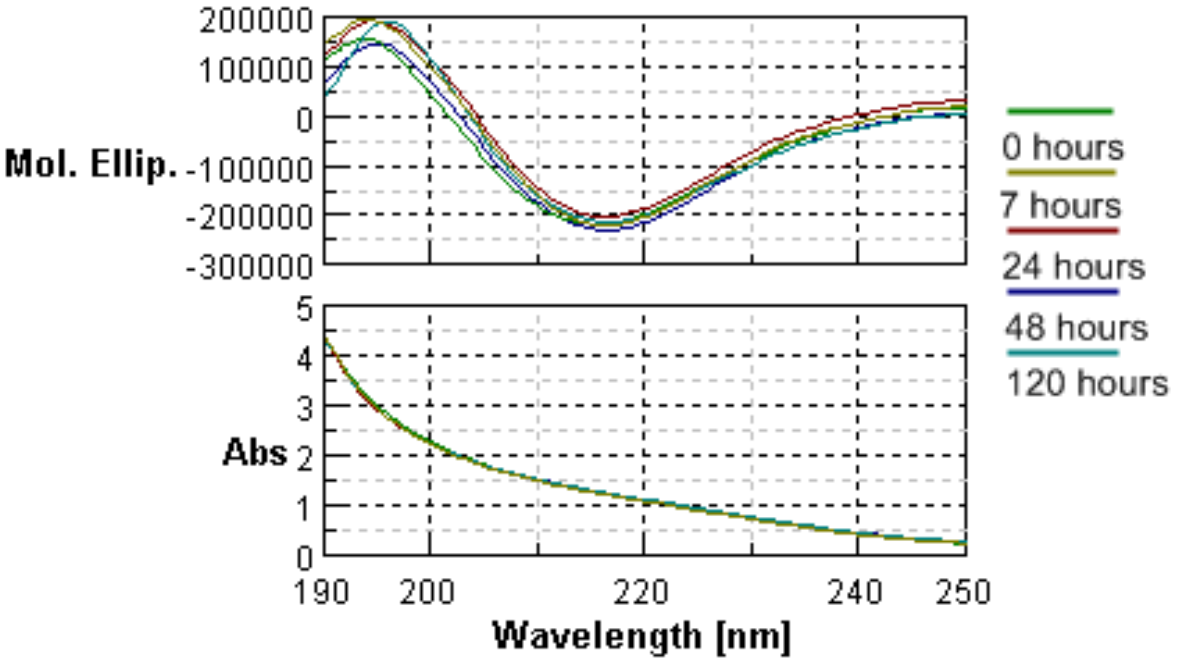

Fig. 58: Time dependent CD-spectra of 20 µM Aβ 42 from 0.1 % ammonia stock solution diluted with 50 mM phosphate buffer plus 100 µM substance H in MeOH.

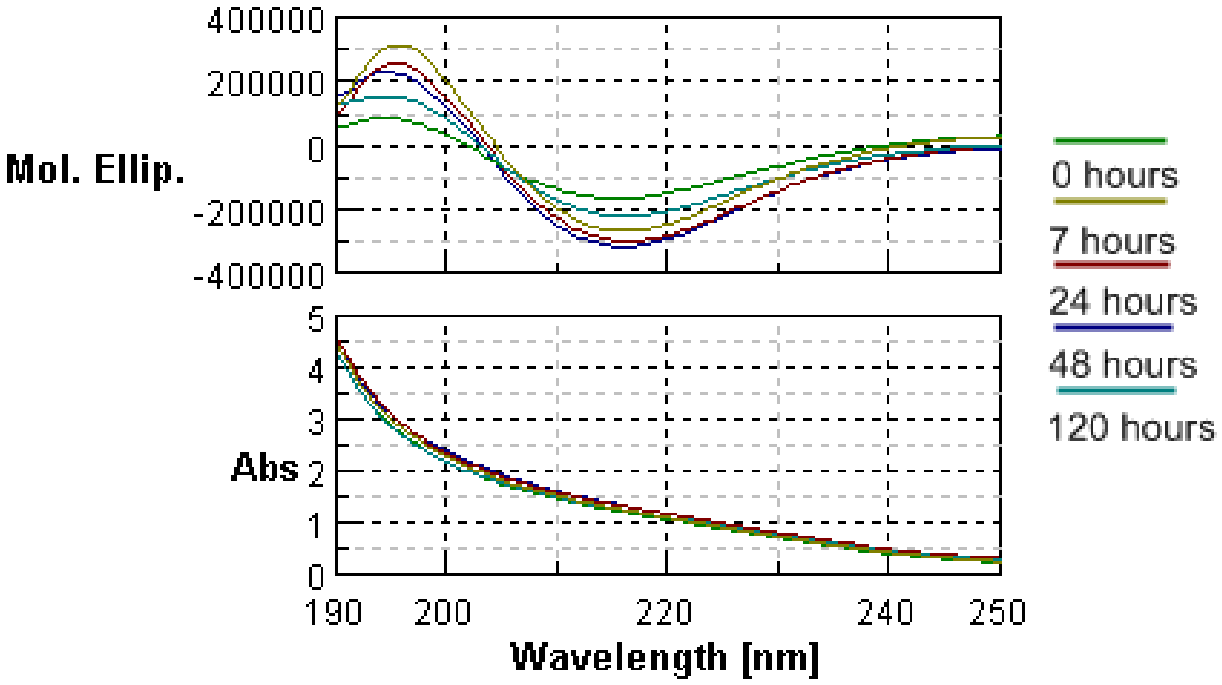

Fig. 59: Time dependent CD-spectra of 20 µM Aβ 42 from 0.1 % ammonia stock solution diluted with 50 mM phosphate buffer plus 5 % MeOH.

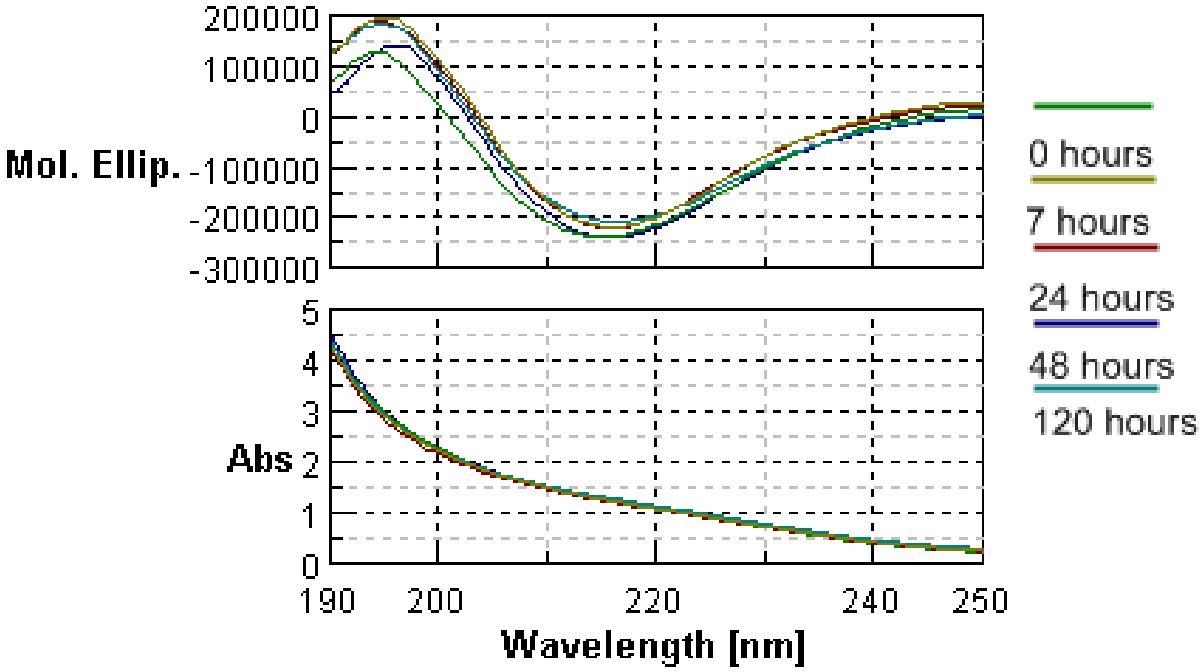

Fig. 60: Time dependent CD-spectra of 20 µM Aβ 42 from 0.1 % ammonia stock solution diluted with 50 mM phosphate buffer plus 10 µM substance H in MeOH.

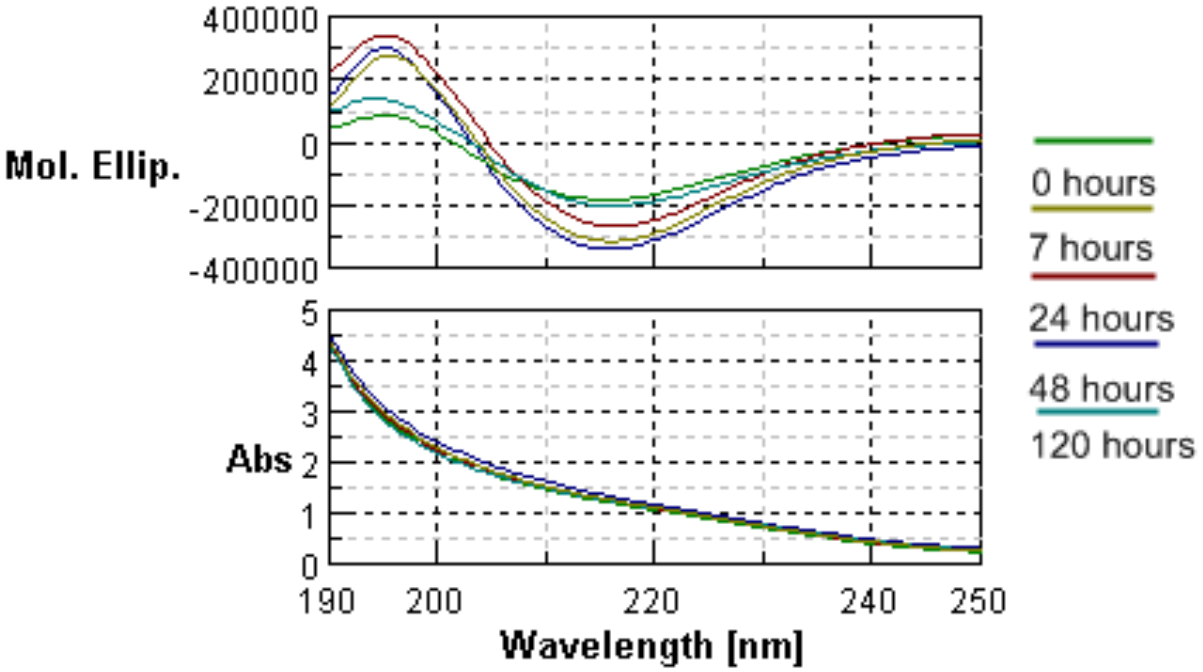

Fig. 61: Time dependent CD-spectra of 20 µM Aβ 42 from 0.1 % ammonia stock solution diluted with 50 mM phosphate buffer plus 0.5 % MeOH.

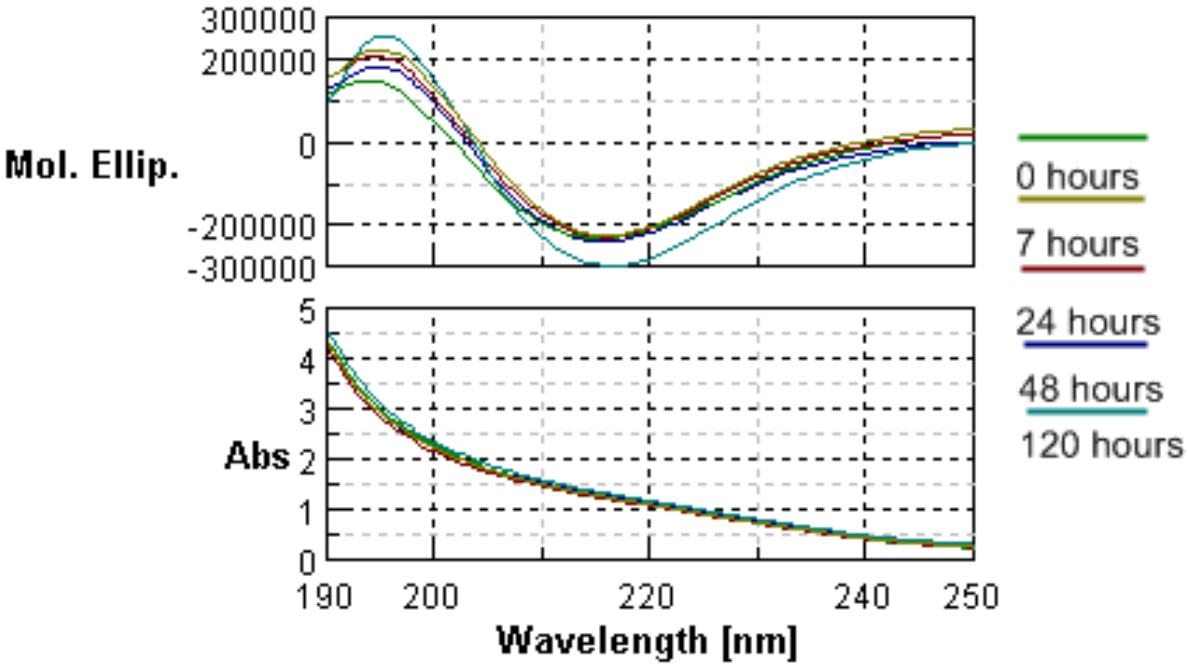

Fig. 62: Time dependent CD-spectra of 20 µM Aβ 42 from 0.1 % ammonia stock solution diluted with 50 mM phosphate buffer plus 1 µM substance H in MeOH.

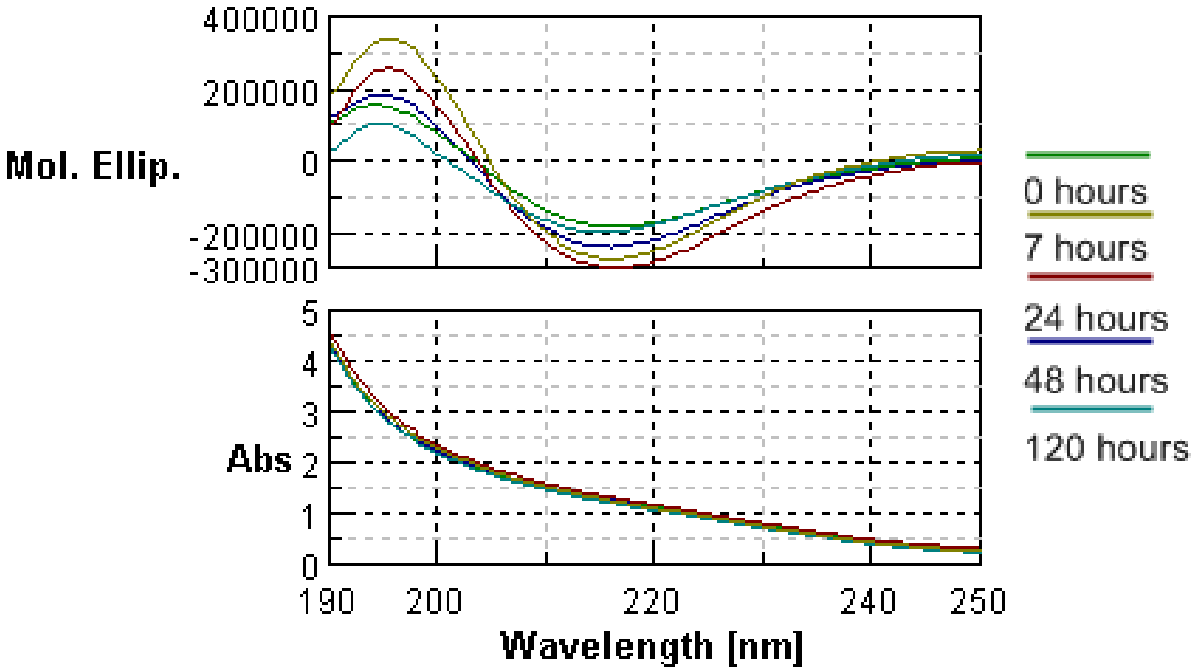

Fig. 63: Time dependent CD-spectra of 20 µM Aβ 42 from 0.1 % ammonia stock solution diluted with 50 mM phosphate buffer plus 0.05 % MeOH.

Different concentrations of substance H dissolved in MeOH were measured by means of the CD spectrophotometr. Values were gained from various wavelenghts at the minimum, 220 nm, 195 nm in time. Resulting molar ellipsis versus time curves are shown in figures 64 to 66.

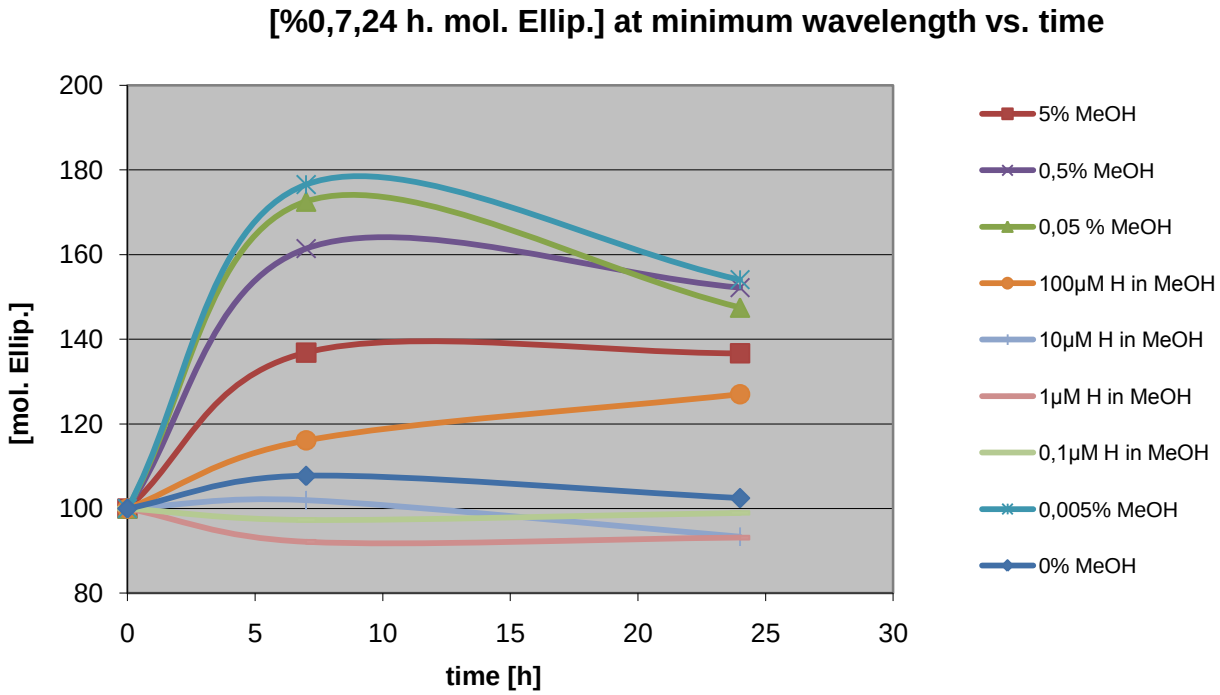

Fig. 64: Time dependent progressions of molar ellipsis values [%] at the minimum wavelength obtained from 20 µM Aβ 42 solutions with 0.1-100 µM substance H and/or 0.005-5 % MeOH.

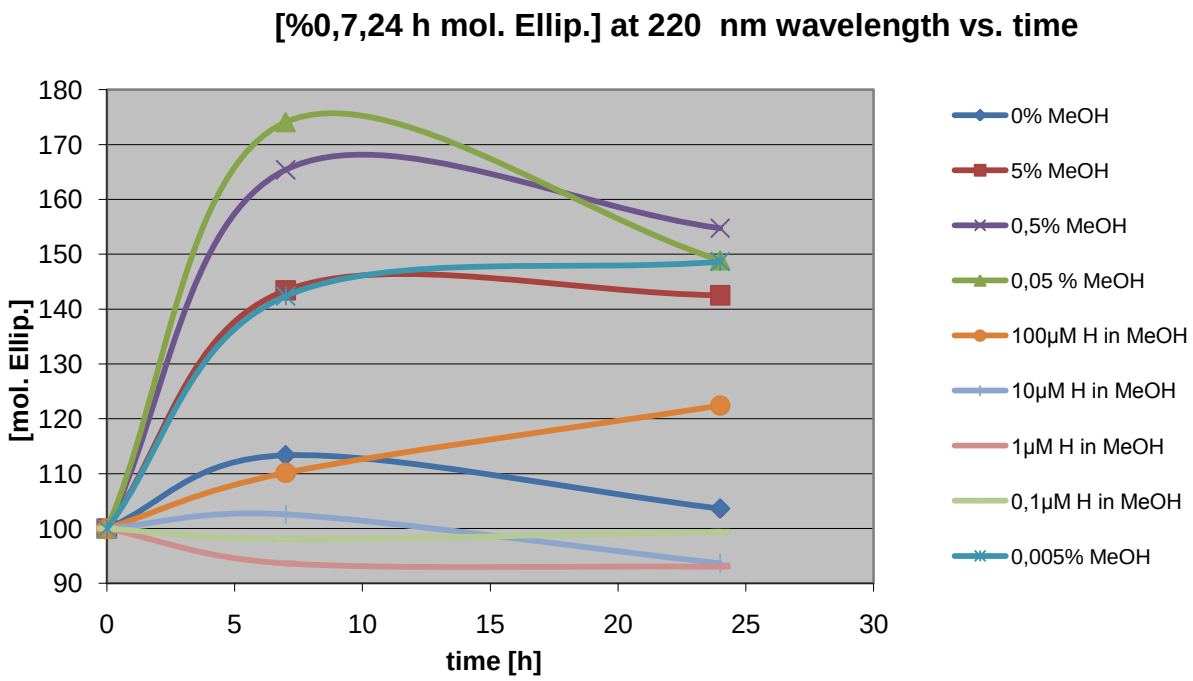

Fig. 65: Time dependent progressions of molar ellipsis values [%] at the 220 nm wavelength obtained from 20 µM Aβ 42 solutions with 0.1-100 µM substance H and/or 0.005-5 % MeOH.

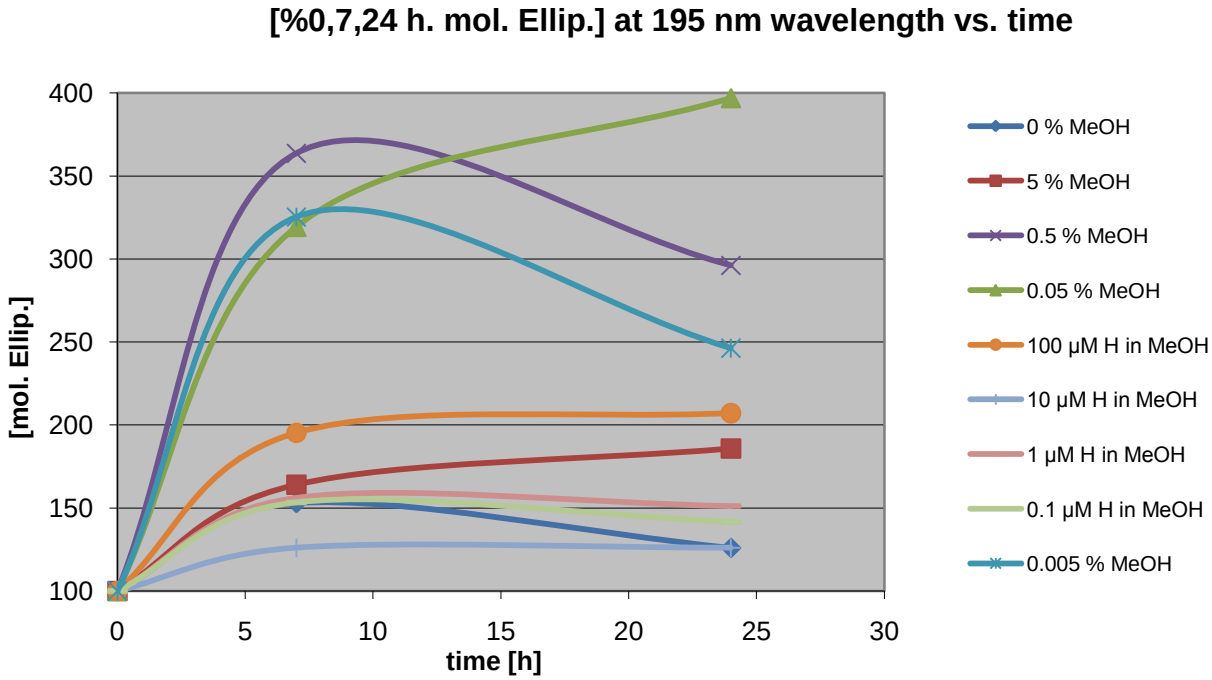

Fig. 66: Time dependent progressions of molar ellipsis values [%] at the 195 nm wavelength obtained from 20 µM Aβ 42 solutions with 0.1-100 µM substance H and/or 0.005-5 % MeOH.

Based on normalised molar ellipsis-graphs the slopes of these curves were calculated after linear regression analysis using points between 0 and 7 h.,0. 7 and 24 h. or 0 and 24 hours. Results are summarized in table 6.

Substance H in Methanol									
	Minimum			220 nm			195 nm		
	0, 7 h	0, 7, 24 h	0, 24 h	0, 7 h	0, 7, 24 h	0, 24 h	0, 7 h	0, 7, 24 h	0, 24 h
0 % MeOH	1.103	0.0257	0.1023	1.9092	0.0163	0.151	7,561	0.582	1.0785
5 %MeOH	5.2651	1.2413	1.5275	6.2012	1.4326	1.7718	9,1437	3.1463	3.5729
0.5 %MeOH	8.7778	1.6698	2.1755	9.3415	1.7395	2.2803	37,663	5.9153	8.1738
0.05 %MeOH	10.365	1.3369	1.9792	10.584	1.3825	1.9792	31,34	10.919	12.371
0.005 %MeOH	10.939	1.5883	2.2534	6.0549	1.7192	2.2534	32,184	4.0958	6.094
100 µM sub.H	2.2976	1.036	1.1258	1.4506	0.8949	0.9344	13,613	3.7635	4.4642
10 µM sub. H	0.2815	-0.3197	-0.2769	0.3653	-0.3127	-0.2644	3,7195	0.8834	1.0851
1µ M sub. H	-1.1283	-0.2223	-0.2868	-0.9087	-0.2426	-0.29	8,0194	1.6812	2.1321
0.1 µM sub. H	-0.3867	-0.0171	-0.0434	-0.2775	-0.0049	-0.0243	7,6172	1.281	1.7317

Tab. 6: Summary of slopes of normalised, time-dependent molar ellipsis curves of the experiments with 0.1-100 µM substance H dissolved in MeOH and 0.005-5 % MeOH as additional control samples.

The fifth experiment with Congo Red and Meclocycline Sulfosalicylate was made. Both substances in the water were dissolved and in different time points were measured by the same method as the previous measurement. The concentration was still 20 µM in solution. For measurement, the solution containing the inhibitor in amount of 23 µl, 15.3 µl of amyloid (50 µl of 300 mM) and 191.7 µl of phosphate buffer were used. CD- spectra of each sample are shown in figures 67-75.

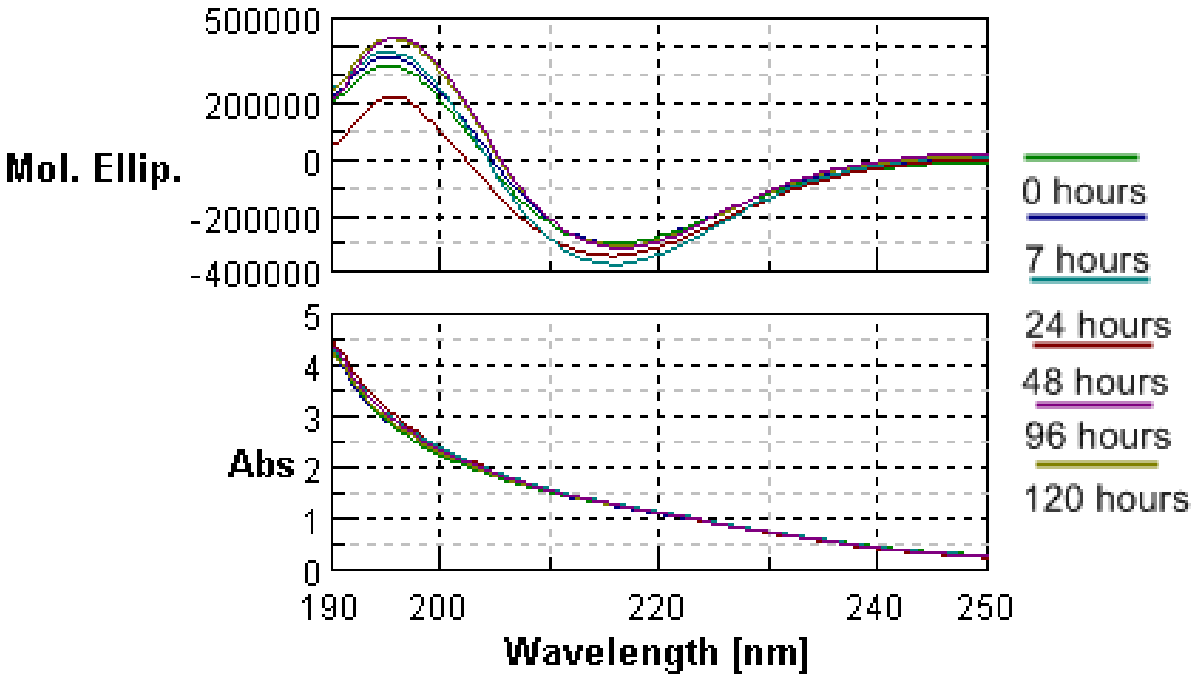

Fig. 67: Time dependent CD-spectra of 20 µM Aβ 42 from 0.1 % ammonia stock solution diluted with 50 mM phosphate buffer.

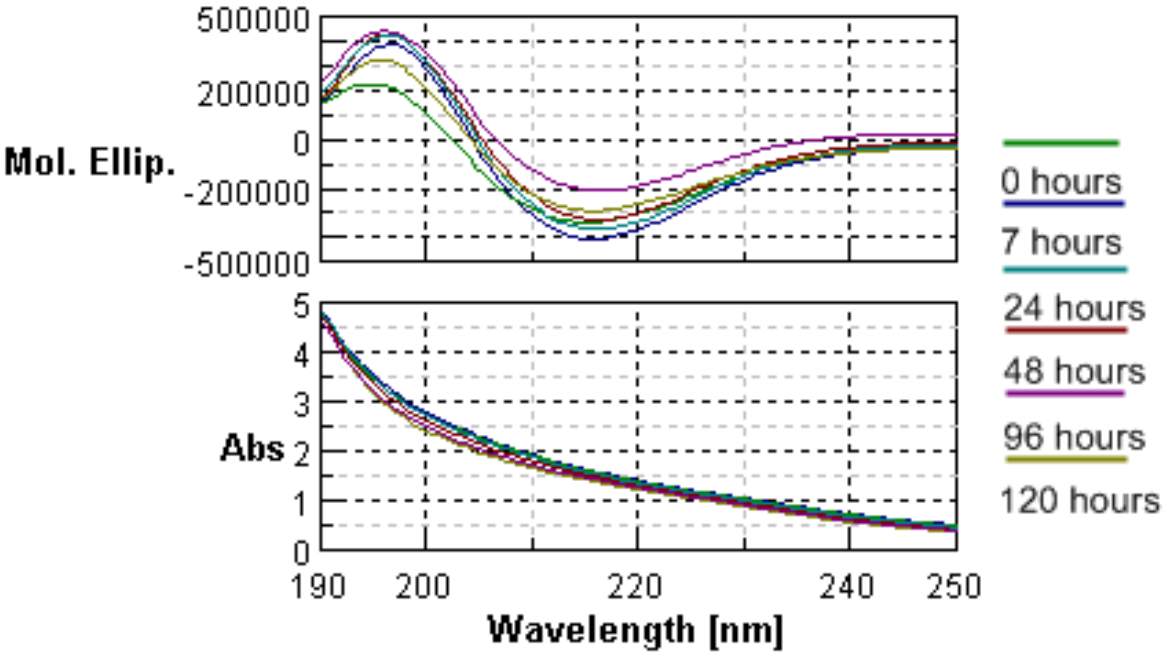

Fig. 68: Time dependent CD-spectra of 20 µM Aβ 42 from 0.1 % ammonia stock solution diluted with 50 mM phosphate buffer plus 1 mM Congo Red.

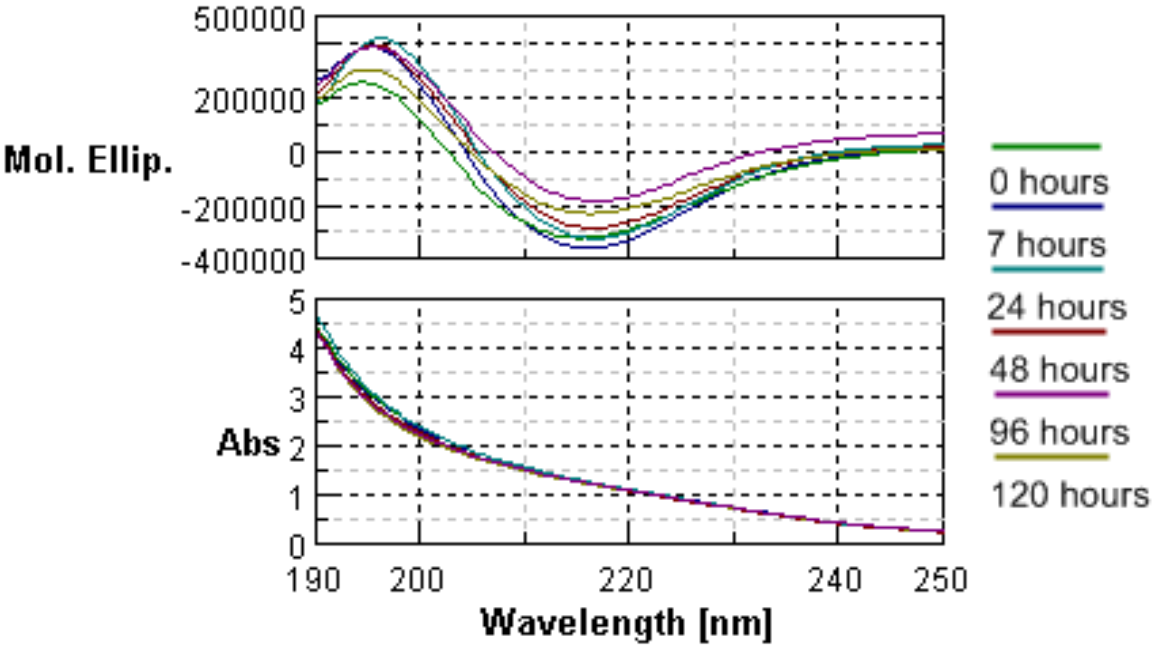

Fig. 69: Time dependent CD-spectra of 20 µM Aβ 42 from 0.1 % ammonia stock solution diluted with 50 mM phosphate buffer plus 100 µM Congo Red.

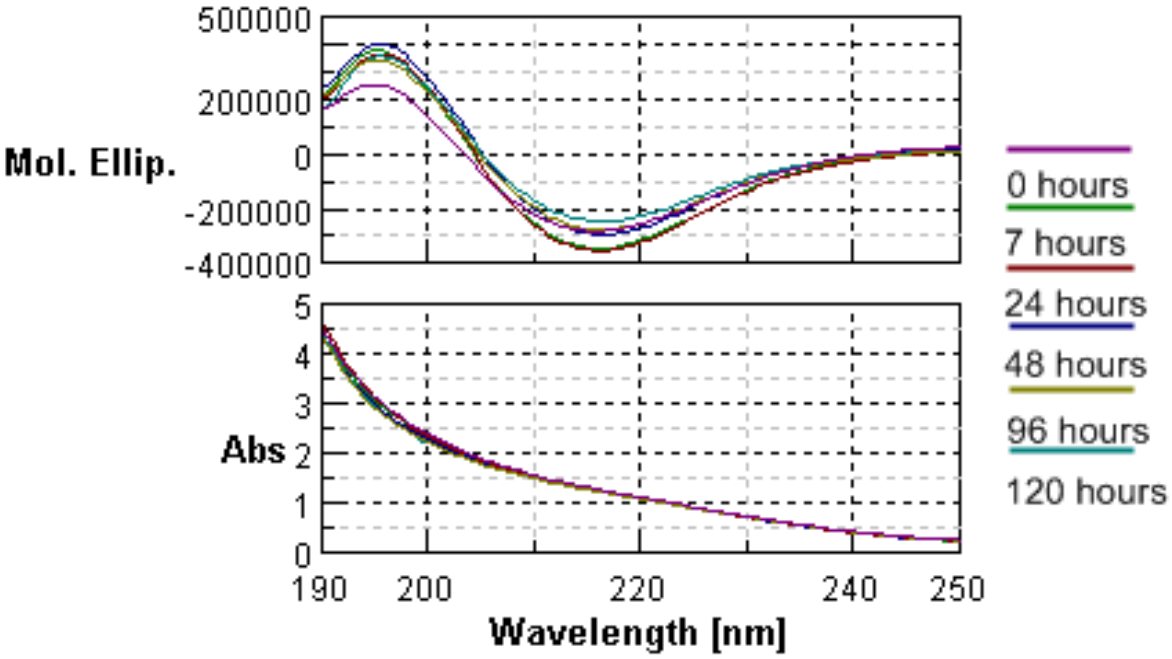

Fig. 70: Time dependent CD-spectra of 20 µM Aβ 42 from 0.1 % ammonia stock solution diluted with 50 mM phosphate buffer plus 10 µM Congo Red.

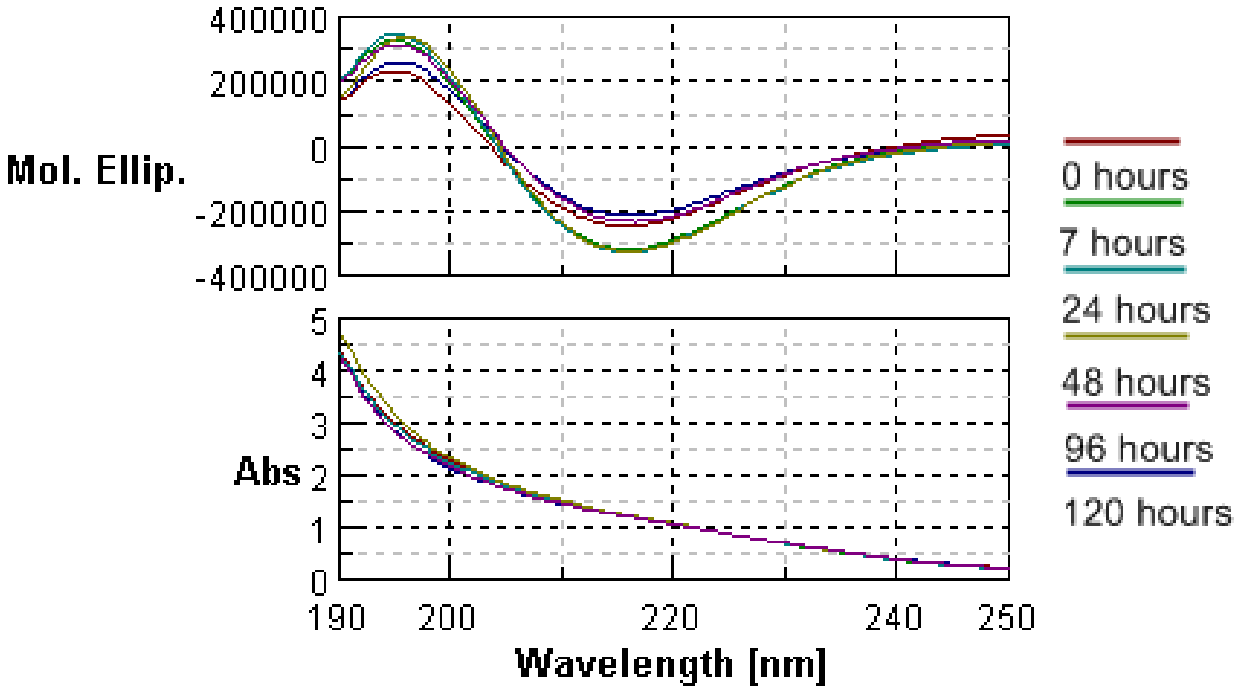

Fig. 71: Time dependent CD-spectra of 20 µM Aβ 42 from 0.1 % ammonia stock solution diluted with 50 mM phosphate buffer plus 1 µM Congo Red.

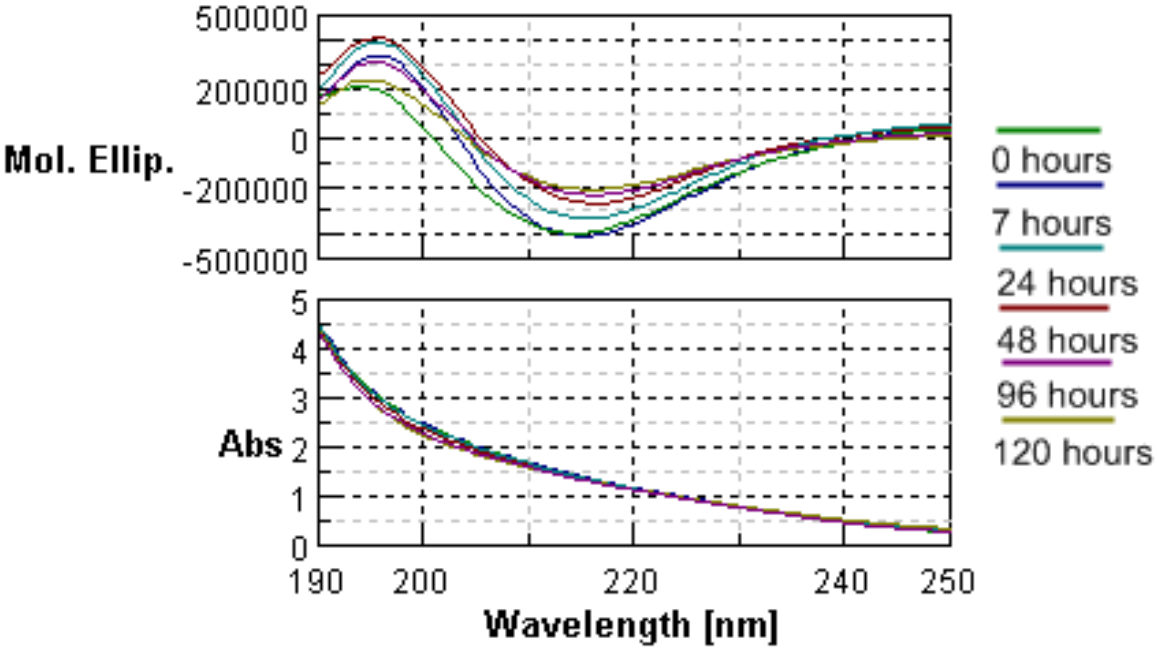

Fig. 72: Time dependent CD-spectra of 20 µM Aβ 42 from 0.1 % ammonia stock solution diluted with 50 mM phosphate buffer plus 1 mM Meclocycline Sulfosalicylate.

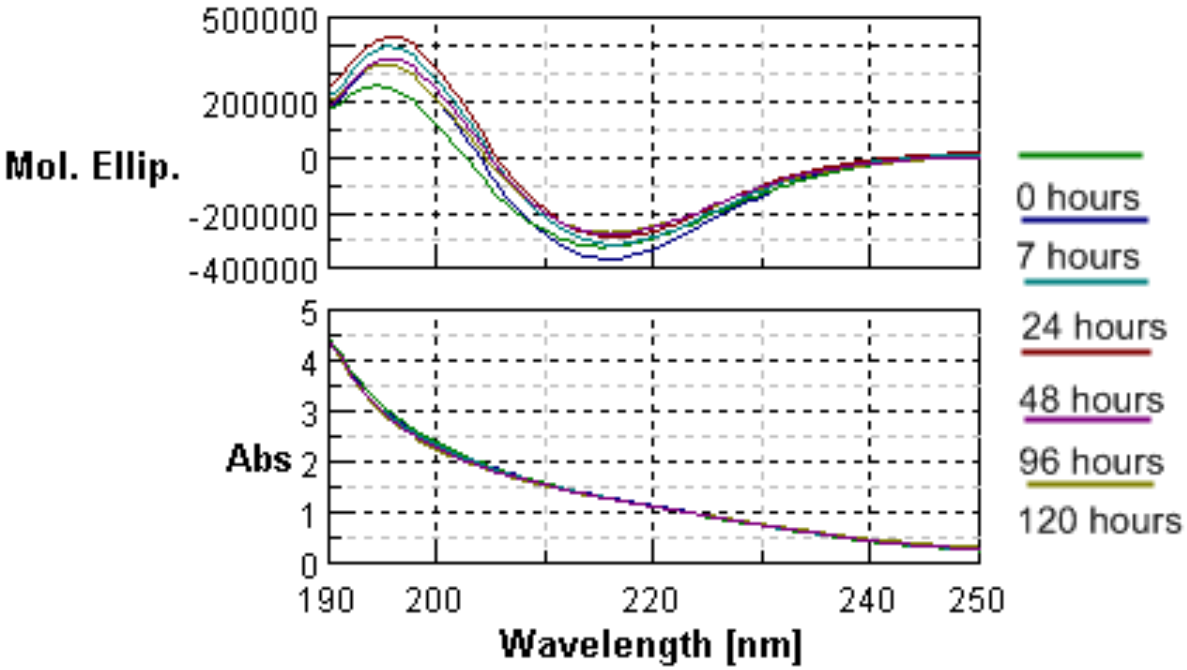

Fig. 73: Time dependent CD-spectra of 20 µM Aβ 42 from 0.1 % ammonia stock solution diluted with 50 mM phosphate buffer plus 100 µM Meclocycline Sulfosalicylate.

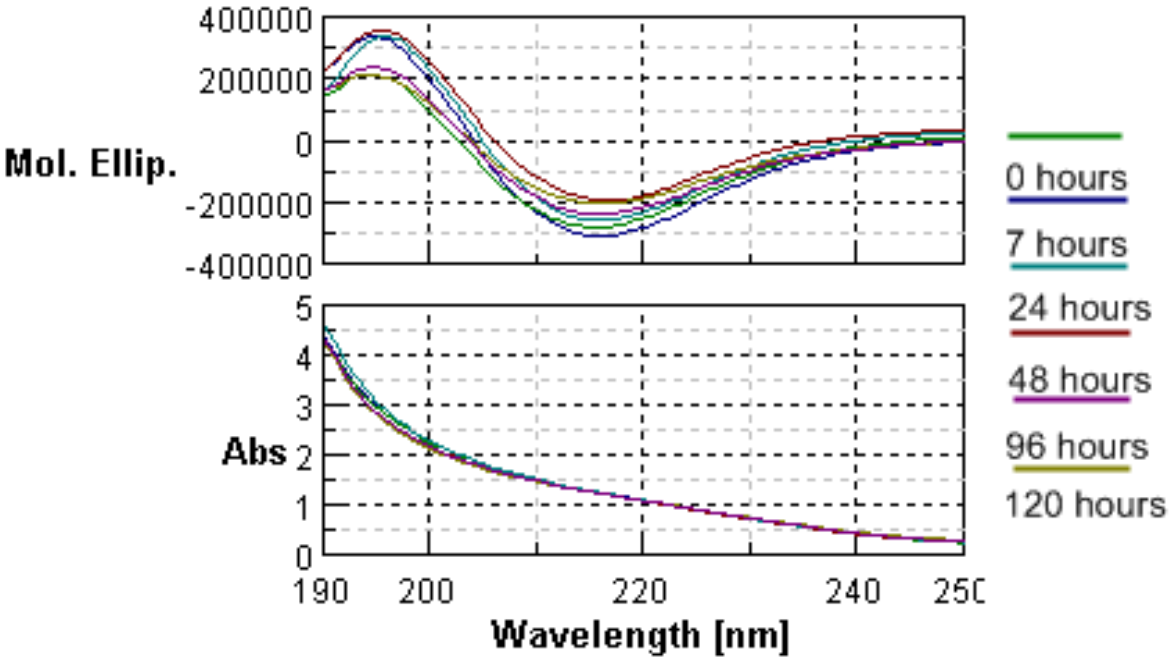

Fig. 74: Time dependent CD-spectra of 20 µM Aβ 42 from 0.1 % ammonia stock solution diluted with 50 mM phosphate buffer plus 10 µM Meclocycline Sulfosalicylate.

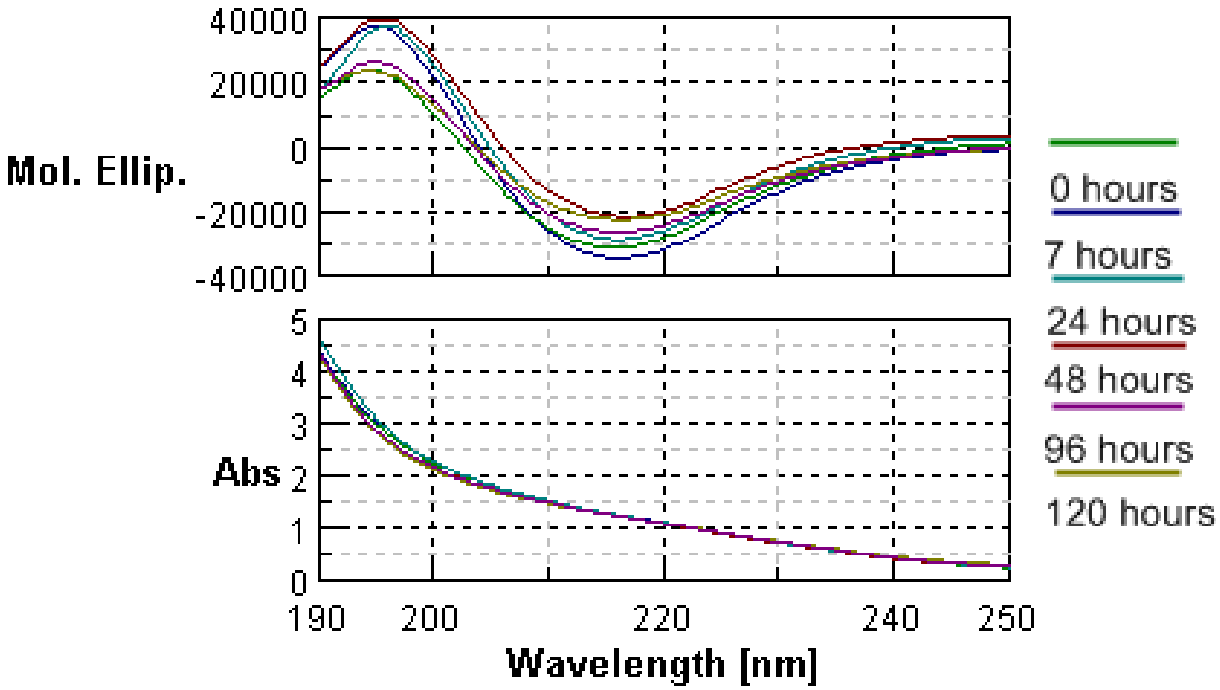

Fig. 75: Time dependent CD-spectra of 20 µM Aβ 42 from 0.1 % ammonia stock solution diluted with 50 mM phosphate buffer plus 1 µM Meclocycline Sulfosalicylate.

Different concentrations of Congo Red and Meclocycline Sulfosalicylate dissolved in water were measured by means of the CD spectrophotometer. Values were

gained from various wavelengths at the minimum, 220 nm and 195 nm in time. Resulting molar ellipsis versus time curves are shown in figures 76 to 78.

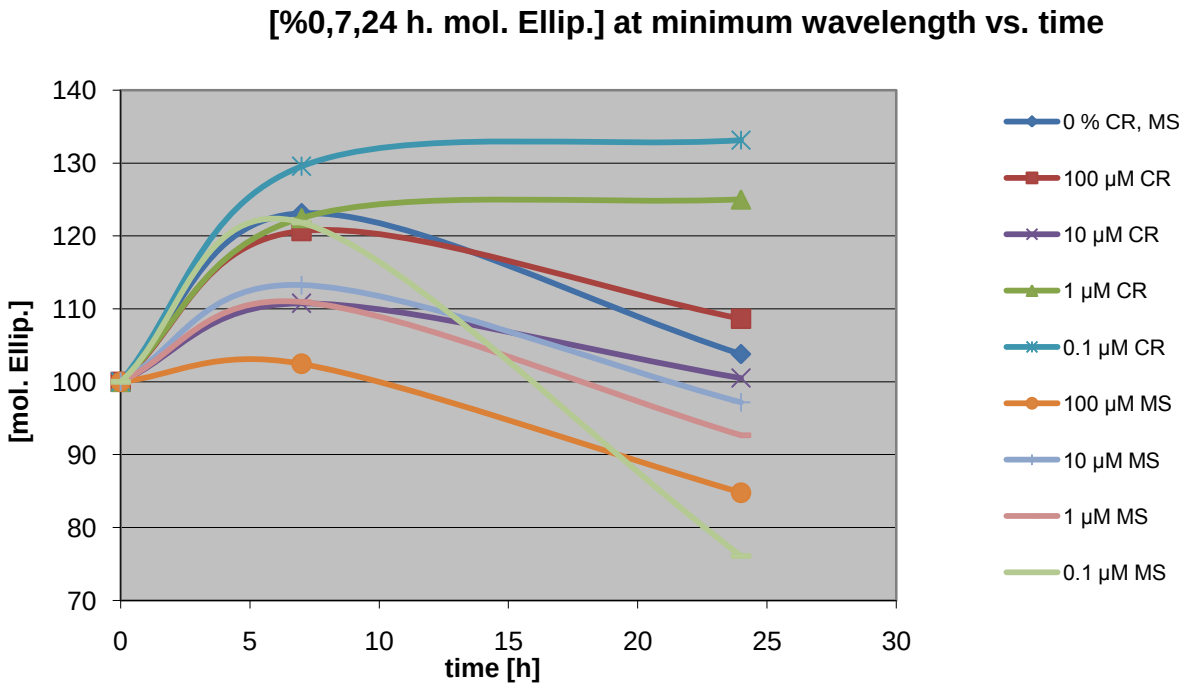

Fig. 76: Time dependent progressions of molar ellipsis values [%] at the minimum wavelength obtained from 20 µM Aβ 42 solutions with 0.1-100 µM Congo Red and Meclocycline Sulfosalicylate and blank value.

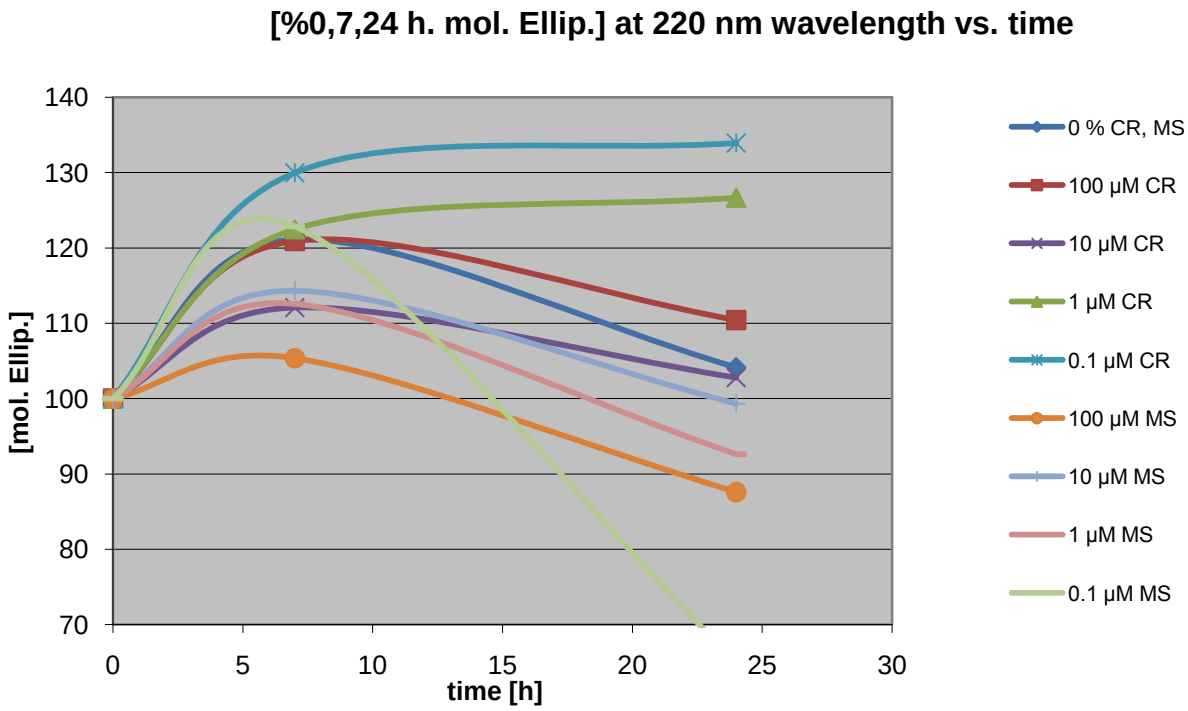

Fig. 77: Time dependent progressions of molar ellipsis values [%] at the 220 nm wavelength obtained from 20 µM Aβ 42 solutions with 0.1-100 µM Congo Red and Meclocycline Sulfosalicylate and blank value.

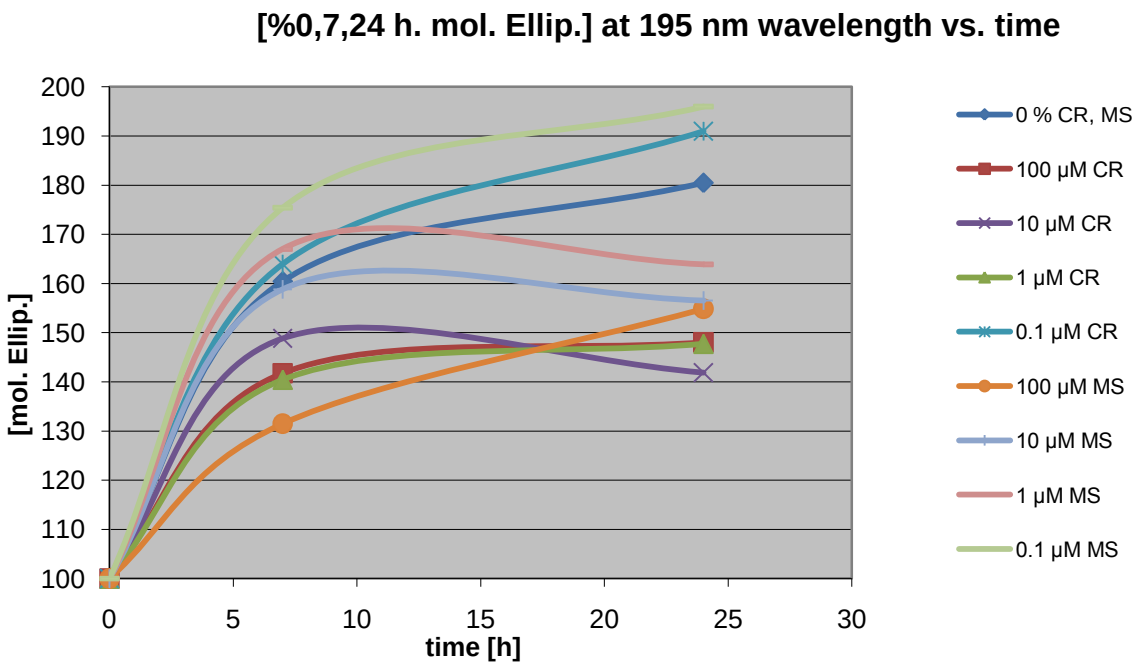

Fig. 78: Time dependent progressions of molar ellipsis values [%] at the 195 nm wavelength obtained from 20 µM Aβ 42 solutions with 0.1-100 µM Congo Red and Meclocycline Sulfosalicylate and blank value.

Based on normalised molar ellipsis-graphs the slopes of these curves were calculated after linear regrassion analysis using points between 0 and 7 h., 0, 7 and 24 h. or 0 and 24 hours. Results are summarized in tab. 6.

Congo Red (CR) and Meclocycline Sulfosalicylate (MS)									
	Minimum			220 nm			195 nm		
	0, 7 h	0, 7, 24 h	0, 24 h	0, 7 h	0, 7, 24 h	0, 24 h	0, 7 h	0, 7, 24 h	0, 24 h
0 % CR, MS	3.3008	-0.0826	0.1581	3.0157	-0.0456	0.1722	8.638	2.9499	3.3545
100 µM CR	2.9524	0.1617	0.3602	2.9902	0.2386	0.4344	5.9667	1.6981	2.0017
10 µM CR	1.5374	-0.0951	0.021	1.7255	-0.0079	0.1154	6.9779	1.3439	1.7447
1 µM CR	3.2103	0.8766	1.0426	3.2108	0.9507	1.1115	5.801	1.7	1.9902
0.1 µM CR	4.2241	1.1637	1.3814	4.2805	1.1941	1.4137	9.1388	3.3817	3.7912
100 µM MS	0.3516	-0.7099	-0.634	0.7675	-0.6154	-0.517	4.4993	2.1166	2.286
10 µM MS	1.893	-0.2715	-0.118	2.0467	-0.1857	-0.027	8.404	1.8922	2.3554
1 µM MS	1.5638	-0.4497	-0.306	1.7929	-0.4686	-0.308	9.5742	2.1321	2.6615
0.1 µM MS	3.12	-1.31	-0.996	3.2647	-1.819	-1.458	10.772	3.4807	3.9994

Tab. 7: Summary of slopes of normalised, time-dependent molar ellipsis curves of the experiments with 0.1-100 µM Congo Red and Meclocycline Sulfosalicylate dissolved in water and compared with additional control samples.

4.7 Results

Before studying effects of inhibitors on Aβ-oligomerization, effects of the organic solvents DMSO, EtOH, MeOH and CH_3CN - which should be used to dissolve the inhibitors - on CD-spectra were analysed. It was shown that CD-spectra of optical

active DMSO were concentration dependent, whereas no concentration dependent effects on CD-spectra were found for EtOH as well as for MeOH and CH_3CN. Even solutions containing 0.05 % DMSO revealed in slightly changed CD-spectra.

The effects of Curcumin, substance H, Congo Red and Meclocycline Sulfosalicylate on the Aβ-oligomerization were studied by CD-spectroscopy.

All inhibitors were prepared in the same way. First, substances were dissolved in organic solvents and were then diluted in a row to ensure same volumina of substance solutions in all samples. Then, inhibitors or appropriate amounts of organic solvents alone (as blanks) were mixed with prepared Aβ-solutions, ammonia and 50 mM phosphate buffer to achieve 20 µM Aβ 42 solution with or without inhibitors. All samples were incubated at least for 72 or 96 hours at 37 °C and were measured at each time point (unless otherwise specified at 0, 7, 24, 48, 72 or 96 hours). In general, the biggest differences occurred between 0 and 7 hours incubation after beginning the reaction. The maximum progression of the curves in the spectra was observed after 48 hours, then the curves started to degenerate. In spectra, the minimum was around 220nm, at which the presence of β-sheet structures can be detected. Differences between curves were compared by values from 0, 7, 24 h at different wavelengths (minimum, 220 nm, 195 nm). In order to normalise for possible different starting values, molar ellipsis values at 0 h were set to 100 % and graphs were drawn from 0 over 7 to 24 hours for the values at the minimum wavelengths (app. 216-219 nm), 220 nm and 195 nm. Based on normalised molar ellipsis-graphs the slopes of these curves were calculated after linear regression analysis using points between 0 and 7 h, 0, 7 and 24 h or 0 and 24 hours.

For the Curcumin studies, the substance was dissolved in DMSO as well as EtOH in order to investigate possible differences in the effects dependent on the solvent used. Using DMSO as solvent resulted in difficultly interpretable data. No concentration dependent effect of Curcumin on the Aβ-oligomerization was observed. Considering only the DMSO data, in comparison to the control sample (0 % DMSO) the oligomerization procress seemed to be accelerated by DMSO indicated by the data from 0-7 hours. Subsequently, slopes from 0-24 hours decreased significantly because the maximum values had been reached after app. 7 hours and then the slopes started to decrease again. Thus, DMSO was not suitable for these studies due to two reasons. On

the one hand, DMSO influenced the CD-spectra because of its optical activity. On the other hand, spectra revealed an enhancing effect of DMSO on Aβ-oligomerization. On the contrary, EtOH exhibited no concentration dependent effect on CD-spectra. According to this, it was possible to confirm concentration dependent effects of Curcumin on Aβ-oligomerization including the 24 hours values (220 nm, 0-24 h, control slope: 2.296; Curcumin 100µM: 0.781, 10 µM: 0.931, 1 µM: 1.329, 0.1 µM: 1.691). Considering the influence of EtOH alone, it was remarkable that 0.1 and 0.01 % EtOH seemed to delay Aβ-oligomerization, whereas higher and lower concentration of EtOH (1 %, 0.001 %) did not affect the progression of CD-spectra in comparison to the control. Presence of Curcumin reduced Aβ-oligomerization additionally to EtOH except at 0.1 % EtOH. This effect should be further investigated and maybe enlighten a possible role of EtOH onto the oligomerization process of Aβ 42.

Furthermore, the potential preventing Aβ 42 oligomerization of substance H was investigated. It was dissolved in MeOH and tested in concentration from 0.1 to 100 µM. In comparison to the control sample (0 % MeOH), it seemed that substance H accelerated the Aβ 42 oligomerzation process. But when slope values were related to the corresponding MeOH values, a significant, partly concentration dependent effect was observed (table 6). In this regard, MeOH strongly accelerated Aβ 42 oligomerization compared to the control and thus covered the reducing effect of substance H.

The proposed disintegrating substances Congo Red and Meclocycline Sulfosalicylate were also tested. Both were dissolved in water and inhibited also the Aβ 42 oligomerization process in a concentration dependent manner.

4.8 Discussion

Effects of inhibitors on Aβ-oligomerization were investigated by CD-spectroscopy. Selected inhibitors, such as Curcumin, Congo Red, substance H and Meclocycline Sulfosalicylate can bind to amyloid and delay the onset of Aβ oligomerization. The mechanism of inhibitory reaction is proposed to base on binding to the β-sheets, which can easily be detected by a CD-method.

Curcumin contains symmetrical phenol groups, which can bind to Aβ and delay the oligomerization. The inhibitory effect of Curcumin on the aggregation had been proved for several times and also its Aβ disaggregation properties in low concentrations

was promoted (Nakagami et al., 2002). The other inhibitors such as Congo Red, composed of a sulfonated structure with hydrophobic bridges can also bind to Aβ sheets as well as Meclocycline Sulfosalicylate, which is tetracyclic compound, has the same effect on Aβ. Also their inhibitory effects were proven.

With regard to the published IC_{50} values of Curcumin (361.11 ± 38.91 μM), Congo Red (10 ± 0.29 μM) and Meclocycline Sulfosalicylate (0.25 ± 0.07 μM) different concentration dependent effects on the Aβ-oligomerization were expected (Necula et al., 2007; for substance H no IC50 value is currently known. Interestingly, the most significant inhibiting effects on Aβ oligomerization were shown around their IC_{50} values, in particular for Curcumin (in EtOH) at a concentration of 100 μM, for Congo Red at 10 μM and for Meclocycline Sulfosalicylate at 0,1 μM after 24 hours. Since it was also reported that some inhibitors can promote fibrilization, it is possible that substances may support fibrilization at higher concentrations leading to inconclusive concentration-effect relationships.

At the same time a western blot analysis tool as well as a fluorescence assay based on ThT were developed in the lab, which were able to reproduce some data of this diploma thesis. It was able to show the effects of Congo Red by the western blot assay by analysing the inhibition of Aβ-oligomer formation (Rybka, 2009). By means of the ThT-fluorescence assay the concentration dependent inhibition of fibril formation by Congo Red and Curcumin were confirmed.

One important point which complicates the experimental procedures should be mentioned. The Aβ-oligomerization process is a very dynamic one which is dependent on pH-value and time, but also on temperature. Thus, every preparation step including dissolution should be carried out at least on ice. Once the Aβ-oligomerization has started it leads also to changes in the stock solution which results in different oligomerization ratios at the beginning of each single experiment. Thus, appropriate control samples in each experiment as well as e.g. centrifugation before the usage of the stock solution (to separate fibrils as pellets) and fast dissolution of Aβ 42 are strongly recommended. As shown in this thesis the influence of a little amount of ammonia can result in enhanced oligomerization probably due to changes solubility of Aβ 42. Other research groups dissolve the Aβ 42 with a strong acid, evaporate this and redissolve in DMSO for further storage. This should also be tried out. However, in general a

procedure for the CD-measurement of the Aβ 42 oligomerization was established. Based on these data, the method can further be developed and might be used for drug screening with regard to their Aβ 42 oligomerization inhibiting and plaques disintegrating properties.

5 Summary

The main aim of this study was to establish a CD-method which enables studies about the Aβ 42 oligomerization process. This was achieved by developing a measurement protocol to determine the CD-spectra of Aβ 42 solutions. Fast working during the dissolution and preparation of Aβ 42 solutions on ice are necessary to provide meaningful start spectra. The optimum found concentration of Aβ 42 for these tests was 20 µM. Addition of ammonia accelerated the progression of the Aβ 42 oligomerization and was necessary in order to gain reasonable experimental durations. The influence of organic solvents on the Aβ 42 oligomerization process should not be neglected. DMSO is optical active, MeOH and EtOH affected the speed of the Aβ 42 oligomerization process in a concentration dependent manner. This has to be considered since several groups store their Aβ 42 stock solutions in DMSO and this might influence their published results. However, the methods for the storage and usage of Aβ 42 solutions has to be optimized in order to start with a defined amount of only Aβ 42 monomers, since western blotting (Rybka, 2009) showed that Aβ 42 monomer solution might be contaminated by and by with formed oligomers. For this, techniques as ultrafiltration or centrifugation seem to be the most practicable purification steps. With regard to the inhibitor studies, it was able to confirm data from literature. The strongest concentration dependent effects were shown for all investigated substances (Curcumin, Congo Red, Meclocycline Sulfosalicylate) around their published IC_{50} values. In general, a CD-method to screen for inhibitors of the Aβ 42-oligomerization process was established. However, due to the high amount of Aβ 42 (200 µl of a 20 µM solution for one sample) and the complex data analysis, other techniques might be used to screen for inhibitors of the Aβ 42-oligomerization process as e.g. fluorescence assays based on fluorescence shifts of Thioflavin T or Resveratrol after binding to already formed fibrils. Nevertheless, together with western blots (differentiation between monomers, oligomers and polymers) and fluorescence assays (detection of fibril formation) the CD method can provide very useful and important data (differences in the secondary structures) in order to examine and evaluate the mechanisms of Aβ oligomerization and also its inhibition by specific compounds.

6 References

Aggarwal, B. B., Surh, Y.-J., Shishodia, S. (2007). The molecular targets and therapeutic use of Curcumin heath and disease. S.: 1-2.

Ahn, J. S., Lee, J.-H., Kim, J-H., Paik, S. R (2007). Novel method for quantitative determination of amyloid fibrils of α-synuclein and amyloid β/A4 protein by using Resveratrol. *ScienceDirect*, S. 367: 259-265.

Akaishi, T., Morimoto, T., Shibao, M., Watanabe, S., Sakai-Kato, K., Utsunomiya-Tate, N., Abe, K. (2008). Structural requirements for the flavonoid fisetin in inhibiting fibril formation of amyloid β protein. *Neuroscience Letters*, S. 444, 280-285.

Barrow, C. J. (2007). Abeta peptide and Alzheimer disease, S: 216.

Basha, F. Z., Atta-ur-Rahman (2006). Bioactive natural products. *Elsevier links*, S.: 786.

Berova, N., Nakanishi, K., Woody, R. W. (2000). Circular dichroism of peptides and proteins. S.: 601-612.

Blazer, D. G., Steffens, D. C. (2009). The american psychiatric publishing textbook of Geriatric Psychiatry, S: 122-124.

Carter, J., Lippa CF. (2001). Beta-amyloid, neuronal death and Alzheimer´s disease. *BenthamDirect links*, S 1(6): 733-7.

Feldman, H. H., Jacova, C., Robillard, A., Garcia, A., Chow, T., Borrie, M., Schipper, H. M., Blair, M., Kertesz, A., Chertkow, H. (2008). Diagnosis and treatment of dementia: 2. Diagnosis. *Canadian Medical Association or its licentors*, S. 178(7): 825-836.

Fisher, A. (1998). Advances in Alzheimer´s disease and Parkinson´s disease, S: 109.

Greenberg, A., Breneman, C. M., Liebman, J. F. (2000). The amide linkage. S.: 600.

Kim, H., Park, B.-S., Lee, K.-G., Choi, Ch. Y., Jang, S. S., Kim, Y.-H., Lee, S.-E. (2005). Effects of naturally occuring compounds on fibril formation and oxidative stress of β-amyloid. *Journal of agricultural and food chemistry*, S. 53: 8537-8541.

Kim, D.S.H.L., Park, S.-Y., Kim J.-Y. (2001). Curcuminoids from Curcuma longa L. (Zingiberaceae) that protect PC12 rat pheochromocytoma and normal human umbilical vein endothelials cells from βA (1-42) insult. *Neuroscience Letters*, S. 303: 57-61.

Guerois, R., Lopéz de la Paz, M. (2006). Protein design. S.: 256-271.

Hof, P. R., Mobbs, Ch. V. (2000). Functional Neurobiology of aging. *Amyloid hypothesis,* S: 22: 333.

Jang, M. M., Piao, X. L., Kim, J. M., Kwon, S. W., Park, H. J. (2008). Inhibition of cholinesterase and amyloid-β aggragation by resveratrol oligomers from Vitis amurensis. *Physiotherapy research,* S. 22: 544-549.

Jiskot, W., Crommelin, D. J. A. (2005). Methods of structural analysis of protein pharmaceuticals. S.: 92-96.

Kominos, D. (1995). Toward understanding amyloid aggregation. *Biophysical journal*, S:. 739-740.

Maccioni, RB., Munoz, JP., Barbeito L. (2001). The molecular bases of Alzheimer´s disease and other neurodegenerative disorders. *Elsevier links*, S. 32(5): 367-81.

McLaurin, J., Golomb, R., Jurewicz, A., Antel, J. P., Fraser, P. E. (2000). Inositol stereoizomers stabilize an oligomeric aggregate of Alzheimer amyloid-β peptide and inhibit Aβ induced toxicity. *The journal of biological chemistry,* S. 24: 18495-18502.

McLaurin, J., Kierstead, M. E., Brown, M. E, Hawkes, Ch. A., Lambermon, M. H. L., Phinney, A. L., Darabie, A. A., Cousins, J. E., French, J. E., Lan, M. F., Chen, F., Wong, S. S. N., Mount, H. T. J., Fraser, P. E., Westaway D., St George-Hyslop P. (2006). Cyclohexanehexol inhibitors of Aβ aggregation prevent and reverse Alzheimer phenotype in a mouse model. *Nature medicine,* S. 7: 801-808.

Octave, JN. (2005). Alzheimer disease: cellular and molecular aspects. *Medical Bulletin,* S. 160 (10-12): 445-9.

Patterson, Ch., Feightner, J. W., Garcia, A., Hsiung, G.-Y. R., MacKnight, Ch., Sadovnick, A. D. (2008). Diagnosis and treatment of dementia: 1. Risk assessment and primary prevention of Alzheimer disease. *Canadian Medical Association or its licensors,* S. 178(5): 548-556.

Ransohoff, R. M., Benveniste, E. N. (1996). Cytokines and the CNS. *Neurodegenerative cascade*, S: 13.

Rattan, S. I. S., Kassem, M.(2006). Prevention and treatment of age-related diseases. *Therapy*, S: 52-59..

Richter, R. W. (2004). Alzheimer´s disease: A Physician´s Guide to Practical Management, S: 1-6.

Ringe, D., Petsko, G. A. (2004). Protein structure and function. S.: 1-17.

Rost, F. W. D., (1995). Fluorescence microscopy. S.: 385.

Rybka, J. (2009). Development and optimization of a disintegrator western blot assay based on the detection of Amyloid-beta oligomers, a potentially harmful species during Alzheimer disease. S.: 69.

Sachdev, P. (2003). The aging brain: the neurobiology and neuropsychiatry of aging. *Blood brain barrier*, S: 155.

Sarbadhikari, S. N. (2006). Depression and dementia: progress in brain reseach, clinical applications and future trends. *Blood brain barrier*, S: 97-103.

Sigma-Aldrich (2009) www.sigmaaldrich.com

Sirgurdsson, E. M. (2005). Amyloid proteins: methods and protocols. *Circular dichroism*, S. 36-37.

Sisodia, S. S., Tanzi, R. E. (2007). Alzheimer disease: advances in genetics, molecular and cellular biology. *Clearance*, S: 41.

Smith, H. J. (2007). Protein misfolding in neurodegenerative diseases, S: 75-76.

Toy, E. C., Uthmann, E., Uthmann, M., Braun, E. J. (2008). Case files. *Morfology*, S.: 119-120.

Verbeek, M. M., de Waal, R. M. W., Vinters, H. V. (2000). Cerebral amyloid angiopathy in Alzheimer disease and related disorders. *Blood brain barrier*, S: 23-26.

Vojáček, J., Malý, M. (2004). Arteriální a žilní trombóza v klinické praxi. *Zánět,* S: 29.

WHO (2001).

http://www.searo.who.int/LinkFiles/Health_and_Behaviour_alzheimers.pdf

Yang, F., Lim, G. P., Begum, A. N., Ubeda, O. J., Simmons, M. R., Ambegaokar, S. S., Chen P., Kayed, R., Glabe, Ch. G., Frautschy, S. A., Cole, G. M. (2005). Curcumin inhibits formation of amyloid β oligomers and fibrils, binds plagues, and reduces amyloid in vivo. The journal of biological chemistry, S. 7: 5892-2005.